

**SELF-ASSEMBLY AND RHEOLOGY OF  
BLOCK COPOLYMER WITH  
POLYMER ADDITIVES OR PARTICLE SUSPENSIONS**

**ABHINAV MAHESWARAN PRAGATHEESWARAN**

**NATIONAL UNIVERSITY OF SINGAPORE**

**2014**

**SELF-ASSEMBLY AND RHEOLOGY OF  
BLOCK COPOLYMER WITH  
POLYMER ADDITIVES OR PARTICLE SUSPENSIONS**

**ABHINAV MAHESWARAN PRAGATHEESWARAN**

(B.Tech, Anna University, India)

A THESIS SUBMITTED FOR THE DEGREE OF  
**DOCTOR OF PHILOSOPHY**

DEPARTMENT OF  
CHEMICAL AND BIOMOLECULAR ENGINEERING

**NATIONAL UNIVERSITY OF SINGAPORE**

**2014**

## DECLARATION

---

I hereby declare that this thesis is my original work and it has been written by me in its entirety. I have duly acknowledged all the sources of information which have been used in the thesis. This thesis has also not been submitted for any degree in any university previously.



---

**Name:** Abhinav Maheswaran Pragatheeswaran

**Date:** 21/7/2014

## ACKNOWLEDGEMENT

---

I would like to express my special appreciation and thanks to my advisor Associate Professor Shing Bor Chen, for his consistent and thoughtful advice, continuous encouragement and help during the course of this work.

I would also like to thank my committee members, Associate Professor Liang Hong and Associate Professor Saif A. Khan for their constructive criticisms and excellent advices to this study. I could always count on them to help me see things from another point of view.

This work has received a great deal of support and assistance from the lab officer Jamie Woon Chee Siew. I would like to acknowledge Tan Evan Stephen and Ang Wee Siong for their help on the operation of the equipment in the initial stage of my project.

Many thanks also go to all my lab mates for their support and helpful discussions. Without them, the atmosphere in the lab would not have been so unforgettable. Thanks are also due to my friends at NUS for their encouragement and enjoyable talks and jokes during the numerous evening tea sessions.

Finally, I would like to express my heartfelt gratitude to my parents and fiancée for their continuous support and encouragement, which enabled me to overcome difficulties and hardship encountered in the course of this study.

# TABLE OF CONTENTS

---

<b>DECLARATION</b> .....	<b>i</b>
<b>ACKNOWLEDGEMENT</b> .....	<b>i</b>
<b>TABLE OF CONTENTS</b> .....	<b>ii</b>
<b>SUMMARY</b> .....	<b>vii</b>
<b>LIST OF TABLES</b> .....	<b>x</b>
<b>LIST OF FIGURES</b> .....	<b>xi</b>
<b>NOMENCLATURE</b> .....	<b>xv</b>
<b>1. Research Background and Objectives</b> .....	<b>17</b>
1.1. Block copolymer self-assembly .....	17
1.2. Overview of Pluronic triblock copolymers .....	18
1.3. Micellization in Pluronics .....	21
1.3.1. CMC and CMT .....	21
1.3.2. Micellization mechanism .....	21
1.3.3. Size and shape of micelles .....	22
1.4. Gelation in Pluronics .....	24
1.4.1. CGC and CGT.....	24
1.4.2. Gelation mechanism.....	25
1.4.3. Structure and rheology of gel.....	25
1.5. Applications of Pluronics .....	27
1.6. The role of additives.....	27
1.6.1. Effects of salts.....	28

1.6.2.	Effects of solvents.....	28
1.6.3.	Effects of classical surfactants .....	29
1.7.	Motivation .....	30
1.7.1.	Effects of poly(ethylene oxide).....	30
1.7.2.	Effects of poly(acrylic acid).....	32
1.7.3.	Mixed PEO-PPO-PEO copolymers .....	33
1.7.4.	Effects of polymeric additives on corn starch suspension .....	35
1.8.	Objectives.....	36
1.9.	Thesis organization .....	38
<b>2.</b>	<b>Materials and Methods .....</b>	<b>40</b>
2.1.	Materials.....	40
2.1.1.	Pluronic triblock copolymers.....	40
2.1.2.	Poly(ethylene oxide).....	40
2.1.3.	Poly(acrylic acid).....	41
2.1.4.	Corn starch .....	41
2.1.5.	Others .....	42
2.2.	Sample Preparation .....	42
2.2.1.	Preparation of pluronic solution.....	42
2.2.2.	Preparation of particle suspension .....	43
2.3.	Equipment .....	43
2.3.1.	Dynamic light scattering (DLS).....	43
2.3.2.	Differential scanning calorimetry (DSC).....	44
2.3.3.	UV-visible spectrophotometer .....	45
2.3.4.	Fourier transform infrared (FTIR) spectroscopy .....	45

2.3.5.	Rheometer .....	46
2.3.6.	Tube inversion technique and cloud point (CP) measurements.....	47
2.3.7.	Nuclear magnetic resonance (NMR) .....	47
2.3.8.	Small angle X-ray scattering (SAXS).....	48
2.3.9.	Optical microscopy .....	48
2.3.10.	Polarized light microscopy (PLM).....	49
2.3.11.	Cryogenic transmission electron microscopy (Cryo-TEM).....	49
<b>3.</b>	<b>Effect of Poly (ethylene oxide) on Sol-Gel Behavior of Pluronic F127 .....</b>	<b>50</b>
3.1.	Introduction .....	50
3.2.	Results and discussion.....	51
3.2.1.	Critical gelation temperature (CGT).....	51
3.2.2.	Gelation time and strength of gel.....	54
3.2.3.	Critical micellization temperature (CMT) .....	57
3.2.4.	Micelle characterization.....	62
3.2.5.	Correlation between micellization and gelation .....	70
3.3.	Conclusion.....	73
<b>4.</b>	<b>Effect of Poly (acrylic acid) on Sol-Gel Behavior of Pluronic F127 .....</b>	<b>74</b>
4.1.	Introduction .....	74
4.2.	Results and discussion.....	76
4.2.1.	Critical micellization temperature.....	76
4.2.2.	Enthalpy of micellization.....	83
4.2.3.	Gelation.....	90
4.2.4.	Comparison with other commonly studied additives.....	95

4.3.	Conclusion.....	96
<b>5.</b>	<b>Sol-Gel Behavior of Pluronic Binary Mixture with Non-identical PPO</b>	
	<b>Block Lengths .....</b>	<b>98</b>
5.1.	Introduction .....	98
5.2.	Results and discussion.....	100
5.2.1.	Critical micellization temperature.....	100
5.2.2.	Size analyses .....	103
5.2.3.	Cloud point (CP) studies.....	105
5.2.4.	Gelation and rheology.....	107
5.2.5.	Microstructure.....	112
5.3.	Conclusion.....	116
<b>6.</b>	<b>Effect of Pluronics and Other Additives on Rheology of Corn Starch</b>	
	<b>Suspension .....</b>	<b>118</b>
6.1.	Introduction .....	118
6.2.	Choice of CS packing fraction .....	120
6.3.	Results & Discussion .....	123
6.3.1.	Effects of F127.....	123
6.3.2.	Effects of PEO homopolymer.....	125
6.3.3.	Yielding.....	126
6.3.4.	Solvent effect of PEG200 .....	130
6.3.5.	Interaction between CS particles and PEO .....	133
6.3.6.	Discussion.....	135
6.4.	Conclusion.....	140



<b>7. Conclusions and Recommendations.....</b>	<b>142</b>
7.1. Conclusions .....	142
7.2. Recommendations .....	145
<b>BIBLIOGRAPHY.....</b>	<b>149</b>
<b>PUBLICATIONS &amp; CONFERENCES .....</b>	<b>166</b>
<b>APPENDIX.....</b>	<b>167</b>
Effect of PEO contributed viscosity on F127 micelle size.....	167
Effect of PEO on <sup>1</sup> H-NMR spectra of 1%F127 .....	168
SAXS Analysis.....	170
<sup>13</sup> C-NMR for F127+L64 mixture .....	172
Effect of F127 concentration on CMT of F127/PAA/H <sub>2</sub> O system .....	173
Thermoreversibility of micellization process in F127/PAA/H <sub>2</sub> O.....	174

## SUMMARY

---

Polymer self-assembly in nano scale has received a great deal of attention in the last two decades and the number of scientific applications and products based on the principle of self-assembly is still briskly growing. Moreover, fundamental processes in life sciences such as the properties and stability of lipid membranes and their interactions with proteins, DNA, etc. are governed by the phenomenon of self-assembly. Pluronics® (PEO-PPO-PEO, PEO = poly (ethylene oxide), PPO = poly (propylene oxide)) are non-ionic amphiphilic triblock copolymers. In the last decade, major research studies on Pluronics have focused on the application of these copolymers and their efficiency in pharmaceutical, therapeutic and lithographic applications. Nevertheless, relatively little is known about the influence of relevant additives in the formulations along with the Pluronics on micellization and gelation properties of Pluronic surfactants, and what the underlying mechanisms are.

In this thesis work, a comprehensive study on the influence of additives, namely non-ionic homopolymer (poly (ethylene oxide); PEO), ionic homopolymer (poly (acrylic acid); PAA), triblock copolymer (Pluronic® L64 or P105) and a particle suspension (corn starch; CS) on the micellization and gelation behavior of Pluronic® F127 in H<sub>2</sub>O is carried out. Differential scanning calorimetry, dynamic light scattering, dye solubilization technique and nuclear magnetic resonance are used to study the micellization behavior while the rheology, gelation and structural analysis of the systems are characterized by

rheometry, tube inversion method, cryogenic TEM, small angle X-ray scattering and polarized light microscopy.

The results show that both the homopolymers PEO and PAA have similar impact on the gelation of F127, i.e., both increase the critical gelation temperature (CGT) and decrease the gel strength with homopolymer concentration. From micellization experiments, it is found that the heat of micellization ( $\Delta H$ ) drastically reduced with the addition of PAA, depicting its effect on changing the local environment for PPO blocks to alleviate their need for dehydration, while this effect is not observed with the addition of PEO. However, both the homopolymers decrease the critical micellization temperature (CMT) of F127. The effect of PAA is strongly dependent on the pH of the medium. Next the incorporation of Pluronic L64 or P105 to F127 results in formation of mixed micelles. It is also observed that with increase in temperature, two hard gels of different crystalline structure are formed in F127/L64/H<sub>2</sub>O systems, while such a complex behavior is not seen in F127/P105/H<sub>2</sub>O system. Finally, the incorporation of Pluronic F127 reduces the shear thickening behavior of CS suspensions because of the increased thermodynamic contribution to viscosity that dominates over the hydrodynamic influences.

Previously unobserved behavior such as the advancement of the micelle formation points of F127 in the presence of homopolymers (PEO and PAA), and two gel phases behavior of F127+L64 mixture are observed, and a greater understanding of the interactions between amphiphilic copolymers and polymeric additives in aqueous medium is achieved. The findings prove to be beneficial in

the optimization of copolymer formulations engineered for the use in pharmaceutical or biomedical applications and other industries as well.

## LIST OF TABLES

---

Table 3.1 Effects of molecular weight of PEO on CGT, $t_{gel}$ , $\tau_{co}$ and $G_0'$ of 20% F127 .....	53
Table 3.2 Effects of PEO concentration on CGT, $t_{gel}$ , $\tau_{co}$ and $G_0'$ of 20wt% F12754	
Table 3.3 Effect of molecular weight of PEO on hydrodynamic size of 1% F127 .....	66
Table 3.4 Effect of concentration of PEO on hydrodynamic size of 1% F127 ....	67
Table 5.1 CP temperatures of pure Pluronics and their mixtures .....	105
Table 6.1 Effect of PEO concentration on $G'$ (Pa), yield Stress (Pa) and thixotropic loop area (Pa/S) of CS suspension; PEO M.W = 2k; CS conc. = 44% .....	127
Table 6.2 Effect of CS : PEO ratio and PEO M.W on the shift of -OH peak relative to pure CS .....	135

## LIST OF FIGURES

---

Figure 1.1 Schematic representation of AB diblock copolymer forming micelle in a selective solvent .....	17
Figure 1.2 Pluronic grid .....	19
Figure 1.3 Schematic representation of the association mechanism of PEO-PPO-PEO in water .....	22
Figure 1.4 Clear gel formed in 20% Pluronic F127 at 40°C .....	25
Figure 2.1 Chemical structure of PEO-PPO-PEO (Pluronic) .....	40
Figure 2.2 Chemical structure of PEO (left) and PAA (right) .....	40
Figure 2.3 FESEM images of corn starch granules .....	41
Figure 2.4 Image of rheometer AR G2 with cone and plate geometry (left) and with the solvent trap (right).....	46
Figure 3.1 Effects of molecular weight of PEO on gelation of F127/water system; F127 conc. = 20 wt% .....	52
Figure 3.2 Loss factor $\tan(\Theta)$ vs. temperature for 20 wt% F127 .....	55
Figure 3.3 Storage and loss moduli as a function of stress for 20% F127 in the presence of Class B PEO homopolymers at 37°C; the number of data points (not shown for clarity) for each decade of logarithmic stress is 12 .....	55
Figure 3.4 Thermograms of F127 in presence of PEO of different M.W.; F127 conc. = 20%; PEO conc. = 6% .....	58
Figure 3.5 Effect of MW of 6% PEO on CMT of 20% F127 (top); Effect of PEO conc. on CMT of 20% F127 (bottom); CMT of 20% F127 = $12.6 \pm 0.1^\circ\text{C}$ .....	59
Figure 3.6 Plot of count rate against temperature from DLS; arrows mark the CMTs of three different samples with F127 at 0.5% and PEO at 4% .....	60
Figure 3.7 Plot of average hydrodynamic radius against temperature for 0.5% F127 with PEO at 4% .....	62
Figure 3.8 Effect of molecular weight of Class A PEO on intensity distribution of F127/water system; PEO conc. = 4%; F127 conc. = 1% .....	64

Figure 3.9 Effect of molecular weight of Class B PEO on intensity distribution of F127/water system; PEO conc. = 2%; F127 conc. = 1% .....	64
Figure 3.10 Cryo-TEM micrographs of 10% F127 (A), 10% F127 + 5% PEO35k (B) and 10% F127 + 5% PEO200 (C) .....	70
Figure 4.1 Effect of temperature on UV-vis absorption spectra for DPH in F127/PAA (1.8k)/H <sub>2</sub> O system (top) and in F127/PAA (450k)/H <sub>2</sub> O system (bottom); F127 conc. = 1% .....	77
Figure 4.2 Effect of PAA concentration on CMT of F127 obtained by DPH technique; F127 conc. = 1% .....	78
Figure 4.3 Effect of pH on CMT of F127/PAA/H <sub>2</sub> O obtained by DPH technique; F127 conc. = 1% .....	78
Figure 4.4 Solution pH vs. temperature; Effect of high M.W PAA (A and B) and low PAA (C and D); The arrow marks the CMT as detected by DPH solubilization technique .....	80
Figure 4.5 Effect of pH on size distribution of 1% F127 + 0.05% PAA (450k) system at 40°C .....	81
Figure 4.6 DSC thermograms of 17.5% F127 in the presence of PAA at various concentrations; PAA 1.8k (top) and PAA 450k (bottom); Estimated uncertainty: $\Delta H \pm 0.2$ J/g .....	84
Figure 4.7 Effect of pH on DSC Thermograms of 17.5% F127 + 4% PAA 1.8k (top) and 17.5% F127 + 0.5% PAA 450k (bottom); Estimated uncertainty: $\Delta H \pm 0.2$ J/g .....	86
Figure 4.8 Effects of PAA (1.8k) on the gel behavior of F127 at different concentrations; 20% (red), 17.5% (blue, circles) and 16% (yellow) at natural pH and 17.5% (blue, squares) at pH = 5 .....	90
Figure 4.9 Effect of PAA molecular weight on the gel behavior of 17.5% F127; Low M.W PAA (blue) and high M.W PAA (red) .....	90
Figure 4.10 Effects of PAA (1.8k) conc. on oscillatory temperature sweeps of F127/water system; F127 conc. = 17.5% .....	94
Figure 4.11 Effects of PAA (450k) conc. on oscillatory temperature sweeps of F127/water system; F127 conc. = 17.5% .....	94

Figure 4.12 DSC Thermograms of 17.5% F127 with the addition of PAA (1.8k) and PEO (2k); Estimated uncertainty:  $\Delta H \pm 0.2$  J/g ..... 95

Figure 5.1 DSC thermograms of various weight ratios for F + L (left) and F + P (right); F:F127, P:P105, L:L64 ..... 100

Figure 5.2 Light scattering intensity vs. temperature for 1%F (a), 1%L (b), 1%F + 1%L (c), 1%P (d) and 1%F + 1%P (e); F:F127, P:P105, L:L64 ..... 102

Figure 5.3  $R_h$  distribution of pluronic mixture F + P (F:F127 and P:P105) at 40°C (left) and 60°C (right)..... 104

Figure 5.4  $R_h$  distribution of Pluronic mixture F+L (F:F127 and L:L64) at 40°C (left) and 60°C (right)..... 104

Figure 5.5 Sol-gel behavior of F+L (F:F127, L:L64) system determined by tube inversion technique ..... 107

Figure 5.6 Oscillatory temperature sweeps of varying ratios of F: L (F:F127, L:L64) with total polymer concentration fixed at 25% ..... 108

Figure 5.7 Images of tilted glass tubes with the mixture 12.5% F127 + 12.5% L64 at different temperatures; the sample appearance did not change after one week ..... 109

Figure 5.8 Oscillatory temperature ramp up and ramp down for 14% F + 11%L (left) and 12.5%F + 12.5%L (right); F:F127, L:L64 ..... 110

Figure 5.9 Effect of heating rate (left) and cooling rate (right) on  $G^*$  of 12.5%F127+12.5%L64 mixture ..... 110

Figure 5.10 Oscillatory temperature sweep for the mixture 1% F127 + 1% L64 ..... 111

Figure 5.11 SAXS patterns for the mixture 12.5% F + 12.5% L at different gel regions; Inset: SAXS pattern for soft gel region of 14%F + 11%L; (F:F127, L:L64) ..... 112

Figure 5.12 Oscillatory temperature sweeps of varying ratios of F127: P105 with total polymer concentration fixed at 25% ..... 116

Figure 6.1 Flow curves of CS suspension at different weight fractions ..... 121

Figure 6.2  $(\tau/\eta_m\dot{\gamma})$  vs. Re plot curves for CS weight fractions studied in Figure 6.1 ..... 121



Figure 6.3 Physical appearance of CS suspended in water for concentration just above the maximum packing fraction ( $\phi_m$ )..... 123

Figure 6.4 Flow curves of 44% CS with increasing F127 concentration; control = pure 44% CS ..... 124

Figure 6.5 Flow curves of 44% CS with increasing PEO2k concentration (left); with increasing molecular weight of 1% PEO (right); control = pure 44% CS.. 125

Figure 6.6 Effect of concentration of PEO2k on oscillatory stress sweep (left) and thixotropy (right) of CS suspensions; CS concentration = 44% ..... 126

Figure 6.7 Photographs of pure CS (A), CS + PEO2k (B) and CS + PEO20k (C) suspensions on the rheometer plate after cone withdrawal; CS conc. = 44%; PEO conc. = 4% ..... 129

Figure 6.8 Shear flow curves of 44% CS in various fraction of PEG200/water 130

Figure 6.9 Microscopic images of 1% CS in various fraction of PEG200/water; pure water (A), 25% PEG200 (B), 50% PEG200 (C), 75% PEG200 (D), pure PEG200 (E)..... 132

Figure 6.10 Effect of PEG M.W. on FTIR spectra for CS : PEG weight ratio = 7.5:2.5 ..... 133

Figure 6.11 Effect of weight ratio of CS : PEG on FTIR spectra; total concentration =10 wt%; PEG M.W. = 2k..... 134

Figure 6.12 Relative viscosity vs. shear stress for CS suspension with increasing PEO weight percentages; CS conc. = 44%; PEO M.W = 2k; control = pure 44% CS..... 136

Figure 6.13 Effect of pH on flow curves of 44% CS in water..... 137

## NOMENCLATURE

---

<b>Abbreviations</b>	<b>Descriptions</b>
BO	Butylene oxide
CAC	Critical association concentration
CGC	Critical gelation concentration
CGT	Critical gelation temperature
CMC	Critical micellization concentration
CMT	Critical micellization temperature
CP	Cloud point
Cryo-TEM	Cryogenic Transmission electron microscopy
CS	Corn starch
DI-water	Deionized water
DLS	Dynamic light scattering
DPH	1,6-Diphenyl-1,3,5-hexatriene
DSC	Differential scanning calorimetry
FTIR	Fourier transform infrared spectroscopy
HBD	Hydrogen Bond Donating
HLB	Hydrophilic to lipophilic balance
Hz	Hertz
NMR	Nuclear magnetic resonance
NOESY	Nuclear Overhauser effect spectroscopy
PAA	Poly (acrylic acid)
PaS	Pascal-second
PEO	Poly (ethylene oxide)
PLM	Polarized light microscopy
PPO	Poly (propylene oxide)

SAXS	Small angle X-ray scattering
SDS	Sodium dodecyl sulfate
SO	Styrene oxide
TEM	Transmission electron microscopy

<b>Symbols</b>	<b>Descriptions</b>
% w/v	Weight per volume percentage
$\Delta H$	Heat of micellization
$\mu$	Viscosity
D	Hydrodynamic diameter
d	Translational diffusion coefficient
G'	Storage modulus
G''	Loss modulus
$K_b$	Boltzmann's constant
mol%	Mole percentage
$M_w$	Molecular weight
$^{\circ}\text{C}$	Degree Celsius
R	Gas constant
T	Temperature
wt%	Weight percentage

## 1. Research Background and Objectives

---

### 1.1. Block copolymer self-assembly

Surfactants are surface active agents with both hydrophilic (water-loving) and hydrophobic (water-hating) parts in them. Small molecular surfactants have been studied extensively in the 20<sup>th</sup> century and have found a wide range of industrial applications.<sup>1-4</sup> Large amphiphilic molecules (block copolymers) represent a new frontier in the field of surfactant science and technology. Their macromolecular nature affords a range of architectures, length scales, time scales, and levels of interactions much broader than those obtainable in small amphiphilic molecules.<sup>5</sup> However, such variety brings great challenges in characterization and understanding of the self-assembly in amphiphilic block copolymers.

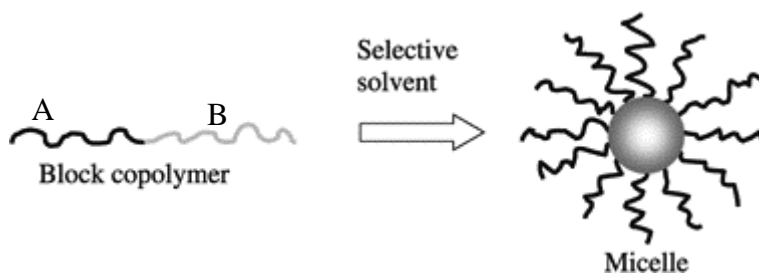


**Figure 1.1** Schematic representation of AB diblock copolymer forming micelle in a selective solvent

Block copolymers are composed of chemically dissimilar chains connected covalently with each other. A simple example is an AB diblock copolymer as shown in the Figure 1.1. This AB copolymer in solvent incompatible to B block will result in formation of micelles (microphase separation) with B blocks

forming the core of the micelle and A blocks forming the corona (Figure 1.1). Earlier studies on self-assembly of block copolymers were focused in organic solvents, but recently their self-assembly in aqueous media is also being explored. In general, the mechanism behind the self-assembly (micellization process) is different in organic and aqueous media.<sup>5</sup> In organic medium, the self-assembly is usually exothermic (enthalpy driven micellization) and hence the copolymers tend to dissolve at high temperature. In contrast, the self-assembly is endothermic (entropy driven process) in aqueous medium and hence with increase in temperature the driving force for self-assembly also increases. In various applications, constant efforts are being made to utilize this temperature triggered self-assembly property of block copolymers.<sup>6-9</sup> Spontaneous self-assembly requiring no special processing steps is a vital aspect of block copolymer nanostructures and hence suitable for large scale industrial production.

## 1.2. Overview of Pluronic triblock copolymers

Poly (ethylene oxide) – poly (propylene oxide) – poly (ethylene oxide) (PEO-PPO-PEO) triblock copolymers are a subset of amphiphilic block copolymers also commercially available as Pluronics® (BASF laboratories, Wyandotte, USA) or Synperonics® (ICI laboratories, Wilton, UK). US Food and Drug administration (FDA) guide has presented Pluronic F127 as an inactive ingredient for different types of formulations (e.g. inhalation, oral, ophthalmic or topical formulations).<sup>7</sup> A considerable number of patents associating Pluronics have been registered in the USA [www.uspto.gov](http://www.uspto.gov). At low temperature, both PPO and PEO blocks of the copolymers are soluble in water (unimers). With increase

in temperature, the PPO blocks become relatively hydrophobic and gradually become insoluble in water while PEO blocks are still soluble. Aggregation of insoluble PPO blocks results in self-assembly of these molecules into micelles when either the critical micellization concentration (CMC) or critical micellization temperature (CMT) is reached. At high enough concentration, the micelles can pack themselves to form liquid crystalline structures (physical gels) above the critical gelation temperature (CGT). Both the micellization and gelation processes are thermoreversible.<sup>10</sup>

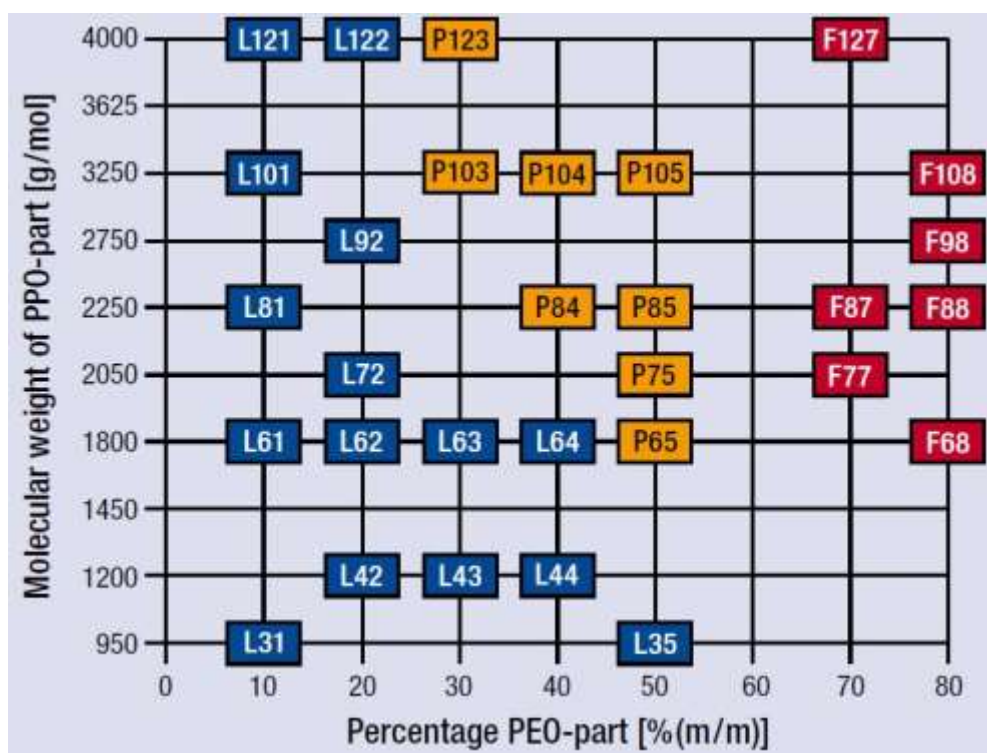


**Figure 1.2** Pluronic grid

Pluronic are different from classical low molecular weight non-ionic surfactants  $C_xE_y$  ( $y$ -ethylene glycol;  $x$ -alkyl ethers) in a number of ways: 1) the

peculiarity of pluronics is that their CMC and surface activity depend very intensely on temperature than those for the classical non-ionic surfactants. The CMC value of Pluronic changes by more than an order of magnitude for a 10°C increase in temperature.<sup>11, 12</sup> 2) While classical surfactants afford a rather limited variation of their hydrophobic and hydrophilic parts, pluronics allow adjustment of the hydrophobe/hydrophile (PPO/PEO) composition and total molecular weight to get a series of triblock copolymers called a Pluronic grid (Figure 1.2).<sup>13</sup> The molecular weights of Pluronics are typically in the range 2000 – 20,000 Da and their PEO compositions are in the range of 10 to 80%. On the vertical axis of Figure 1.2, moving up the grid indicates an increase in length of the hydrophobic (PPO) center blocks and moving right along the lateral axis indicates an increase in weight percentage of the hydrophilic (PEO) blocks. A certain minimum PPO block size is required for sufficient block segregation and subsequent expression of amphiphilic properties. Each copolymer in the grid is given a code with a letter to define its physical form at room temperature (L - liquid, P - paste, F - flake (solid)) followed by two or three digits. The first digit (or first two digits) indicates the length of PPO block. Multiplying this number by 300 gives the approximate molecular weight of the hydrophobic PPO block. The last digit indicates the mass fraction of PEO block. Multiplying this number by 10 gives the percentage of hydrophilic PEO block in the copolymer. For example, the Pluronic species with the code 'F127' remains as solid flakes ('F') at room temperature with a PPO molecular weight of approximately 3600 g/mol ('12' times 300), and is 70% by weight PEO ('7' times 10).

### **1.3. Micellization in Pluronics**

#### **1.3.1. CMC and CMT**

A micelle is an aggregation of surfactants in a selective solvent. Micellization (process of micelle formation) of PEO-PPO-PEO copolymers in water takes place above a critical micellization concentration (CMC) at constant temperature or above a critical micellization temperature (CMT) for a given concentration.<sup>11, 12, 14</sup> Both CMC and CMT are parameters of great fundamental value. The CMC or CMT of pluronics can be determined by a number of techniques such as dynamic light scattering (DLS),<sup>15-17</sup> differential scanning calorimetry (DSC),<sup>12, 16, 18, 19</sup> dye solubilization technique,<sup>16, 20</sup> surface tension method<sup>12</sup> and fluorescence spectroscopy.<sup>11, 21</sup> The unimer-to-micelle transition is not sharp, but takes place over a concentration of decade or temperature of 10 K due to the broad molecular weight distribution of these copolymers.<sup>10, 14</sup>

#### **1.3.2. Micellization mechanism**

The mechanism behind the micellization processes of Pluronics in water is the hydrophobic effect i.e. the principle preventing oil and water to mix in a liquid phase.<sup>22</sup> At low temperature both PEO and PPO blocks of Pluronics are hydrophilic and hence soluble in water. With increase in temperature, the PPO blocks become relatively hydrophobic while the PEO blocks remain hydrophilic. These hydrophobic PPO blocks aggregate with each other in order to dissipate the “ice-like shell” of water molecules formed around them to form micelles (Figure 1.3). The polymer chains that contribute to the micelles are always in dynamic equilibrium with the free polymer chains in the bulk.



Thermodynamics of micelle formation in pluronics has been studied by Alexandridis et al.<sup>11</sup> From differential scanning calorimetry (DSC) studies it is found that the micellization process is associated with large endothermic heat which is linearly dependent on the size of PPO block.<sup>12</sup> The endothermic heat is attributed to the dehydration of PPO blocks and it is called the heat of micellization ( $\Delta H$ ). Thermodynamically, this positive  $\Delta H$  indicates the transition from unimers to micelles is enthalpically disfavored. Nevertheless the enthalpy is overcome by the strong increase in entropy which arises from the dissipation of water molecules in the system. Therefore the micellization of PEO-PPO-PEO copolymers in water is an entropy driven process, and hence CMC values for the pluronics decrease sturdily with increase in the temperature.<sup>12, 15</sup>

### 1.3.3. Size and shape of micelles

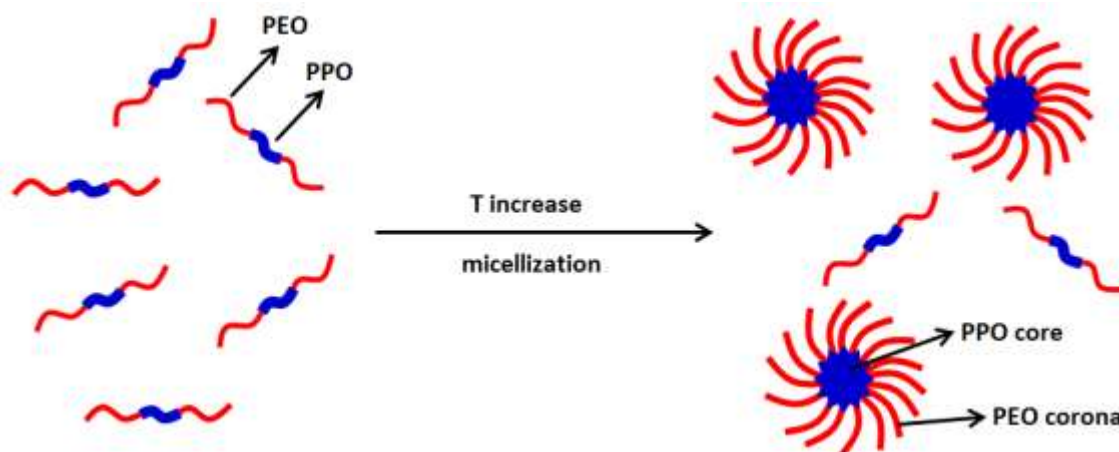


**Figure 1.3** Schematic representation of the association mechanism of PEO-PPO-PEO in water

The size and shape of micelles formed from the self-assembly of PEO-PPO-PEO block copolymers have been investigated by many researchers.<sup>12, 16, 23-</sup>

<sup>25</sup> Rassing and Attwood were the first to detect the spherical shape of Pluronic F127 micelles using light scattering technique.<sup>25</sup> Direct visualization of micelles<sup>26,</sup>  
<sup>27</sup> using cryogenic transmission electron microscope (Cryo-TEM) confirmed the spherical structure of micelles obtained by scattering techniques. The core of the micelles is assumed to be free of water, while the corona of the micelles is still hydrated. As a result the effective volume fraction of the micelles are 2 to 3 times greater than the actual volume fraction.<sup>12</sup>

The number of copolymer chains present in a micelle is called as aggregation number of the micelle. Both the aggregation number and the size of micelles are least affected by the concentration<sup>12</sup> while temperature has interesting effects on PEO-PPO-PEO micelles. With increase in temperature the aggregation number of the micelles increases due to the enhanced tendency of the unimers to separate from the solvent. This effect tends to increase the size of the micelles. However the rise in temperature also dehydrates the PEO corona of the micelles, reducing the size of the micelles. Such a dual effect of temperature keeps the hydrodynamic radius of Pluronic micelles to remain almost independent of temperature.<sup>15</sup> The polydispersity of the micelle size decreases with the temperature.<sup>16</sup> Effective concentration of the micelles also increase with temperature until all the unimers are part of micelles, or the volume fraction of micelles is so high that they form crystalline structure to form gel.<sup>23</sup>

The CMC and CMT values strongly depend on the structure and molecular weight of PEO-PPO-PEO copolymers.<sup>11</sup> For the copolymers with same hydrophilic (PEO) length, the copolymer with a larger hydrophobic (PPO)

domain form micelles at lower temperatures. For the copolymers with same hydrophobic (PPO) length, the CMT or CMC increases with the length of hydrophilic (PEO) blocks which indicates that the micelle formation becomes more difficult for the molecules with higher hydrophilic nature. However, the effect of PEO blocks is less pronounced when compared to the effect of PPO blocks on CMT or CMC and on the enthalpy of micellization ( $\Delta H$ ) which indicates that the hydrophobic (PPO) blocks are the primary factor in the micellization process. For the pluronics with same PPO/PEO ratio but different molecular weight, the copolymer with higher molecular weight form micelles at lower CMT or CMC.

#### **1.4. Gelation in Pluronic**

At higher concentrations ( $> 15\text{wt } \%$ ), PEO-PPO-PEO block copolymers in water form a variety of lyotropic liquid crystalline phases.<sup>28-30</sup> Cubic, hexagonal packed cylinder, lamellar, and bicontinuous cubic structures have all been observed. Owing to their finite yield stress which prevents them from flowing under their own weight, these are often termed as ‘gels’. However, the gel properties result from the ordered microstructure of the micelles and not from the cross linking between the polymer chains as seen in a conventional polymer gel.

##### **1.4.1. CGC and CGT**

The gelation in Pluronic takes place above a critical gelation concentration (CGC) at constant temperature or above a critical gelation temperature (CGT) for the given concentration. The parameter CGT is very vital in Pluronic since most of the applications bank on this sol-gel transition

temperature.<sup>7</sup> The onset of gelation can be characterized by techniques such as tube inversion technique<sup>31, 32</sup> and rheometer.<sup>32-36</sup>

#### 1.4.2. Gelation mechanism

The gels seen in PEO-PPO-PEO systems are due to the ordered microstructure of micelles.<sup>28-30, 33</sup> The gels are physical i.e. there exists no cross links which are found in conventional polymer gel. In the micellar regime, the volume fraction of the micelles increases with both temperature and concentration. When this volume fraction crosses the critical value of hard-sphere crystallization the system undergoes a transition from sol to gel state.<sup>30</sup> Figure 1.4 shows the clear gel seen in 20 wt% Pluronic F127 in water at 40°C.



**Figure 1.4** Clear gel formed in 20% Pluronic F127 at 40°C

#### 1.4.3. Structure and rheology of gel

The temperature induced gelation in Pluronic F127 is reflected in drastic increase in storage modulus.<sup>37</sup>  $G'$  approached a steady value after the formation of gel and this steady value increases with increase in polymer concentration.

Pluronics in unimer and in micellar state exhibit only Newtonian behavior.<sup>30</sup> The gel state of Pluronics shows shear thinning behavior.<sup>38</sup>

The lyotropic crystalline phases exhibit thermotropic behavior i.e. reversible transitions take place between different phases with increase in temperature. Alexandridis et al<sup>28</sup> studied the lyotropic liquid crystalline (LLC) phases of Pluronics L62, L64 and P105. They reported that the number of LLC phases and the thermal stability of the LLC phases increase with increase in PEO content and the M.W. of copolymers in the order L62 < L64 < P105. The impact of diblock (PEO-PPO) impurities that are present in the commercial Pluronics on the microstructure of Pluronic F127 is also reported in the literature.<sup>33</sup> F127 used as received from the chemical company BASF forms a face-centered cubic structure while the pure F127 (free from diblock impurities) forms a body-centered cubic structure.

Systems with storage modulus higher than loss modulus ( $G' > G''$ ) with  $G'$  exceeding 1 kPa are termed as hard gels. Soft gels also have  $G'$  greater than  $G''$  but  $G'$  stays below 1 kPa. Sol has very low storage modulus and  $G'' > G'$ ,<sup>31, 39</sup>. However, whether or not  $G'$  exceeds  $G''$  depends upon the choice of frequency, therefore a fixed frequency of 1 Hz has been used by Booth and coworkers to obtain consistent results.<sup>39</sup> The tube inversion technique has shown to give results in excellent agreement with hard gel boundary obtained from rheometry and has been used to prepare gel phase diagrams for a number of systems. However the tube inversion technique cannot determine the soft gel boundary since soft gels flow when the tube is tilted owing to their low yield stress (< 40Pa).

### 1.5. Applications of Pluronics

The ability of pluronics to form thermoreversible micelles and gels has created substantial interest in their use in pharmaceutical applications. The self-assembly of block copolymer melts is also used to produce well-ordered nanostructured templates with domain spacing of ~10nm for electronic applications.<sup>40-</sup><sup>42</sup> Many excellent reviews are available describing the pharmaceutical applications of Pluronic block copolymer micelles and gels.<sup>7, 8, 43, 44</sup> Pluronic copolymers have led to increased solubilization of hydrophobic drugs and prolonged drug release profiles for ophthalmic,<sup>45, 46</sup> rectal,<sup>47, 48</sup> topical,<sup>49, 50</sup> and injectable<sup>51, 52</sup> purposes. However, Pluronics in pharmaceutical field are mostly used in combination with other excipients (eg. cross linked PAA) to optimize the rheological (gel strength, gelation time, CGT), solubilization, and bio-adhesive properties.<sup>7, 53, 54</sup> In lithographic applications, additional homopolymers or small molecules are often blended with Pluronics to enhance their microphase segregation. These additions can also be used to alter the domain spacing and morphology without a need for synthesis of new block copolymers.<sup>40, 55</sup>

### 1.6. The role of additives

Studies on the effect of additives on the surfactant behavior of Pluronics are essential for two main reasons. 1) Suitable additives can be used to tune the properties of Pluronics to match the particular needs of a specific application. For instance, the gel strength of F127 can be modified by adding inorganic salts and organic solvents, thereby influencing the drug release rate of the gel.<sup>56, 57</sup> 2) The presence of third component whose intended role is different from the Pluronics

in the same product formulation may change the desired properties of Pluronics. Therefore an in-depth knowledge on the role of various relevant additives on the behavior of Pluronics is crucial in order to engineer an optimized formulation.

Commonly studied additives on the sol-gel behavior of Pluronics are inorganic salts, solvents (methanol, ethanol, etc.) and classical surfactants (SDS, TTAB, CTAB, etc.). These components are often present in drug delivery formulations in order to improve the solubility of active compounds and also to tune the other relevant properties.

### **1.6.1. Effects of salts**

Addition of salts having anions and cations of different sizes and polarizabilities, resulted in either an increase or decrease in cloud point of the micelles.<sup>58</sup> The onset of micelle formation was also shifted in the same direction as the cloud points but to a relatively lesser degree.<sup>10, 59</sup> The mechanism was discussed in terms of the salt's effect on the structure of water. For instance, the decrease of CMT and cloud point in the presence of NaCl is attributed to a decreased hydration of copolymer chains due to an increase of water structure. NaSCN (sodium thiocyanate), a water structure breaker, was found to increase the CMT.<sup>60-62</sup> The presence of sodium chloride also decreased the gelation temperature and increased the gel strength of Pluronic F127.<sup>63</sup>

### **1.6.2. Effects of solvents**

Most commonly studied solvents with Pluronics are methanol, ethanol and butanol.<sup>19, 35, 36</sup> Methanol and ethanol delay the onset of micellization and

suppress the micelle formation in Pluronics. Propanol and butanol favor the micellar aggregates resulting in advancement of the onset of micelle formation. The effects of these solvents are also explained in terms of their effect on the water structure. Methanol and ethanol act as water structure breaker and hence result in increased Pluronic solubility while butanol acts a water structure maker resulting in decreased solubility of Pluronics. The sol-gel boundary of F127 is least disturbed in the presence of ethanol concentrations of 10 to 20 wt% but it is much increased when the ethanol concentration is 30 wt%.

### **1.6.3. Effects of classical surfactants**

The effects of cationic surfactant tetradecyltrimethylammonium bromide (TTAB) and anionic surfactant sodium dodecyl sulfate (SDS) have been comprehensively investigated.<sup>17, 18, 64-68</sup> The studies include isothermal titration calorimetry (ITC), light scattering, differential scanning calorimetry (DSC) and small angle neutron scattering (SANS). The following sequence of events is reported upon addition of SDS to Pluronics at a concentration well above the copolymer CMC. At low SDS concentration, SDS binds to copolymer micelles to form mixed micelles. The binding is reasoned due to the hydrophobic interactions between copolymers and the SDS molecules. Further addition of SDS leads to breakdown of these copolymer micelles followed by the binding of SDS molecules directly onto unassociated Pluronic unimers, forming a unimer Pluronic + micellar SDS complexes. The SDS binds to the hydrophobic PPO blocks of copolymer, reducing their hydrophobicity and therefore enabling them to remain not aggregated in solution. The CMT of F127 is also reported to be slightly



decreased in the presence of SDS. This may possibly be due to the action of SDS as 'nuclei' for the formation of copolymer micelles close to the micellization point. With increase in SDS concentration the breakdown of copolymer micelles also leads to the reduction of the gel region in Pluronics.

## **1.7. Motivation**

Significant research on Pluronics over the past two decades has now led to clear understanding of both micellization and gelation processes in Pluronics. In the present decade there exists a rapidly growing body of work that studies the use of Pluronics in pharmaceutical and in other scientific fields. However, bulk of these studies focus on the application of these Pluronics and their efficiency in pharmaceutical, therapeutic and lithographic applications. Relatively little is known about the changes that the relevant additives bring to the micellization and gelation behaviour of the Pluronic surfactants, and their underlying mechanisms. For the additives such as salts, solvents and classical surfactants, even though the underlying mechanisms are still debatable their impacts on the sol-gel behavior of Pluronics are well documented. But investigation on the impacts of polymeric additives is scarce in the literature.

### **1.7.1. Effects of poly(ethylene oxide)**

Poly (ethylene oxide) homopolymer (PEO) of sufficient molecular weight is reported to suppress the gelation in Pluronics. Gilbert et al.<sup>69</sup> were the first to report the rise in CGT of F127 in the presence of PEO homopolymer with molecular weight of 2k, 10k and 20k g/mol based on tube inversion method. A similar finding for gelation suppression using rheometry<sup>32</sup> was later documented

along with a decrease in storage modulus.<sup>70</sup> It was also reported that the solubility of hydrophobic drug in F127/water system can be increased by addition of a small amount of PEO.<sup>71</sup> For PEO with  $MW \leq 1000$  g/mol, however, the CGT of F127 was found to decline in the study by Zhang et al.,<sup>72</sup> where PLGA-PEO-PLGA was the main copolymer in their investigation with PLGA denoting poly(lactic acid-co-glycolic acid). They proposed and addressed several mechanisms to account for the experimentally observed effect of PEO. Despite the existence of the aforementioned gelation studies, there exists only scarce investigation on the micellization and its correlation with gelation of F127 in the presence of PEO. Only in a very recent work, did Ricardo et al.<sup>70</sup> use dynamic light scattering to measure the micelle size of F127 with added PEO (MW = 6k and 35k) along with gelation examination by rheometry and small angle X ray scattering. They reported an increase in micelle size and a face-centered cubic structure of the formed gels.

From the aforementioned discussion, it is seen that the existing studies have reported the loss of gelation in F127 in the presence of PEO of sufficient molecular weight. However the literature lacks any studies on the impact of PEO on micellization properties such as CMT and  $\Delta H$  (enthalpy heat of micellization) of Pluronics. In addition the underlying mechanism for the loss of gelation is also unclear. As a part of this thesis work, a comprehensive study on the micellization behavior of F127/PEO/water is carried out and a greater understanding in the loss of gelation is established (Chapter 3).

### 1.7.2. Effects of poly(acrylic acid)

Recently, Carbomers (cross linked poly acrylic acid (PAA) polymers) combined with F127 are used as an ‘*in situ* temperature sensitive hydrogel’ for ophthalmic drug delivery.<sup>8, 53</sup> While Carbomer is added to improve the mucoadhesive property of F127 it could also alter the other desired properties such as CMT, enthalpy of micellization ( $\Delta H$ ), CGT and gel strength of F127. Since the above mentioned properties are very crucial in ophthalmic drug delivery or as such in any other applications, sound knowledge on the influence of PAA homopolymer on these properties and their interaction with F127 are of utmost importance. In the dilute regime, light scattering studies<sup>73, 74</sup> witnessed large sized complexes for the system Pluronic/PAA/H<sub>2</sub>O. The only previous study on the concentrated regime of Pluronic/PAA/H<sub>2</sub>O system is by Dos Santos<sup>75</sup> et al., who studied the effect of PAA on liquid crystalline phases formed in concentrated aqueous Pluronic P104 using small angle X-ray scattering (SAXS). They found that the ordered structures in the P104/H<sub>2</sub>O systems are destroyed by the addition of PAA.

While the size analysis in dilute regime and microstructure analysis in concentrated regime are reported, the literature lacks any information on micellization and gelation behavior such as the variation of CMT, enthalpy of micellization ( $\Delta H$ ), CGT, gel rigidity ( $G'$ ) and thermoreversibility of pluronics in the presence of PAA. As a part of this thesis work, the micellization and gelation behavior of Pluronic/PAA/H<sub>2</sub>O system are explored for the first time (Chapter 4).

The obtained results might shed light on how to design a F127/PAA hydrogel with desired drug loading capacity and sol-gel transition temperature.

### 1.7.3. Mixed PEO-PPO-PEO copolymers

Micellar stability, drug loading capacity, micelle size and distribution are important characteristics for effective use of the polymeric micelles as drug delivering carriers.<sup>76</sup> Only limited copolymers are being used in drug carrying applications because they can meet requirements. Although Pluronics have been extensively studied for their potential use in drug delivery, they have not found wide commercial application for drug solubilization purpose, primarily because of their low drug loading capacity.<sup>43</sup> For Pluronics, more hydrophobic species have a high drug loading capacity but a poor stability, while the behavior is reversed for more hydrophilic ones.<sup>43</sup> Therefore, mixing two Pluronic copolymers with different block lengths to form mixed micelles could be a promising solution to this problem.<sup>43, 77</sup>

In general, for a mixture of two block copolymers, the micelles can be any of the two types: (1) mixed micelles containing both polymer species, and (2) two separate families of micelles each incorporating only one polymer species (separate or pristine micelles). Formation of mixed micelles was reported for the mixture  $EO_{99}-PO_{69}-EO_{99} + EO_{45}-BO_{14}-EO_{45}$  by Liu et al.<sup>78</sup> and for the mixture  $EO_{135}-BO_{20}-EO_{135} + EO_{82}-SO_9-EO_{82}$  by Nagila et al.,<sup>79</sup> where BO and SO represent butylene oxide and styrene oxide, respectively. As stated in the latter work, the hydrophobicity of BO block is estimated to be 5-6 times that of a PO block while the hydrophobicity of SO block is twice that of BO block. Separate

micelles were reported for the mixture  $\text{EO}_{62}\text{-PO}_{39}\text{-EO}_{62} + \text{EO}_{45}\text{-BO}_{14}\text{-EO}_{45}$  by Harrison et al.<sup>80</sup>

It can be found from these studies that the mixture of copolymers with similar hydrophobicity most likely forms mixed micelles, although the hydrophobic blocks could be different in length and chemical structure. Therefore for Pluronic copolymers, mixtures with similar PPO block lengths are expected to form mixed micelles since they have equivalent hydrophobicity. This has indeed been verified using light scattering.<sup>31</sup> For the mixtures with different PPO block lengths or hydrophobicity, there exist different claims on the nature of micelles. Gaisford et al.<sup>81</sup> used a UV spectrometric method to find that mixtures F77+F127 and F87+F127 with dissimilar PPO block lengths exhibited two different CMT values. This observation led them to claim separate micellization for those having dissimilar PPO block lengths. Very recently, Zhang et al. used differential scanning calorimetry (DSC) to detect two endothermic peaks for the system F127+F68 with dissimilar PPO block lengths, and interpreted this finding as a result of separate or independent micellization.<sup>82</sup> Having similar observation in an early study on P105+L64 with different PPO block length,<sup>83</sup> Zhou et al., on the contrary, speculated otherwise without further investigation because structural analysis was the main focus in their study.

The literature outlined above indicates that further investigations are required to unravel the nature of micelles in Pluronics with dissimilar PPO block lengths. Moreover, there are very few studies on gelation behavior of mixed Pluronics.<sup>31, 84</sup>

As a part of this thesis work, the micellization and gelation behavior of two Pluronic mixtures (F127 + L64 and F127 + P05) of different PPO block lengths are studied in detail (Chapter 5).

#### **1.7.4. Effects of polymeric additives on corn starch suspension**

Shear thickening suspensions are those who show increase in viscosity with shear stress/rate.<sup>85-87</sup> These suspensions at low stresses can flow freely like any other normal liquid. When the fluid encounters a sudden stress they can solidify (rapid increase in viscosity) almost instantly. In recent times, this impact hardening property of these suspensions is of great interest for scientists to make liquid armor such as flexible bullet proof jackets, bomb blankets, jump boots, etc.<sup>88-91</sup> The effects of particle concentration, size, size distribution, shape and continuous phase viscosity on the shear thickening property are well documented in the literature.<sup>86, 87, 92</sup> The hardening/solidification process of these suspensions is triggered by the high stress/impact.

Corn starch (CS) in water is often used to demonstrate the shear thickening behavior in classrooms owing to its easy availability and low cost. CS suspensions have also been used by researchers<sup>87, 92-95</sup> to probe the shear thickening mechanism. Though a significant number of studies have used CS/H<sub>2</sub>O suspension to study the different characteristics of shear thickening effect, the rheology of CS suspension has not been studied by modifying the composition of the continuous phase or by the adding polymers to the suspension. As a part of this thesis work, the shear thickening behavior of corn starch (CS)/H<sub>2</sub>O suspension with a block copolymer Pluronic F127, a homopolymer PEO and a

solvent PEG200 will be studied (Chapter 6). The idea behind adding Pluronic is to impart the temperature triggered viscosity increasing ability of F127 to the shear thickening suspension (corn starch suspended in water) to see if the shear thickening is enhanced or not.

## 1.8. Objectives

Whether it is the micellization/gelation aspect in aqueous medium for pharmaceutical applications or the structural ordering aspect for electronic applications, a sound understanding of the self-assembly behavior and interaction of Pluronics with the relevant additives is of utmost importance. The objective of this thesis is to advance the understanding of the sol-gel behavior and rheology of Pluronic/H<sub>2</sub>O system in presence of non-ionic homopolymer (PEO), ionic homopolymer (PAA), other Pluronics with different hydrophobic block length (Pluronics L64 and P105) and particle (corn starch). Pluronic 'F127' will be used in particular, because of its high stability, bio-adhesive characteristics, thermoreversible gelling ability at room temperature and non-toxic properties, which makes it a suitable vehicle for drug formulations.<sup>7, 13, 96</sup> The research described in this thesis, specifically, aims to meet the following objectives:

**Objective 1:** To investigate the effect of PEO chain length on micellization and gelation of Pluronic F127 (Chapter 3)

The goal here is to investigate the micellization of F127/PEO/H<sub>2</sub>O system in a wide range of PEO molecular weight (200-35k g/mol). This would shed more

light on the mechanism behind the loss of gelation in F127 in presence of PEO reported in the literature as discussed earlier. The focus is placed on the effects of chain length and concentration of PEO on CMT,  $\Delta H$ , micelle size, CGT, gel strength and thermoreversibility of F127. We intend to examine the effects of PEO addition on the self-assembly behavior and microstructure, and seek the correlation between micellization and gelation.

**Objective 2:** To investigate the effect of PAA on micellization and gelation of Pluronic F127 (Chapter 4)

In this work, the aim is to investigate the micellization and gelation behavior of F127/PAA/H<sub>2</sub>O system for the first time. The focus is placed on the effects of pH, concentration and molecular weight of linear PAA on CMT,  $\Delta H$ , CGT, gel strength and thermoreversibility of F127. This study herein might shed light on how to design a F127+PAA hydrogel with desired sol-gel properties to be used in ocular drug delivery applications and could possibly be extended to other applications as well.

**Objective 3:** To examine the sol-gel behavior of Pluronic binary mixtures of different hydrophobic block lengths in aqueous medium (Chapter 5)

The aim of this work is to examine the micellization and gelation of mixed Pluronics with different hydrophobic block lengths in aqueous medium. We study the two mixtures F127+P105 and F127+L64 (F127: EO<sub>98</sub>PO<sub>67</sub>EO<sub>98</sub>; P105: EO<sub>37</sub>PO<sub>56</sub>EO<sub>37</sub>; L64: EO<sub>13</sub>PO<sub>30</sub>EO<sub>13</sub>) for the following reasons: (1) the CMT values of parent Pluronics are very close to each other in F127+P105, but far apart



in F127+L64, allowing us to study the effect of CMT difference on the self-assembly, (2) the parent Pluronics in each of the two mixtures form spherical micelles with different sizes, discernable by DLS, and (3) the properties of these Pluronics fall in the range that can be conveniently characterized by various characterization techniques.

**Objective 4:** To examine the effect of Pluronic F127, PEO homopolymer and a binary solvent (PEG200:H<sub>2</sub>O) on the rheology of corn starch (CS) suspension (Chapter 6)

The aim of this work is to examine the influence of block copolymer F127, homopolymer PEO and solvent PEG200 on the rheology of CS suspension. The focus is placed on the effects of F127 concentration and temperature on the shear thickening behavior of suspension. The effects of PEO concentration and molecular weight will also be investigated. We intend to elucidate the mechanisms behind the observed changes in the rheology of CS suspension.

## 1.9. Thesis organization

This thesis is organized as follows. Chapter 1 introduces the research background for block copolymer self-assembly and the role of additives. The objectives and the scopes of this research work have also been pointed out. The materials and methods will be described in Chapter 2. Chapter 3 presents the results and discussion for the study of interaction between poly (ethylene oxide) homopolymer and Pluronic F127. Chapter 4 describes the effects of pH,

concentration and molecular weight on the interaction behavior of poly (acrylic acid) and Pluronic F127. Micellization and gelation behavior of Pluronic binary mixtures will be presented in Chapter 5. Chapter 6 will focus on discussing the effect of Pluronics and poly (ethylene oxide) on the rheology of corn starch suspensions. Finally, Chapter 7 concludes the thesis and gives some recommendations for future work.

## 2. Materials and Methods

---

### 2.1. Materials

#### 2.1.1. Pluronic triblock copolymers

Pluronic F127, F68, L64 were purchased from Sigma Aldrich and Pluronic P105 was obtained from BASF as a gift. Pluronics were used as received without any further purification. Pluronic has a chemical formula as shown in Figure 2.1.

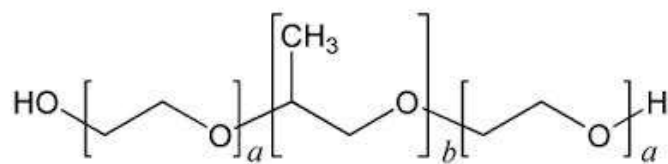


**Figure 2.1** Chemical structure of PEO-PPO-PEO (Pluronic)

#### 2.1.2. Poly(ethylene oxide)

Poly (ethylene oxide) (PEO) with repeating unit molecular structure as illustrated in Figure 2.2 is a non-ionic homopolymer. PEO from Sigma Aldrich with an average of molecular weight of 200, 600, 1k, 1.5k, 2k, 10k, 20k, 35k, 100k, 400k g/mol were used as received.

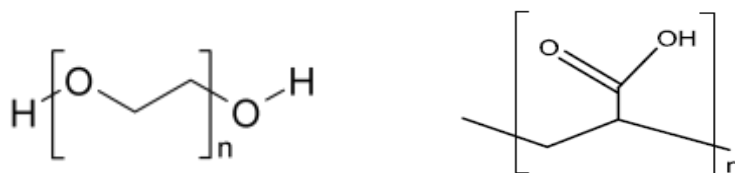


**Figure 2.2** Chemical structure of PEO (left) and PAA (right)

### 2.1.3. Poly(acrylic acid)

Poly (acrylic acid) (PAA) with repeating unit molecular structure as illustrated in Figure 2.2 is a weak polyelectrolyte. When dissolved in water, carboxylic acid groups of PAA will lose their protons and acquire a negative charge. PAA is highly sensitive to the changes of pH. At pH 6.5 or above, it becomes almost completely dissociated and highly charged in the solution. PAA from Sigma Aldrich with an average of molecular weight of 1.8k g/mol and 450k g/mol were used as received.

### 2.1.4. Corn starch

Corn starch (CS) particle suspension in water is often used to demonstrate the shear thickening behavior in class rooms owing to its easy availability and low cost. CS particles are non-Brownian particles with an average diameter of 15  $\mu\text{m}$ . The hydroxyl groups on the surface render hydrophilic nature to the CS particles. CS particles were purchased from Sigma Aldrich and used as received. The FESEM images of CS particles are shown in Figure 2.3.

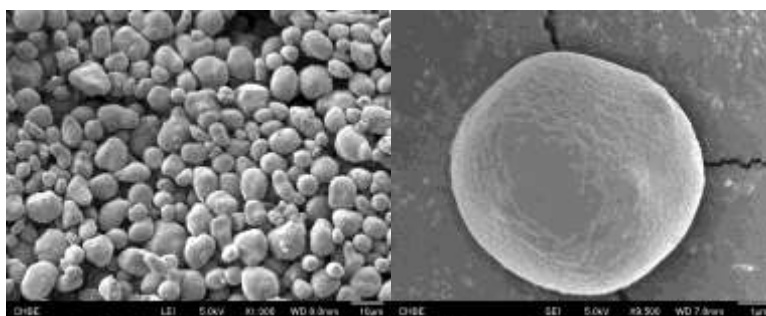


**Figure 2.3** FESEM images of corn starch granules

### **2.1.5. Others**

High purity sodium hydroxide pellets (NaOH), hydrochloric acid fuming 37% (HCl), chloroform (analytical reagent grade), ethanol (ACS grade) and methanol (ACS grade) were purchased from Merck. 1,6-Diphenyl-1,3,5-hexatriene (DPH) with  $\geq 97.5\%$  purity was purchased from Fluka. Propionic acid (ACS grade), glycerol ( $\geq 99.5\%$ ), deuterium oxide (99.9 atom % D), and DMSO ( $\geq 99.5\%$ ) were purchased from Sigma Aldrich. Deionized water with a resistivity of  $18 \text{ M}\Omega\cdot\text{cm}$  was obtained from a Pure Lab Maxima water purification system (ELGA). All glassware was cleaned, and rinsed thoroughly with deionized water prior to use.

## **2.2. Sample Preparation**

### **2.2.1. Preparation of pluronic solution**

Poly (ethylene oxide) or poly (acrylic acid) solutions with appropriate concentrations were first dissolved in Millipore water at room temperature. The samples were then gently stirred for 24 hours. The solution was allowed to stand for 24 hours to attain equilibrium. An appropriate amount of Pluronic copolymer was dissolved in Millipore water or in an appropriate weight percentage of PAA or PEO solution by cold method.<sup>13</sup> The solutions were allowed to stand below  $5^\circ\text{C}$  for 24 hours for dilute samples and for 3 days for concentrated samples prior to any experiment to remove air bubbles and to achieve equilibrium. All the samples were prepared in weight to weight percentages (w/w %). For Pluronic solutions with varying pH value, an appropriate amount of HCl or NaOH was

slowly added to the solution, stirred and measured using a pH meter. This procedure was repeated until the desired pH value was obtained. pH was controlled in one direction only.

### **2.2.2. Preparation of particle suspension**

Appropriate amount of polymer (Pluronic or PEO) is added to Millipore water and stirred for 24 hours followed by equilibration time of 24 hours. Suspensions (wt/wt %) were then prepared by adding appropriate amount of corn starch (CS) particles in DI or in an appropriate weight percentage of Pluronic or PEO solution. The suspension is hand stirred initially for 2 minutes followed by magnetic stirring for 15 minutes. Subsequently the suspension is left alone in the room temperature for 10 minutes to relax.

## **2.3. Equipment**

### **2.3.1. Dynamic light scattering (DLS)**

DLS has been used for two purposes in this work; one is to measure the hydrodynamic size of the Pluronic micelles while the other is to find the CMT of Pluronic samples. The hydrodynamic diameter of a polymeric micelle is calculated from the translational diffusion coefficient by using the Stokes-Einstein equation. The average hydrodynamic diameter and size distribution of micellar samples were determined using Zetasizer Nano ZS (Malvern), which applies back scattering (detection angle of  $173^\circ$ ) to measure the intensity-weighted size distribution. In back scattering technique, the laser does not pass through the

entire sample and because the scattered light passes through a shorter path length, multiple scattering effects is reduced allowing us to study the much higher concentrated samples.<sup>97</sup>

CMT of Pluronics at low concentration can be characterized by light scattering method since the unimer-micelle transition will cause a significant increase in the scattering intensity and size.<sup>16</sup> Prior to measurements, samples were filtered through 0.45  $\mu\text{m}$  Millipore syringe filter to prevent any dust particles from affecting the results. The temperature was controlled using a Peltier unit system with an accuracy of  $\pm 0.1^\circ\text{C}$  at  $25^\circ\text{C}$  and  $\pm 0.5^\circ\text{C}$  at  $90^\circ\text{C}$ . A waiting time of 10 to 20 min at an appropriate temperature was allowed prior to any experiment.

### **2.3.2. Differential scanning calorimetry (DSC)**

DSC is a powerful tool to characterize the CMT and the heat of micellization ( $\Delta H$ ) of Pluronic samples since micellization in Pluronic/ $\text{H}_2\text{O}$  system involves endothermic heat.<sup>12, 16</sup> Thermogram (output of the DSC) is the difference in heat energy that is required to maintain the sample and the reference at the same temperature. DSC experiments were performed using a Mettler Toledo DSC822 differential scanning calorimeter. An aluminum crucible was filled with 20 to 30 mg of the sample, and an empty crucible was used as the reference. Samples are carefully loaded in the crucible to prevent any air bubbles. Temperature scans were performed from 0 to 30 (or)  $50^\circ\text{C}$  at a rate of  $2^\circ\text{C}/\text{min}$ .

### 2.3.3. UV-visible spectrophotometer

A Shimadzu UV-3600 spectrophotometer has been used to determine the CMT and CMC of the Pluronics using dye solubilization technique. A stock solution of 0.7 mM DPH in methanol was prepared. 25  $\mu$ L of the DPH/methanol solution was added to 3g of the sample so that the final solution contained about 0.004 mM DPH and 1% v/v methanol.<sup>11, 98</sup> The same DPH concentration (0.004mM) was used for all samples. The solutions were left in the dark to equilibrate for at least 3 h (and no more than 24 h) before the spectroscopic measurement. UV-Vis absorbance spectra were measured in the range of 320-400 nm. The hydrophobic dyes DPH will show high absorbance at 356nm when dye molecules are solubilized into a hydrophobic environment, such as the hydrophobic core of a pluronic micelles.<sup>11, 98</sup> Temperature was controlled using thermo-electrical temperature controller (CPS 240A) with a precision of  $\pm 0.1^{\circ}\text{C}$ . A waiting time of 15 min at an appropriate temperature was allowed prior to any experiment.

### 2.3.4. Fourier transform infrared (FTIR) spectroscopy

FTIR spectra were obtained from Shimadzu FTIR-8400 spectrophotometer to study the hydrogen bonding between the CS particles and the polymers in water. The spectra were recorded using 60 scans of 2  $\text{cm}^{-1}$  resolution in the spectral range of 400 - 4000 $\text{cm}^{-1}$ . Appropriate amount of CS particles were added to polymer aqueous solution, stirred well and one mL of the suspension was dropped onto a flat plate. The sample on the flat plate was left at 60 $^{\circ}\text{C}$  for 24 hours to remove the water content. The dried sample was pelletized along with KBr and



then taken to FTIR spectroscopic studies. All the measurements were made at room temperature.

### 2.3.5. Rheometer

Haake (Rheo Stress 600) rheometer with cone and plate geometry (C60/4, diameter 60 mm and angle 4°) and TA (AR G2) rheometer with cone and plate geometry (C60/1, diameter 60mm and angle 1°) were used to characterize the rheological properties. A Peltier controller unit was used to control the temperature of the sample with an accuracy of  $\pm 0.1$  °C. In this work, rheometer has been used to characterize the following properties: shear flow curve ( $\eta$  vs.  $\tau$ ), yield stress ( $\tau_0$ ), critical gelation temperature and moduli ( $G'$  and  $G''$ ).



**Figure 2.4** Image of rheometer AR G2 with cone and plate geometry (left) and with the solvent trap (right)

A thin layer of silicone oil was applied to some samples, which required long measurement time, to prevent the solvent evaporation in Haake rheometer. For the C60/4 fixture (cone diameter and angle are 60 mm and 4°), a gap distance of 0.1355 mm was fixed to carry out the measurements. This makes sure a constant shear rate at all points within the material, which is the most interesting feature of this geometry. A sample volume of 4 ml was used. Sample loading has been done carefully to ensure the space between the cone and the plate is just filled up, without any spilling. All measurements were repeated three times for each sample.

#### **2.3.6. Tube inversion technique and cloud point (CP) measurements**

The CGT of Pluronic samples were determined using tube inversion technique in order to make comparison with that inferred by rheometry. Capped glass vials with 5ml of samples were placed in the water bath equipped with a digital temperature controlled unit with precision of  $\pm 0.1^{\circ}\text{C}$ . Temperature was increased at a constant rate of  $0.5^{\circ}\text{C}/\text{min}$  (unless specified) and the sample was allowed to equilibrate for 10 minutes at each step. The temperature at which turbidity is visually observed against black background is taken as the cloud point (CP). For the CGT, the test tube is tilted by  $90^{\circ}$  to check if the sample can flow or not. The temperature at which the sample stops flowing is taken as gelation point.

#### **2.3.7. Nuclear magnetic resonance (NMR)**

NMR measurements were carried out on Pluronic samples to observe the possible changes in the Pluronic structure in presence of polymeric additives. Measurements were performed on a Bruker DRX 500 operating at 500 MHz for

proton spectra and 125 MHz for carbon spectra. For NMR analysis alone, Pluronic samples were prepared in deuterium oxide (D<sub>2</sub>O). Replacement of H<sub>2</sub>O by D<sub>2</sub>O does not affect the aggregation behavior of pluronics.<sup>12</sup> The temperature was controlled using a Bruker temperature control unit, and the samples were equilibrated at their respective temperatures for 15 min before every measurement.

### **2.3.8. Small angle X-ray scattering (SAXS)**

SAXS analyses were performed to characterize the liquid crystalline phases of Pluronic samples. SAXS profiles were obtained using a Bruker AXS GmbH with a VANTEC-2000 detector. Each sample was injected into a capillary tube and sealed before placed in the vacuum system. Temperature was controlled using a TCPU sample stage with a peltier ( $\pm 0.1^\circ\text{C}$  precision). Scattering patterns were monitored over a q-range from 0 to 0.5 Å<sup>-1</sup>. Waiting time of 15 min at appropriate temperature was allowed prior to any experiment.

### **2.3.9. Optical microscopy**

Leica DML microscope was used to obtain microscopic images of corn starch (CS) suspensions in polymer solution. The dense CS suspensions were diluted to 1 wt% for microscopic analysis. Micrographs were obtained using Leica DFC 310 FX camera imaging system. All the experiments were carried out at room temperature.

### **2.3.10. Polarized light microscopy (PLM)**

Samples were examined for birefringence using a Nikon polarizing microscope with a hot stage temperature controller. A small drop of sample at temperature lower than 5°C was sandwiched between glass plates to ensure its liquid state upon loading. Then the temperature was increased to the desired value, during which the sample was not disturbed to prevent any unwanted orientation birefringence effect. A waiting time of 20 min at appropriate temperature was allowed prior to any experiment.

### **2.3.11. Cryogenic transmission electron microscopy (Cryo-TEM)**

Cryo-TEM was used to visualize the arrangement of micelles in Pluronic samples. Cryo-TEM micrographs were obtained using a Jeol JEM 2010F. Samples were prepared in the way mentioned by Lam et al.<sup>26</sup> and were maintained at 30 °C before they were frozen. 3 µL of the sample was pipetted onto the grid maintained at high humidity in the FEI Vitrobot Mark IV. A blotting time of 5–10 s was used before the grid was plunged into liquid ethane. The sample was then transferred to the cryo-TEM using a Gatan cryoholder to keep the sample frozen.

### 3. Effect of Poly (ethylene oxide) on Sol-Gel Behavior of Pluronic F127

---

In this chapter, first of all, relevant literatures on the effect of polyethylene oxide (PEO) homopolymer on PEO-PPO-PEO block copolymers are reviewed. The present study is aimed to better understand the mechanism behind the loss of gelation behavior of Pluronic triblock copolymers in presence of PEO. Experimental in this section has been designed by investigating the interaction in mixtures of PEO and Pluronic F127 for a wide range of PEO molecular weight (200 - 35k g/mol) using dynamic light scattering (DLS), differential scanning calorimetry (DSC), rheometry, Cryogenic-TEM and NMR spectroscopy. The interesting interaction mechanisms between F127 and PEO homopolymer will be elucidated and proposed in this chapter.

#### 3.1. Introduction

Gilbert et al.<sup>69</sup> were the first to report the rise in critical gelation temperature (CGT) of F127 in the presence of PEO homopolymer with molecular weight (MW) of 2k, 10k and 20k g/mol based on tube inversion method. A similar finding for gelation suppression using rheometry<sup>32</sup> was later documented along with a decrease in storage modulus.<sup>70</sup> For PEO with  $MW \leq 1k$  g/mol, however, the CGT of F127 was found to decline in the study by Zhang et al.<sup>72</sup>, where PLGA-PEO-PLGA was the main copolymer in their investigation with PLGA denoting poly(lactic acid-co-glycolic acid). They proposed and addressed several mechanisms to account for the experimentally observed effect of PEO. Despite

the existence of the aforementioned gelation studies, there exists only scarce investigation on the micellization and its correlation with gelation of F127 in the presence of PEO. Only in a very recent work, did Ricardo et al.<sup>70</sup> use dynamic light scattering to measure the micelle size of F127 with added PEO (MW = 6k and 35k) along with gelation examination by rheometry and small angle X ray scattering. They reported an increase in micelle size and a face-centered cubic structure of the formed gels.

To seek insight on the underlying mechanisms, micellization and gelation of F127 with addition of PEO homopolymer in a wide range of molecular weight (200 - 35k g/mol) is investigated in this study. The focus is placed on the effects of chain length and concentration of PEO on critical micellization temperature (CMT), micelle size, CGT, gelation time and gel strength. The intention is to explore how the added PEO affects the self-assembly behavior and microstructure, and seek the correlation between micellization and gelation.

## **3.2. Results and discussion**

### **3.2.1. Critical gelation temperature (CGT)**

Critical gelation temperature (CGT) can be determined by different methods, and the result can slightly vary from one method to another.<sup>99</sup> In this study, the crossover between the storage and loss moduli ( $G'$  and  $G''$ ) obtained from oscillatory temperature sweep (1Hz & 2Pa) in the linear viscoelastic regime is taken as CGT.<sup>100, 101</sup> To illustrate the sharp change in mechanical properties

upon gelation, plot the complex modulus  $G^*$  against the temperature for F127 without and with added PEO is plotted in Figure 3.1. For high MW PEO (2k - 35k), the gelation is delayed to a higher temperature and the extent of this delay is higher for larger MW of PEO. This behavior is in good agreement with that reported in the literature.<sup>32, 69</sup> For PEO of lower chain length (MW = 200-1k), 1% PEO did not make noticeable changes to the CGT. However, at higher concentration (8%) CGT is decreased slightly, and the decline is more for lower molecular weight (see Figure 3.1). The estimated CGT is presented in Table 3.1 and 3.2 to show the effects of PEO MW and concentration, respectively.

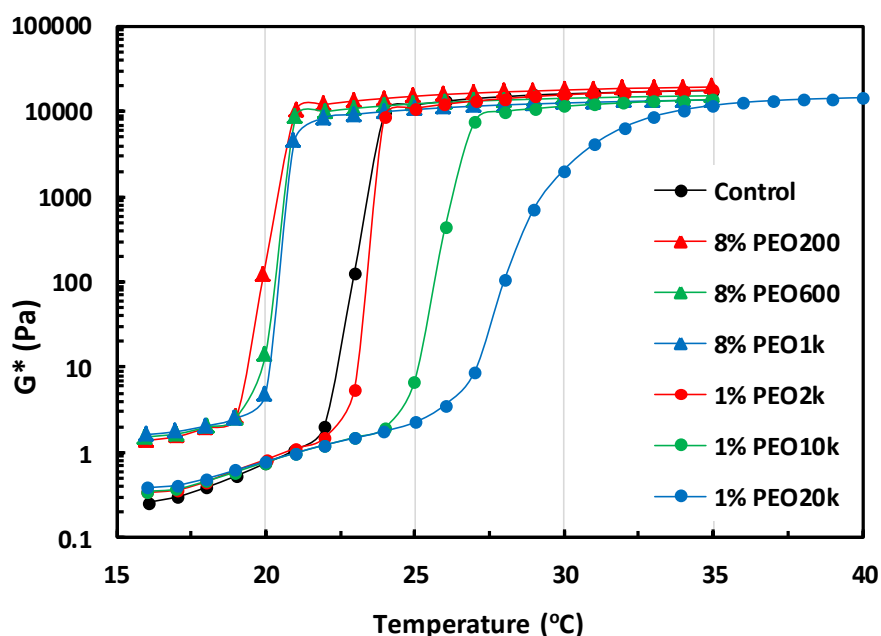


**Figure 3.1** Effects of molecular weight of PEO on gelation of F127/water system; F127 conc. = 20 wt%

Our finding contradicts the behavior reported by Zhang et al.<sup>72</sup> that the extent of CGT decline increases with PEO MW based on tube inversion. To check if the discrepancy arises from different methods to determine CGT, tube inversion

method was also carried out and included the results in parentheses in Table 3.1 for comparison. As seen, the trend remains unchanged although the CGT is slightly lower for each case. The higher CGT by rheometry is due to the temperature ramp speed.<sup>99</sup> Based on this finding of different trends for CGT, the PEO studied in this work is classified into two classes (A and B) as shown in Table 3.1 and 3.2. The deviation of CGT from the value of the pure F127 solution always increases with increasing PEO concentration, regardless of the class (see Table 3.2). But it generally requires a higher concentration for class A to see a noticeable deviation than for class B.

**Table 3.1** Effects of molecular weight of PEO on CGT,  $t_{gel}$ ,  $\tau_{co}$  and  $G_0'$  of 20% F127

	<b>PEO MW (g/mol)</b>	<b>CGT (°C)</b>	<b><math>t_{gel}</math> (s)</b>	<b><math>\tau_{co}</math> (Pa)</b>	<b><math>G_0'</math> (kPa)</b>
20 wt% F127	-	23.0 (22.2)	137	310	21.4
<b>Class A</b> PEO conc. = 8 wt%	200	20.0 (18.8)	131	328	21.3
	600	20.3 (19.0)	133	281	17.9
	1k	21.0 (19.8)	135	245	16.4
<b>Class B</b> PEO conc. = 1 wt%	2k	23.5	138	283	19.4
	10k	25.6	229	226	14.9
	20k	28.5	606	180	12.0
	35k	33.0	-	12	1.5

Estimated uncertainties: **CGT**  $\pm 0.5$  °C;  **$t_{gel}$**   $\pm 5.0$  s;  **$\tau_{co}$**   $\pm 5.0$  Pa;  **$G_0'$**   $\pm 1$  kPa



**Table 3.2** Effects of PEO concentration on CGT,  $t_{gel}$ ,  $\tau_{co}$  and  $G_0'$  of 20wt% F127

	Concentration of PEO (wt%)	CGT (°C)	$t_{gel}$ (s)	$\tau_{co}$ (Pa)	$G_0'$ (kPa)
20 wt% F127	0	23.0	137	310	21.1
Class A PEO1k	2	22.5	136	282	20.0
	4	22.0	135	278	18.6
	8	21.0	135	245	16.4
Class B PEO10k	0.5	24.5	188	267	17.4
	1	25.6	229	226	14.9
	2	31.6	-	31.5	3.9
	4	-	-	-	-

Estimated uncertainties: CGT  $\pm 0.5$  °C;  $t_{gel} \pm 5.0$  s;  $\tau_{co} \pm 5.0$  Pa;  $G_0' \pm 1$  kPa

### 3.2.2. Gelation time and strength of gel

To examine the effect of added PEO on the gel properties, the gelation time and gel strength were measured using oscillatory rheometry. The loss factor  $\tan(\Theta) = G''/G'$  provides a gauge for classification of a material:  $\tan(\Theta) > 1$  for liquid,  $0.1 < \tan(\Theta) < 1$  for weak gel,  $\tan(\Theta) < 0.1$  for strong gel.<sup>102</sup> The time interval between the point at which  $\tan(\Theta)$  reaches the maximum and the point at which  $\tan(\Theta)$  drops to 0.1 is taken as an estimate of the gelation time ( $t_{gel}$ ) as illustrated in Figure 3.2. Note that the initial increase of loss factor arises from the larger increase in loss modulus with temperature prior to gelation. The effect of molecular weight and concentration of PEO on gelation time of F127 can be seen from the data in Table 3.1 and 3.2.

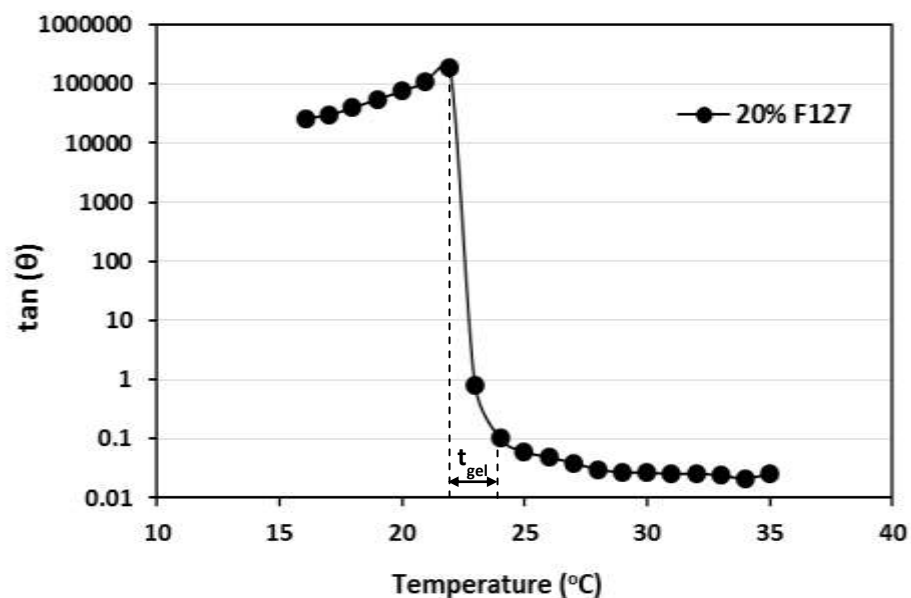


**Figure 3.2** Loss factor  $\tan(\Theta)$  vs. temperature for 20 wt% F127

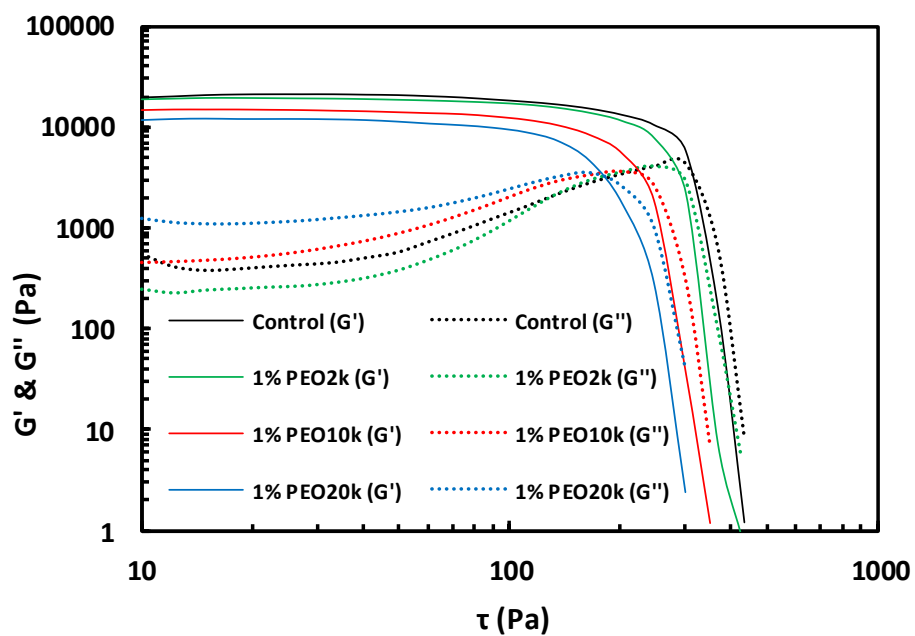


**Figure 3.3** Storage and loss moduli as a function of stress for 20% F127 in the presence of Class B PEO homopolymers at 37°C; the number of data points (not shown for clarity) for each decade of logarithmic stress is 12

Class B PEO was found to increase the gelation time of F127, whereas class A appeared to slightly reduce it. The effect of MW on gelation time is similar to that on CGT of F127. With increasing MW, the gelation time becomes longer, implying that the presence of class B PEO hinders both the initial structural rearrangement of micelles and the subsequent caging to form a packed, ordered gel structure. As such, the mechanical properties could be affected accordingly. To gain a better understanding on this hindering effect of PEO, the rigidity and yielding behavior of the resulting gel is investigated by oscillatory stress sweep (1Hz at 37°C). The temperature is fixed at 37°C because the gel has been developed to a state, in which the complex modulus is nearly independent of temperature as seen in Figure 3.1. The apparent yield stress  $\tau_{co}$  can be measured in number of ways as documented in the literature.<sup>103</sup> In this study, the stress at the crossover of  $G'$  and  $G''$  is adopted as the yield stress<sup>103, 104</sup> as depicted in Figure 3.3. The gel rigidity is gauged by the plateau storage modulus  $G_0'$  at small stress. The results of these mechanical properties are tabulated in Table 3.1 and 3.2. Note that class B PEO showed a drastic change in yield stress and rigidity with respect to PEO MW at 1 wt%, whereas class A PEO gave rise to much smaller changes at this concentration, although the results are not shown.

Except for the system with PEO200, an increase in MW of either class progressively decreased the yield stress and the plateau storage modulus of F127 gel. It indicates that the presence of PEO perturbs the F127 gel structure and hence weakens the network. This disturbing effect is a strong function of PEO MW. In fact, the sample with added 1 wt% PEO35k has no measureable storage

modulus and yield stress at 37°C, revealing the absence of any gel network (the system remains in sol state). From the investigation of gelation time and strength, it is clear that by increasing the chain length of PEO added to F127 solution, both gelation rate and gel strength are reduced. Therefore the addition of PEO not only has an effect on the kinetics of gel formation involving micellar rearrangement but also affects the gel network structure after this process is complete. The decrease in  $G'$  in presence of PEO (Figure 3.3) implies that the stiffness of the gel is decreased by PEO due to their order disrupting effect on F127 via the bridging/flocculation of micelles. Further decrease in  $G'$  with increase in the M.W of PEO implies that the order disrupting effect is more pronounced for high M.W PEO. The micellar aggregates formed in the presence of PEO via bridging/flocculation could result in increased viscous dissipation which explains the greater  $G''$  for majority of the samples when compared to the control.

### **3.2.3. Critical micellization temperature (CMT)**

Since the micellization is the prerequisite for gelation of F127, it is essential to study the former process and characterize micellar samples to seek its correlation with the latter. Differential Scanning Calorimetric (DSC) measurements were carried out for 20 wt% F127 with PEO homopolymer of different chain lengths and concentrations, and the thermograms are shown in Figure 3.4. We see a broad endothermic peak in the spectrum due to dehydration of PPO block of F127 when the temperature becomes high enough.<sup>12</sup> Since the dehydration of PPO block is the driving force for micelle formation, the endothermic peak can be used to characterize the CMT. The temperature for the

onset of endothermic peak is taken as the CMT. The effects of molecular weight and concentration of PEO on the CMT of 20 wt% F127 are provided in Figure 3.5. The obtained CMT of pure 20 wt% F127 is 12.6°C in good agreement with the reported value in the literature.<sup>34</sup>

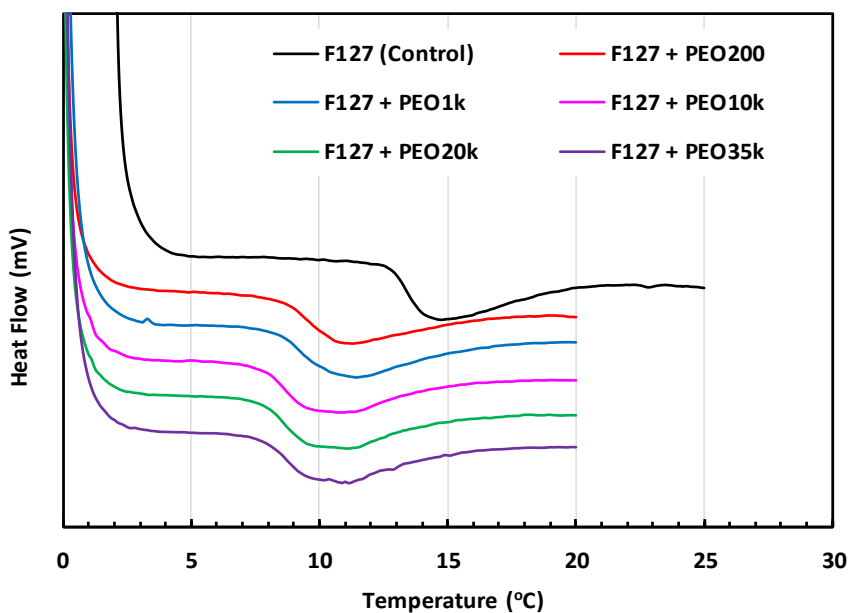


**Figure 3.4** Thermograms of F127 in presence of PEO of different M.W.; F127 conc. = 20%; PEO conc. = 6%

We find that the presence of PEO decreases the CMT of F127 for both classes and this decline increases with increasing chain length (Figure 3.5 (top)) or concentration (Figure 3.5 (bottom)) of PEO homopolymer. The decrease in CMT is expected for class A PEO because it also decreases the CGT of F127. For class B, however, the reason for this behavior was not yet clear at first glance. A detailed comparison also revealed that the change in CMT is much smaller than that in CGT with addition of PEO. For example, addition of 2% PEO20k decreased the CMT of 20% F127 by  $\sim 1.5^{\circ}\text{C}$  only, but gelation became completely

absent in contrast. It indicates that micelle formation at lower temperature due to the addition of PEO does not necessarily promote gelation. The change in heat of micellization (area under the endothermic curve) is well within the uncertainty range of  $\pm 0.2$  g/mol for the samples studied. The decrease in CMT was also observed by adding the PEO homopolymer to another Pluronic (P105).

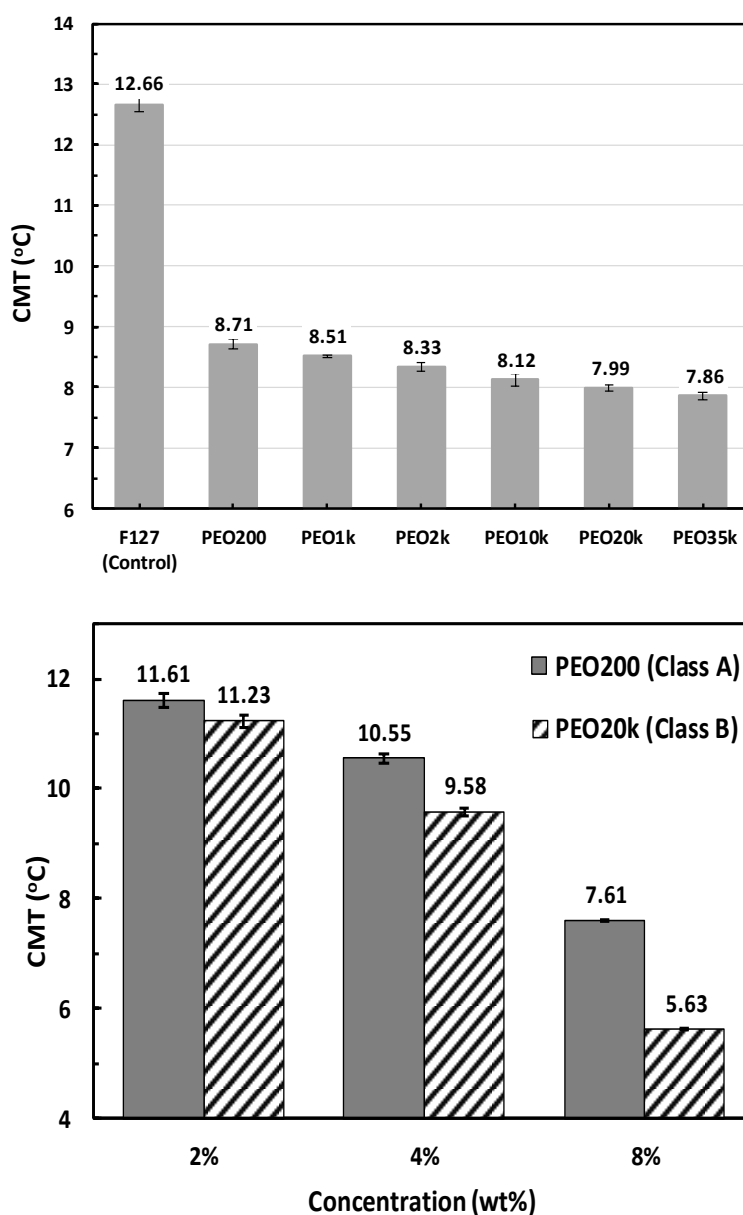


**Figure 3.5** Effect of MW of 6% PEO on CMT of 20% F127 (top); Effect of PEO conc. on CMT of 20% F127 (bottom); CMT of 20% F127 =  $12.6 \pm 0.1^\circ\text{C}$

For F127 at low concentrations, the DSC is not sensitive enough to detect the weak heat flow change. Micellization of such samples can be characterized by light scattering method because the unimer-micelle transition will cause a sharp

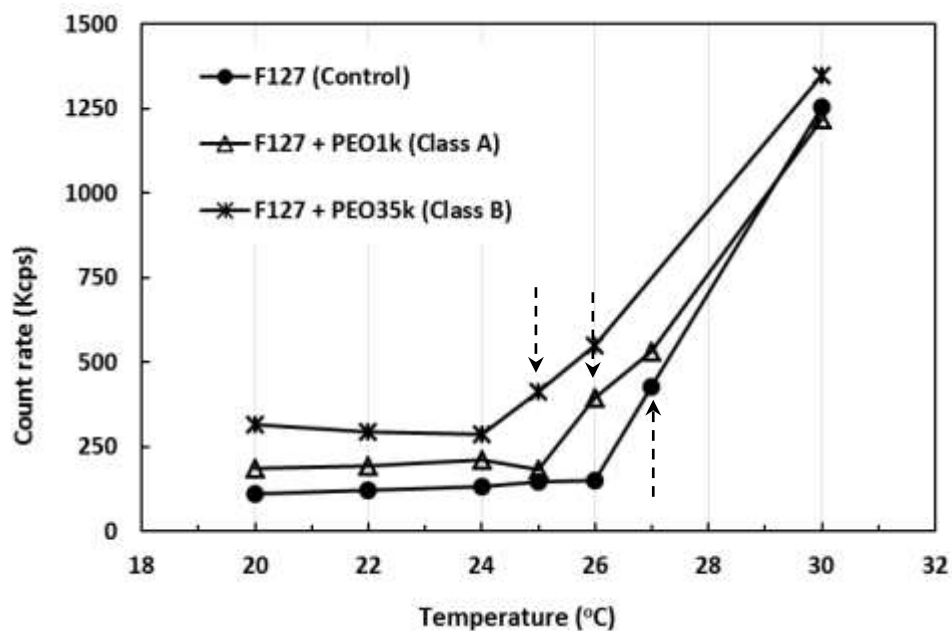


**Figure 3.6** Plot of count rate against temperature from DLS; arrows mark the CMTs of three different samples with F127 at 0.5% and PEO at 4%

increase in the scattering intensity.<sup>12</sup> Figure 3.6 illustrates the change of scattered light intensity (count rate) with temperature for 0.5% F127. As seen, the CMT for F127/PEO1k is around 1°C below that for the pure F127 solution, and becomes around 2°C lower for F127/PEO35k.

As described above, the presence of PEO homopolymer (class A & B) always decreases the CMT of F127; the longer the chain, the greater the decline. This trend is in overt contrast to the gelation behavior, for which the CGT may be increased or decreased, depending on the PEO MW. The effect of additives on

micellization can be elucidated by the change in F127 solubility. It has been known that solubilization of F127 in water arises primarily from hydrogen bonding between the hydrogen atoms of water and the oxygen atoms in the polymer backbone. These oxygen atoms act as proton acceptors during the H-bonding. The study on solute-solvent interactions in a mixed solvent of PEO and water by Singh et al.<sup>105</sup> has found that the mixed solvent shows a decreased hydrogen bond donating (HBD) ability, but an increased hydrogen bond accepting (HBA) ability when compared to pure water. These changes are also found to be more pronounced with increasing PEO concentration and molecular weight. Therefore a PEO/water mixed solvent can decrease the extent of hydrogen bonding with F127, increasing the tendency for F127 to form micelles at raised temperature and leading to a lower CMT. According to Singh et al.,<sup>105</sup> the HBD ability of PEO/water mixed solvent depends more strongly on PEO concentration than on its MW ranging from 200 to 6000 g/mol in their study. Interestingly, our findings also show that the decline in CMT is a weak increasing function of PEO MW when compared to the concentration dependence. In view of this consistency in the trend and dependence, the change in the solvent HBD ability due to the presence of PEO is believed to be one of the possible mechanisms for the observed CMT behavior.

The other plausible explanation rests on how the added PEO affects the water structure. For addition of alcohol to water, methanol and ethanol were found to exert a structure breaking effect on water, while butanol showed the opposite behavior. CMT of Pluronics was increased in the presence of former two



alcohol species, but decreased when the latter was added.<sup>19, 106</sup> Similar to butanol, PEO homopolymer was reported to have a structure promoting effect on water,<sup>107, 108</sup> because of its ability to fit into the tetrahedral water structure. This results in enhanced self-hydration of PEO homopolymer in water, leading to stronger hydrophobicity of F127 in such environment and increased ease for micellization.

### 3.2.4. Micelle characterization

Since gelation has been thought to relate to micellar rearrangement and association to form an ordered network, it is important to characterize micelles with the addition of PEO. For DLS experiments, the F127 concentration must be low enough to avoid multiple scattering. Figure 3.7 shows the temperature dependence of average micelle size for 0.5% F127. For the pure F127 solution,

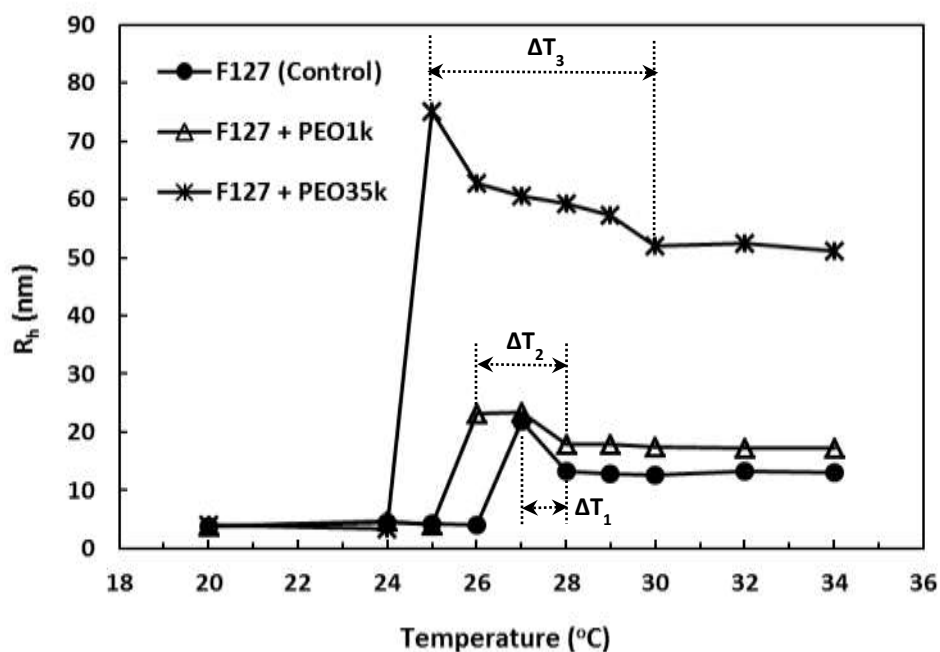


**Figure 3.7** Plot of average hydrodynamic radius against temperature for 0.5% F127 with PEO at 4%

the hydrodynamic radius increases suddenly to about 22 nm at 27°C indicating the formation of micelles, in agreement with what is observed in Figure 3.6. When the temperature is further raised, the micelle size will decrease until reaching a constant (~12.5 nm). This temperature rise  $\Delta T$  above CMT is thought to facilitate the formation of a compact stable micellar structure, i.e., a transition from loose to compact micelles. Similar increase and then decrease in micelle size with increasing temperature has been reported for Pluronic L44 by Naskar et al.<sup>109</sup> recently. They attributed the decrease to the transition of larger to smaller aggregates. Wei et al.<sup>110</sup> reported a similar size variation just above the CMC of a synthesized surfactant (ibuprofen-polyethylene glycol). For the samples in this work, this behavior is also observed for the cases with addition of PEO. However,  $\Delta T$  becomes larger when PEO is added as found from Figure 3.7, and increases with PEO MW.

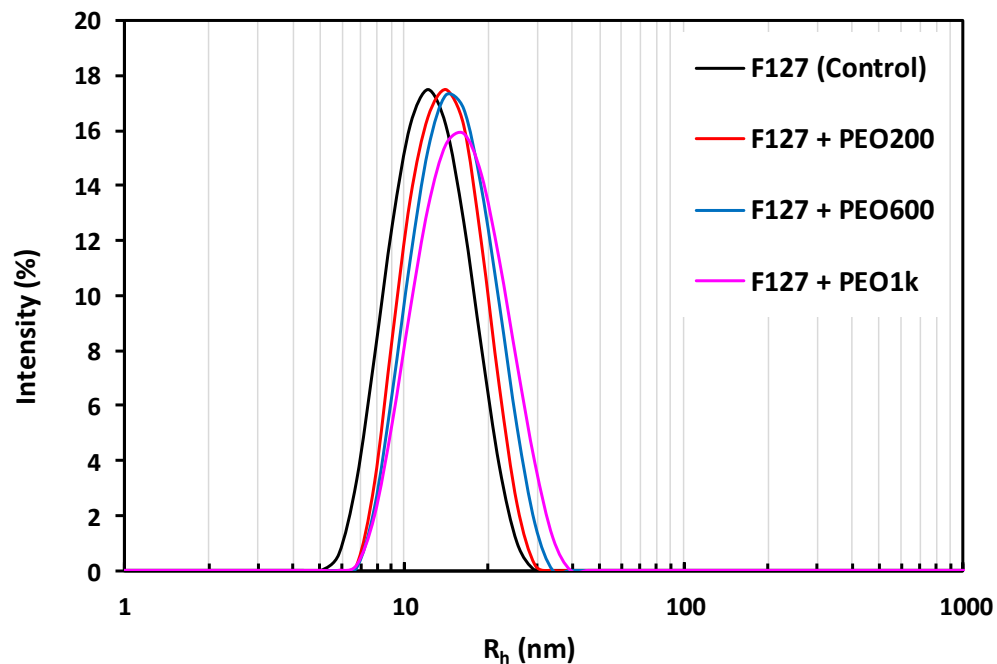


**Figure 3.9** Effect of molecular weight of Class A PEO on intensity distribution of F127/water system; PEO conc. = 4%; F127 conc. = 1%

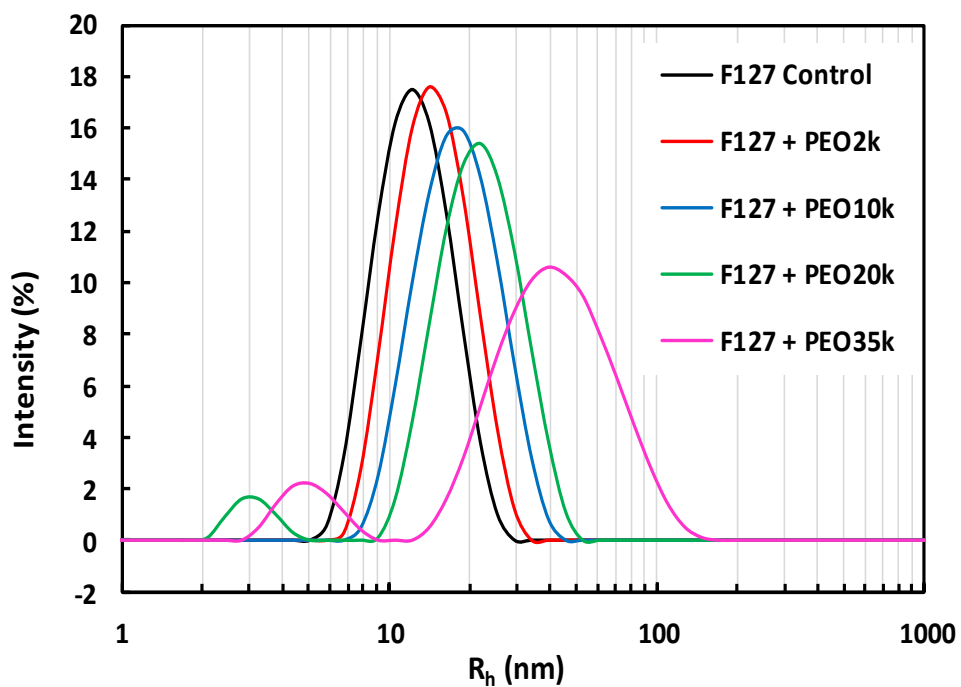


**Figure 3.8** Effect of molecular weight of Class B PEO on intensity distribution of F127/water system; PEO conc. = 2%; F127 conc. = 1%

To further examine the effects of PEO MW and concentration on the

micelle size and size distribution, DLS for 1% F127 at 40°C was conducted to ensure formation of stable micellar structure. The obtained mean hydrodynamic micelle size for pure 1% F127 at 40°C is ~12nm in good agreement with the literature.<sup>99</sup> The effect of PEO of class A and B on the size distribution based on light intensity is shown in Figure 3.8 and 3.9, respectively. The small peak around 3 nm and 5 nm respectively for MW = 20k and 35k is attributed to the scattering of PEO homopolymer in the bulk solution. This has been confirmed by carrying out DLS for PEO solutions without F127, showing similar size peaks. Bimodal distributions have also been reported for PEO with other non-ionic surfactant/water systems.<sup>111, 112</sup>

The quantitative data of micelle size are provided in Tables 3.3 and 3.4. It should be noted that these results are obtained on the basis of micelle diffusion in water. The presence of free PEO may impede the micelle diffusion and hence increase the obtained hydrodynamic radius. In appendix, this effect is assessed by measuring the viscosity of each PEO solution without F127 and correcting the micelle hydrodynamic size accordingly. This correction, however, requires the PEO solution to be treated as a continuum, which is not valid for high MW PEO as the molecules are not much smaller in size than the micelles as seen in Figure 3.9. As such, the correction exercise in this way provides a lower bound, and it is found that the qualitative trend remains unchanged. In what follows, the size results are discussed based on water viscosity.

The hydrodynamic radius of F127 micelles in the presence of PEO of Class A is larger than the counterpart without PEO addition. The modest enlargement

increases with increasing molecular weight of PEO. For PEO of class B, the increase in the average size is more pronounced, showing a stronger dependence on MW of PEO, and the size distribution becomes wider, indicative of increased polydispersity in size as seen in Table 3.3. Also, the size increase becomes more significant for higher PEO concentration, irrespective of the class as seen in Table 3.4. For addition of PEO35k, the size distribution is broadened with the main peak centered at 39.4 nm and extends up to about 147 nm. Since the contour length of a F127 molecule (MW = 12.5k) is far less than 147 nm, it is very unlikely to attain spherical micelles with radius ~147 nm even with incorporation of PEO onto the micelles. The possibility of forming rodlike micelles is also low, according to the Cryo-TEM images that will be shown later. This implies that a number of micelles should have been associated or even merged into a larger one in the presence of PEO with higher MW.

**Table 3.3** Effect of molecular weight of PEO on hydrodynamic size of 1% F127

	PEO MW (g/mol)	Hydrodynamic Radius (nm)	PDI (no unit)
<b>Pure F127</b>	-	12.18 ± 0.18	0.067 ± 0.01
<b>Class A</b> PEO conc. = 4 wt%	200	14.38 ± 0.20	0.066 ± 0.01
	600	15.58 ± 0.68	0.105 ± 0.02
	1k	16.71 ± 0.38	0.120 ± 0.02
<b>Class B</b> PEO conc. = 2 wt%	2k	14.11 ± 0.19	0.099 ± 0.01
	10k	18.92 ± 0.19	0.175 ± 0.01
	20k	21.91 ± 0.21	0.223 ± 0.01
	35k	39.41 ± 1.0	0.359 ± 0.08

**Table 3.4** Effect of concentration of PEO on hydrodynamic size of 1% F127

	<b>Concentration of PEO</b>	<b>Hydrodynamic Radius</b>
<b>Pure F127</b>	-	12.18 ± 0.18
<b>Class A</b> PEO200	2	13.06 ± 0.07
	4	14.38 ± 0.20
	8	16.99 ± 0.32
<b>Class B</b> PEO20k	1	16.34 ± 0.23
	2	21.91 ± 0.21
	4	34.03 ± 0.38

Similar to class B PEO, methanol and ethanol have been reported to suppress the gelation of F127.<sup>106</sup> Addition of ethanol to F127 solutions is found to hinder the formation of F127 micelles.<sup>35, 36, 106</sup> At sufficient concentration of ethanol, the peak of hydrodynamic radius was reported to shift to about 3 nm when compared to 12 nm for pure F127 solution. This considerable size reduction was attributed to the F127 unimers without micellization.<sup>36</sup> Hence, the increased difficulty for F127 to self-assemble into micelles in the presence of ethanol can account for the higher CGT. In contrast to ethanol, addition of PEO of either class always shifts the size peak to higher values, implying that the micellization is never suppressed, consistent with the declined CMT obtained from DSC. Therefore, the mechanism underlying the ethanol effect cannot explain the suppressed gelation of F127 with class B PEO.

Apart from the effect on the onset of micellization, PEO also plays a role in the micellar interactions. As observed, PEO of class A increases the micelles size of F127 slightly, whereas PEO of class B appears to cause aggregation of the micelles. The degree of aggregation seems to increase with increasing chain length of PEO. The earlier belief that neutral polymers do not bind to the non-ionic micelles<sup>113</sup> has been disproved by later research reporting that the neutral polymer (PEO) can interact with non-ionic surfactant micelles to form complexes.<sup>111, 112, 114, 115</sup> These studies used isothermal titration calorimetry and time resolved fluorescence quenching to study the interaction to find that the non-ionic soluble polymer can interact with non-ionic surfactant micelle in two ways: 1) non-ionic homopolymer chains can bind to the hydrophilic micelle corona or may even penetrate into the corona driven by hydrogen bonding, and 2) polymer chains can thread through the hydrophobic micellar core forming “strings of beads”.

For the system in this work, the PPO and PEO blocks constitute the micelle core and corona, respectively. In PEO/water system, there already exist four types of hydrogen bonding in terms of proton donor-acceptor: water-PEO, water-water, PEO-water and PEO-PEO.<sup>116</sup> The PEO-PEO hydrogen bonding involves an end hydroxyl of one PEO and an ether oxygen of the other PEO. In F127/PEO/water system, therefore, hydrogen bonds can also form between the corona EO groups of F127 and homopolymer PEO. Since some hydroxyl groups of F127 may stay on the outer surface of the corona, they can attract PEO homopolymers onto the micellar surface. On the other hand, PEO homopolymers could penetrate into the hydrophilic corona to behave as proton donors.

Therefore, short homopolymer chains may each bind to the corona of one micelle, thereby making the micelle larger. When they are sufficiently long, to the contrary, each may bind to more than one micelle, and hence link the micelles to facilitate their aggregation or clustering as reported for comparable systems.<sup>111, 112</sup> Besides, the high MW PEO homopolymers in the bulk solution can also result in a depletion zone between two micelles, where the osmotic pressure becomes lower than in the bulk, and can give rise to flocculation.

Another possibility could be the interaction between PEO homopolymers and the core PPO of F127 micelles. Phase behavior studies on PEO/PPO/water system showed that the system remained in one phase at either high or low water content, whereas phase separation/immiscibility was observed at intermediate water content.<sup>117</sup> To detect if there exists interaction between PEO homopolymer and F127, we carried out <sup>1</sup>H and <sup>13</sup>C NMR investigations. From <sup>1</sup>H NMR studies (see Figs. A2 and A3 in the appendix), no interaction was found between PPO blocks of F127 and PEO homopolymer. Our <sup>13</sup>C NMR results also could not detect any noticeable conformation change in both PPO and PEO blocks with the addition of homopolymer when compared to the signal peaks for the pure F127 solution at the same temperature. This finding suggests the possibility of depletion flocculation, which could lead to micelle merger and increased aggregation number.

To seek more clues, Cryo-TEM was used to capture the microstructure. The micrographs of 10% F127 without and with addition of PEO 200 (Class A) and PEO 35,000 (Class B) are presented in Figure 3.10. The brighter spots are



micelles, which are surrounded by water appearing in grayish tone.<sup>26</sup> Pluronic F127 is found to have ordered structure in gel state.<sup>27, 38</sup> Although our tested concentration is below the critical gelation concentration (CGC = 15 wt%), the microstructure of pure F127 sample exhibits long range order and each micelle is well separated from surrounding neighbors. This is attributed to a slight increase in the volume fraction of micelles due to removal of some water during the sample preparation.<sup>26</sup> In the presence of PEO of class A, the microstructure ordering does not show a discernible change. However, the addition of PEO of Class B strongly disrupts the micellar arrangement to a disordered state, in which micellar aggregates can also be observed.

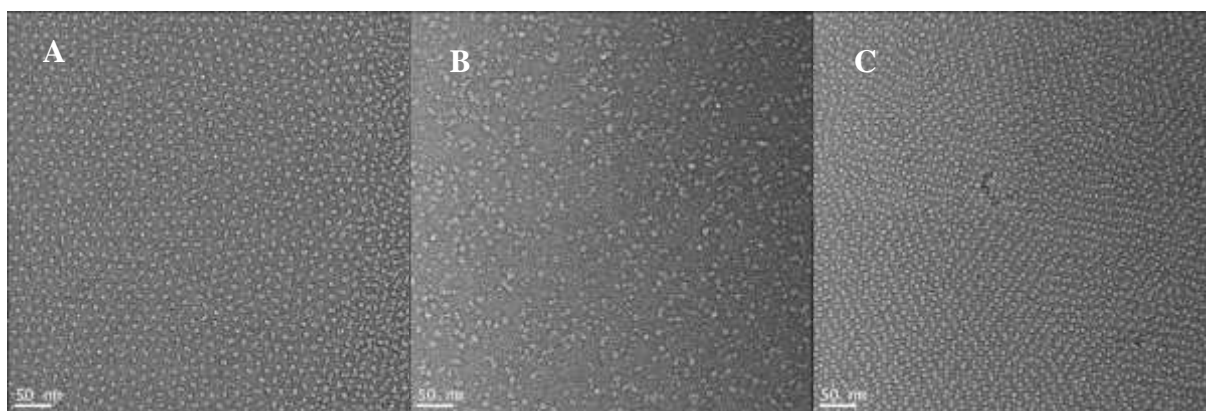
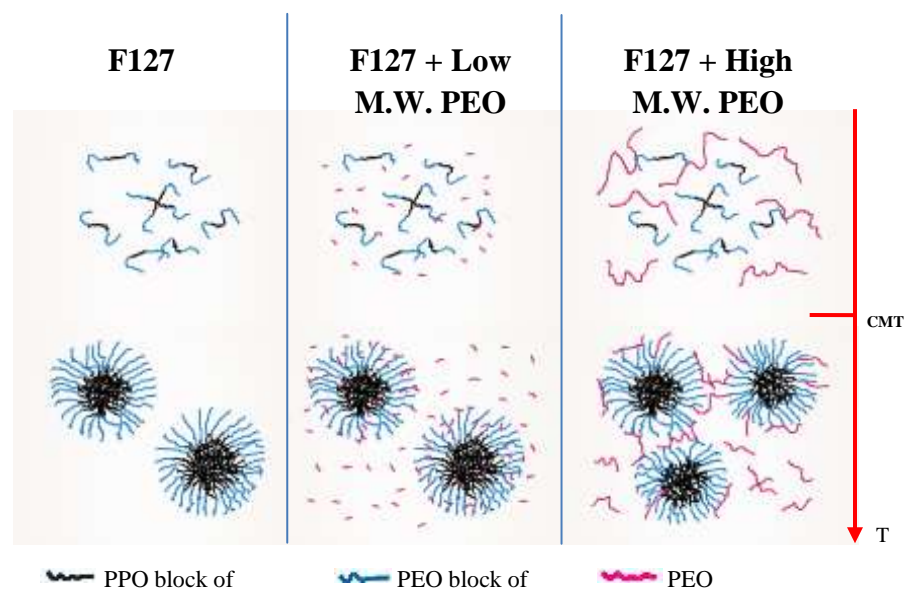


**Figure 3.10** Cryo-TEM micrographs of 10% F127 (A), 10% F127 + 5% PEO35k (B) and 10% F127 + 5% PEO200 (C)

### 3.2.5. Correlation between micellization and gelation

It is interesting to relate the PEO effects on micellization to the gelation behavior. As discussed above, addition of PEO can (1) decrease the HBD ability

of the mixed solvent or promote the water structure, and (2) increase the average micelle size and the polydispersity via bridging micelles or depletion flocculation of micelles. Mezmarich and Love<sup>99</sup> found that an increase in micellar monodispersity arising from addition of hydrophobic drug (methylparaben) could aid gelation of F127, because the micelles would face less sizing defect when undergoing structural ordering during gelation. Suggestively, an increase in size polydispersity of micelles would lead to lattice disruption and hence suppress the gelation as speculated previously by Malmsten and Lindman,<sup>32</sup> who measured the CGT of F127 with added PEO, but did not provide any direct evidence to corroborate this thought.



**Scheme 3.1.** Schematic presentation of F127/PEO/water system (not drawn to scale)

In our opinion, the relative importance between the two aforementioned effects of PEO depends on its molecular weight. For class A PEO, the solvency effect dominates and manifests at high enough concentrations because the

homopolymer is of short chain. The mixture of water and PEO decreases the solvency for F127, making it easier to form micelles as well as gel at lower temperatures. For class B PEO, apart from solvency effect, the bridging/flocculation effect becomes equally or even more important. Formation of micellar clusters by bridging or larger micelles via merger increases the size polydispersity inferred from DLS, leading to more sizing defects for micellar ordering/rearrangement process as evidenced by the Cryo-TEM images and the decreased gel strength from oscillatory rheology. This obstacle is more pronounced with increasing PEO concentration and chain length, accounting for the experimentally observed trend of gelation suppression.

### 3.3. Conclusion

Micellization, gelation and rheology of amphiphilic pluronic triblock copolymer F127 have been investigated in the presence of homopolymer PEO, focusing on the effect of their chain length and concentration. It is found that the CMT of F127 is always decreased irrespective of the chain length of the homopolymer. The decline increases with the chain length and the concentration. This decrease in CMT is attributed to the decreased HBD ability of the mixed solvent and/or the structure promoting effect of PEO on water. To the contrary, the PEO influence on CGT depends on the MW. Low chain length PEO ( $MW \leq 1000$ ) decreases the CGT, while longer chain length PEO ( $MW \geq 2000$ ) either delays the gelation to a higher temperature or even prevents it from happening. The change of CGT in the presence of PEO with low MW is weak when compared to that instigated by PEO of longer chain length.

In general, homopolymer PEO interacts with EO groups of F127 in the micelle corona via hydrogen bonding. For shorter PEO chain, the micelle size of F127 increases slightly due to PEO adsorption on the micellar surface, while aggregation of micelles can take place for longer PEO via bridging. The resulting aggregates or clusters increases the heterogeneity in size and structure, thereby disturbing the micellar ordering as evidenced from the Cryo-TEM images. This disturbing or hindering effect is the reason for gelation suppression.

## 4. Effect of Poly (acrylic acid) on Sol-Gel Behavior of Pluronic F127

---

In this chapter, first of all, relevant literature on the PEO/PAA/H<sub>2</sub>O and Pluronic/PAA/H<sub>2</sub>O systems will be presented. The present study is aimed to study the influence of homopolymer PAA on triblock copolymer F127. Experimental in this section has been designed by investigating the effects of medium pH, concentration and molecular weight of PAA on the sol-gel behavior using UV-spectroscopy, dynamic light scattering (DLS), differential scanning calorimetry (DSC), and rheometry. The interesting interaction mechanisms between F127 and PAA homopolymer will be elucidated and proposed in this chapter.

### 4.1. Introduction

In the literature, numerous investigations on inter-polymer complex formation between PAA homopolymer and non-ionic PEO homopolymer exist.<sup>118-121</sup> According to these studies, the PEO-PAA complex formation is governed by hydrogen bonding between proton accepting ether oxygen atoms of PEO and carboxylic groups of PAA. The interaction is very sensitive to pH because -COOH groups of PAA are protonated at low pH and are available for hydrogen bonding with PEO but at relatively high pH, greater ionization of -COOH groups occurs and are not available for hydrogen bonding. On the other hand, Pluronics are surface active amphiphilic polymers with relatively hydrophobic PPO blocks at center which provides them self-assembling properties unlike PEO homopolymer. However since pluronics also have proton

accepting ether oxygen atoms in their chains, PAA is also expected to form complexes with Pluronics. In the dilute regime, light scattering studies<sup>73, 74</sup> witnessed large sized complexes for the system Pluronic/PAA/H<sub>2</sub>O. The key finding from light scattering studies of Pluronic/PAA/H<sub>2</sub>O is that certain pluronics such as F68, P75 and P85 with small PPO hydrophobes form complexes with PAA only at low pH (= 2) resembling the PAA/PEO/H<sub>2</sub>O system, while pluronics such as F127, P104 and P103 with large PPO hydrophobes form complexes at both pH = 2 and 4.<sup>74</sup> This suggests that hydrophobic interaction also plays a significant role in addition to the hydrogen bonding in determining the complex formation in Pluronic/PAA/H<sub>2</sub>O system. The only previous study on the concentrated regime of Pluronic/PAA/H<sub>2</sub>O system is by Dos Santos<sup>75</sup> et al., who studied the effect of PAA on liquid crystalline phases formed in concentrated aqueous Pluronic P104 using small angle X-ray scattering (SAXS). They found that the ordered structures in the P104/H<sub>2</sub>O systems are destroyed by the addition of PAA.

While the size analysis in dilute regime and microstructure analysis in concentrated regime are reported, the literature lacks any information on micellization and gelation behavior such as the variation of CMT, enthalpy of micellization ( $\Delta H$ ), CGT, gel rigidity ( $G'$ ) and thermoreversibility of Pluronics in the presence of PAA. In the present work, we investigate the micellization and gelation behavior of Pluronic/PAA/H<sub>2</sub>O system for the first time. Pluronic F127 is chosen for this study because of its potential ophthalmic drug delivery applications. The focus is placed on the effects of pH, concentration and

molecular weight of linear PAA on CMT,  $\Delta H$ , CGT, gel strength and thermoreversibility of F127. The obtained results herein might shed light on how to design a F127/PAA hydrogel with desired drug loading capacity and sol-gel transition temperature. The effect of ionic homopolymer PAA is then compared with the effect of non-ionic homopolymer PEO on the sol-gel behavior of F127/H<sub>2</sub>O system to draw some important commonalities and differences between F127/PAA/H<sub>2</sub>O and F127/PEO/H<sub>2</sub>O systems.

## **4.2. Results and discussion**

### **4.2.1. Critical micellization temperature**

In this study, DPH solubilization technique was used to find the critical micellization temperature (CMT) of F127/PAA/H<sub>2</sub>O in dilute regime. The absorbance of DPH at 356nm vs. temperature was plotted and the first inflection point of this curve is taken as the CMT.<sup>98</sup> For the samples for which the inflection point is not obviously present CMT is determined by the point of intersection between two tangential lines. A representative plot is shown in the Figure 4.1, and the as determined CMT is displayed as a function of PAA concentration or pH in Figure 4.2 and 4.3. It is clear from Figure 4.1 that the F127 chains in the presence of PAA can form hydrophobic domains (micelles/aggregates) at a temperature lower than for the pure F127 solution. Further evidence for this CMT reduction is provided in the next section where the micellization enthalpy ( $\Delta H$ ) obtained by DSC will be discussed. It is found that the higher the concentration of PAA, the greater the decrease in CMT (see Figure 4.1 and 4.2). At the same concentration,

the high M.W PAA is more effective in lowering the CMT as shown in Figure 4.2. Also, the CMT increases with increasing pH (depicted in Figure 4.3), and

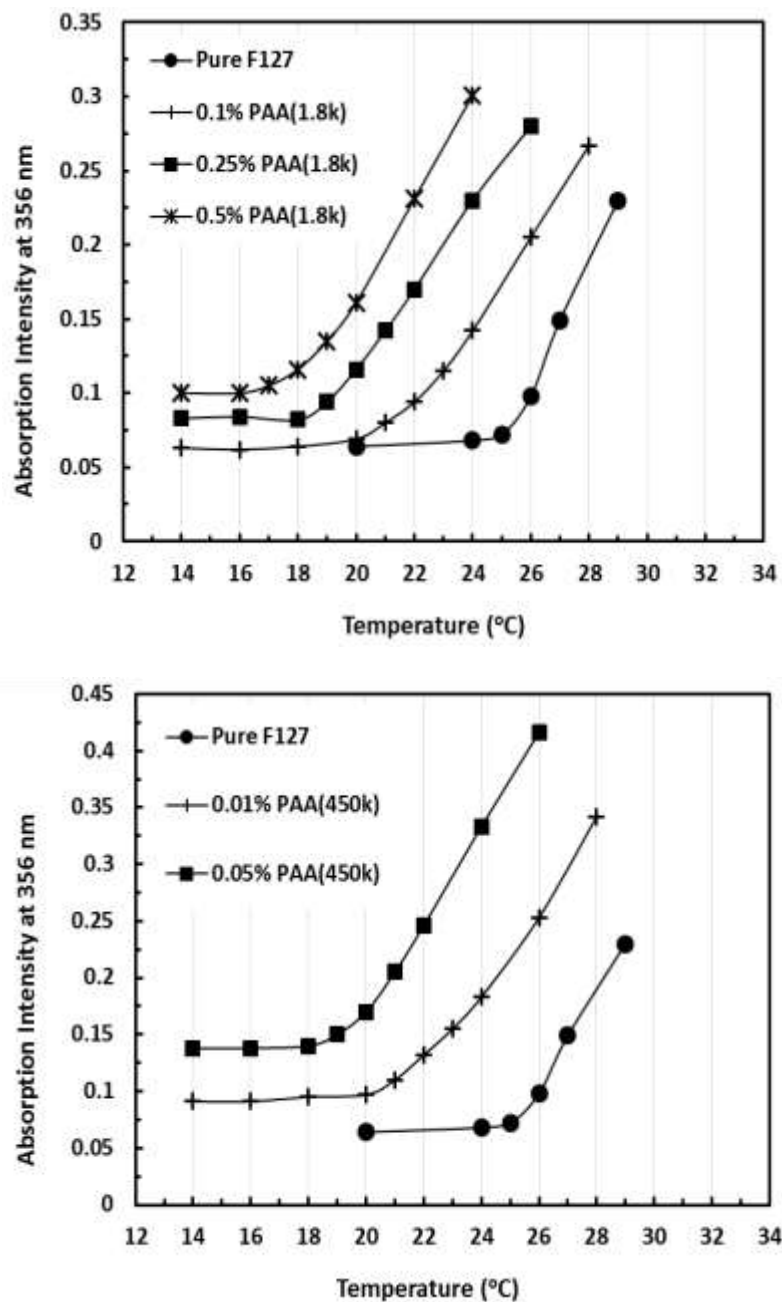


**Figure 4.1** Effect of temperature on UV-vis absorption spectra for DPH in F127/PAA (1.8k)/H<sub>2</sub>O system (top) and in F127/PAA (450k)/H<sub>2</sub>O system (bottom); F127 conc. = 1%



approaches the value of pure F127 (26°C) when pH is raised to 5 or higher. This indicates that the deprotonated PAA chains have a weak effect on the aggregation process of F127.

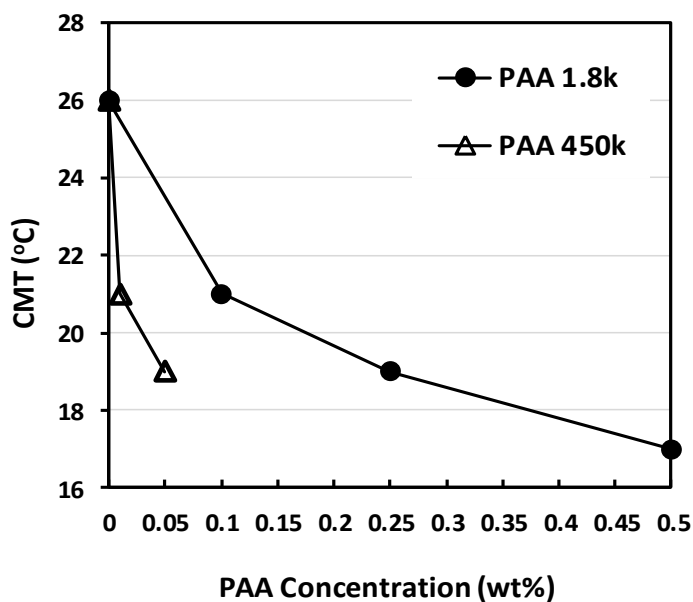


**Figure 4.2** Effect of PAA concentration on CMT of F127 obtained by DPH technique; F127 conc. = 1%

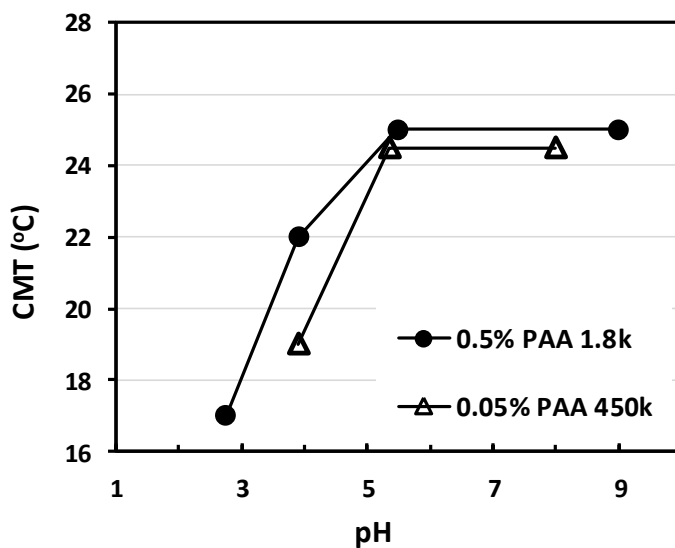


**Figure 4.3** Effect of pH on CMT of F127/PAA/H<sub>2</sub>O obtained by DPH technique; F127 conc. = 1%

The lowering of CMT is thought to arise from the association of F127 chains on PAA. It takes place via hydrogen bonding between ether oxygen of PEO in F127 and carboxylic groups of PAA even below CMT, thereby reducing the dissociation of the acid groups. In fact, earlier studies on homopolymer PEO/PAA/H<sub>2</sub>O systems have shown the existence of PEO-PAA complexes stabilized by hydrogen bonding.<sup>118, 119</sup> To probe the association, we carried out the pH measurement for F127/PAA/H<sub>2</sub>O are carried out and shown in Figure 4.4. It should be noted that the pH of aqueous PAA solutions is <7 because of the dissociation of its acid groups, and the pH values of both pure F127 and pure PAA solutions are independent of the temperature. Figure 4.4A shows a pH increase in the presence of F127, and this increase becomes more significant when the temperature is raised above 20°C, except for the case of 0.01% PAA (1.8k). The pH increase confirms the suppression of -COOH dissociation as a result of hydrogen bonding between PAA and F127. Comparison analysis found that the onset temperature for the greater pH increase, if existent, matches the CMT value (marked by arrows in Figure 4.4) determined by the DPH solubilization technique. This match is also observed for some other samples investigated, although only the selective results are presented in Figure 4.4. With formation of hydrophobic domains, the F127-PAA association is deemed stronger as reflected by the greater pH increase. It may have to do with hydrophobic interaction between PPO and the aliphatic backbone of PAA, which arises and plays a role in enhancing the affinity to facilitate more H-bonding. As mentioned earlier, for PAA (1.8k) at 0.01%, the pH increase is nearly independent of

temperature, as opposed to the behavior of PAA (450k) (cf. Figure 4.4A and 4.4C). Interestingly, there is no detectable change in CMT as well for this case, unless the PAA concentration is increased to higher values, e.g., 0.1% (see Figure 4.4D). The intriguing coincidence indicates that if the PAA concentration/molecular weight is not sufficiently high, the aforementioned affinity enhancement cannot occur or remains too weak to affect the CMT.

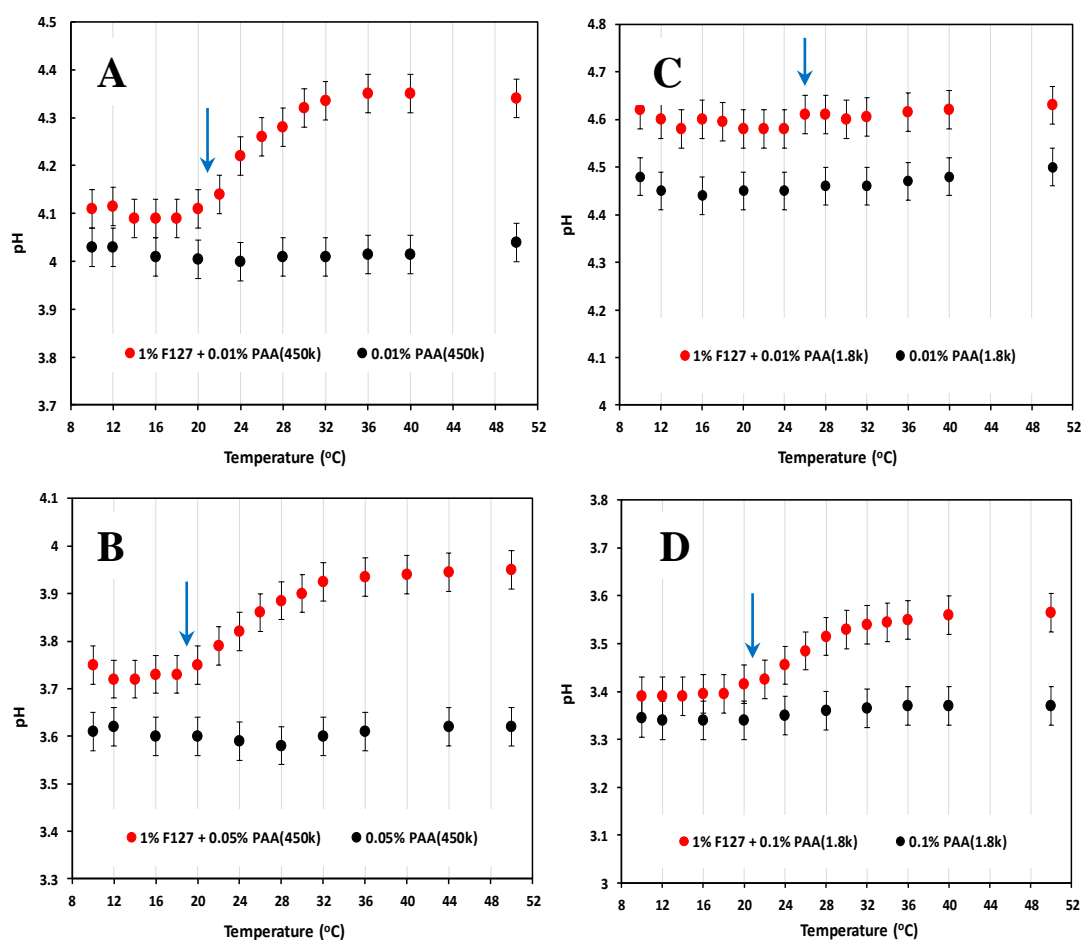


**Figure 4.4** Solution pH vs. temperature; Effect of high M.W PAA (A and B) and low PAA (C and D); The arrow marks the CMT as detected by DPH solubilization technique

To confirm the association of F127 micelles with PAA chains, we performed size analysis using dynamic light scattering (DLS) for the sample 1% F127 + 0.05% PAA (450k) at 40°C (>CMT) with the results shown in the Figure 4.5. At natural pH (~3.9 at 40°C), a bimodal distribution is obtained, as opposed to a single peak at pH=6. This observation is in agreement with the behavior reported for Pluronic P123/pyrene labeled PAA/H<sub>2</sub>O system.<sup>73</sup> The peak at around 100 nm is attributed to the F127-PAA (450k) complexes, which form because bound F127 aggregates on PAA chains can lead to physical crosslinking of different PAA chains into discrete networks. The other peak at around 10 to 15 nm represents the size of free copolymer micelles in the bulk. The figure shows that the complex formation is significant at low pH, but becomes very weak or even absent at higher pH. Note that no such large complexes were detected at any pH for the low M.W. PAA at this concentration, although the results are not shown. It is because the short PAA may only connect a few micelles together,

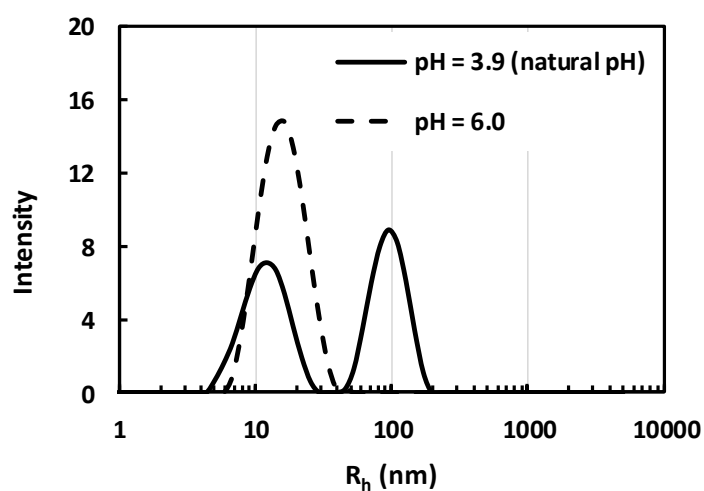


**Figure 4.5** Effect of pH on size distribution of 1% F127 + 0.05% PAA (450k) system at 40°C

instead of forming larger networks distinguishable from free pure micelles in the light scattering experiment.

The recent study on P123/pyrene labeled PAA/H<sub>2</sub>O system using fluorescence technique<sup>122</sup> suggests that pyrene groups attached to PAA are positioned on the PEO/PPO interface of P123 micelles, while the PAA chains prefer to be in PEO environment. It lends support to the dominance of hydrogen bonding for association between PAA and F127 at temperatures above CMT in the present study. Small angle neutron scattering measurements<sup>123</sup> on Pluronic F68/PAA blend systems have earlier shown selective hydrogen bonding between PAA and PEO blocks dominates over the interactions between PAA and PPO blocks.

Possible mechanisms are proposed as follows to account for the formation of F127 micelles on the PAA chains at a temperature lower than that for the pure F127 system. Since EO units can preferentially be associated with the PAA chains, the amount of water required for solvation of the PEO block is reduced by replacement from COOH groups of PAA. As a result, the effective size of the PEO block decreases. It has been known that among the Pluronics with same PPO block size but different PEO block lengths, the CMT decreases with decreasing PEO block length.<sup>11</sup> Hence, in our system, those unimers bound on the PAA chains tend to dehydrate at a temperature lower than for the free unimers in the bulk. They can then either attract one another or act as nuclei to engage some free copolymer chains in the bulk to form micelles on the PAA chains. At low pH, PAA chains are somewhat hydrophobic in nature due to their less extended

conformation.<sup>124</sup> Hydrophobic interactions between the PAA aliphatic backbone and PPO blocks of F127 could enhance their affinity to indirectly facilitate hydrogen bonding, thereby increasing the ease of micellization as well. The reduction of CMT observed in the present study appears to contradict the behavior reported by Costa et al.<sup>122</sup> for Pluronic P123/pyrene labelled PAA (150k)/H<sub>2</sub>O at constant temperature. They claimed that the critical micellization concentration (CMC) remains unaffected, and hence the association could occur only after the formation of free micelles in the bulk water. We reason that the polyelectrolyte concentration ( $5 \times 10^{-7}$  M or  $\sim 0.0075$  wt/wt%) used in their study could be too low to observe any noticeable changes in the CMC.

At high pH, the deprotonated PAA chains lose their ability to associate with F127 unimers. Therefore, the aforementioned nuclei on PAA chains no longer exist to facilitate micellization at low temperature. Moreover, the PAA chains become more extended and relatively hydrophilic, reducing the affinity with PPO blocks. This explains why the CMT is hardly affected by PAA at high pH.

#### **4.2.2. Enthalpy of micellization**

Differential scanning calorimetry (DSC) measurements were carried out for 17.5% F127 with PAA (1.8k) at different concentrations with the thermograms shown in Figure 4.6 (top). Since DSC is not sensitive enough to detect a small heat flow change for F127 at low concentration, high enough concentrations of F127 must be used. On the other hand, it allows us to check if the decrease in CMT caused by PAA also holds true for high F127 concentrations. The endothermic peak observed is attributed to the dehydration of PPO blocks, which

in turn leads to micelle formation.<sup>12, 16</sup> Since the dehydration of PPO blocks is the driving force for micelle formation, the endothermic peak can be regarded as an indicator for the occurrence of micellization with the peak onset and end temperatures representing the beginning and end of this process. Unlike small

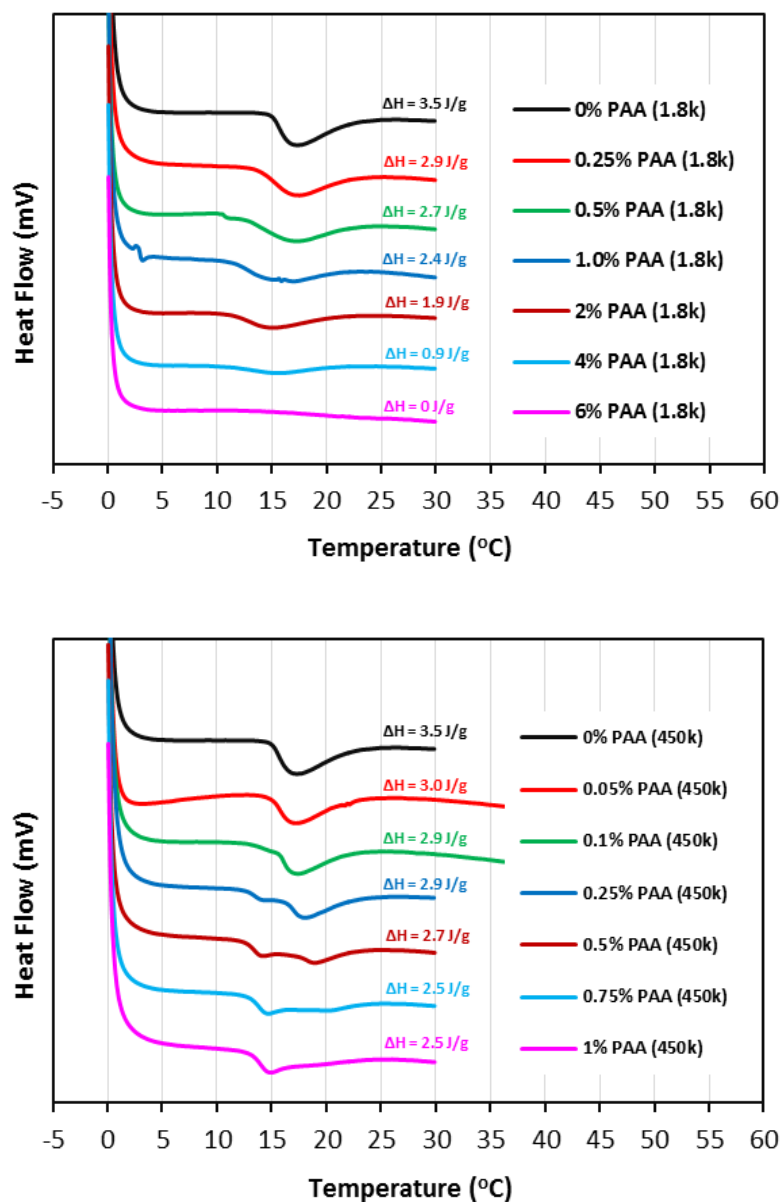


**Figure 4.6** DSC thermograms of 17.5% F127 in the presence of PAA at various concentrations; PAA 1.8k (top) and PAA 450k (bottom); Estimated uncertainty:  $\Delta H \pm 0.2$  J/g

nonionic surfactant, the peak is usually broad for Pluronics because of their broad molecular weight distribution.<sup>10</sup> The enthalpy of micellization ( $\Delta H$ ) can be determined from the area by integrating the endothermic peak.<sup>16, 19</sup>

Figure 4.6 (top) shows that the onset of endothermic peak (deemed as CMT) shifts to a lower temperature with increase in PAA concentration, which is in agreement with the trend obtained earlier via the DPH solubilization technique. The CMT reduction is more significant in the dilute than in the concentrated F127 regime at the same concentration of PAA (see Figure A6 in Appendix). We also find that  $\Delta H$  decreases significantly with increasing PAA concentration. When the PAA (1.8k) concentration reaches 6%,  $\Delta H$  vanishes since no endothermic peak can be detected. At this concentration, the sample remains very clear with the number ratio of EO to COOH equal to about 3.3, meaning that not all of ether oxygen can be involved in hydrogen bonding with PAA even when the degree of dissociation of PAA is zero. Although the result does not necessarily mean the absence of any micelles because the enthalpy could become too small to be detected by DSC, the considerable decrease in  $\Delta H$  reflects the decline in the energy consumed for the PPO dehydration. This behavior is unusual yet interesting when compared to the cases with alcohol as the additive. Addition of ethanol has been reported to reduce  $\Delta H$  and increase the CMT of Pluronic due to its structure breaking effect on water, while butanol shows an opposite behavior because of its structure promoting effect on water.<sup>19</sup>



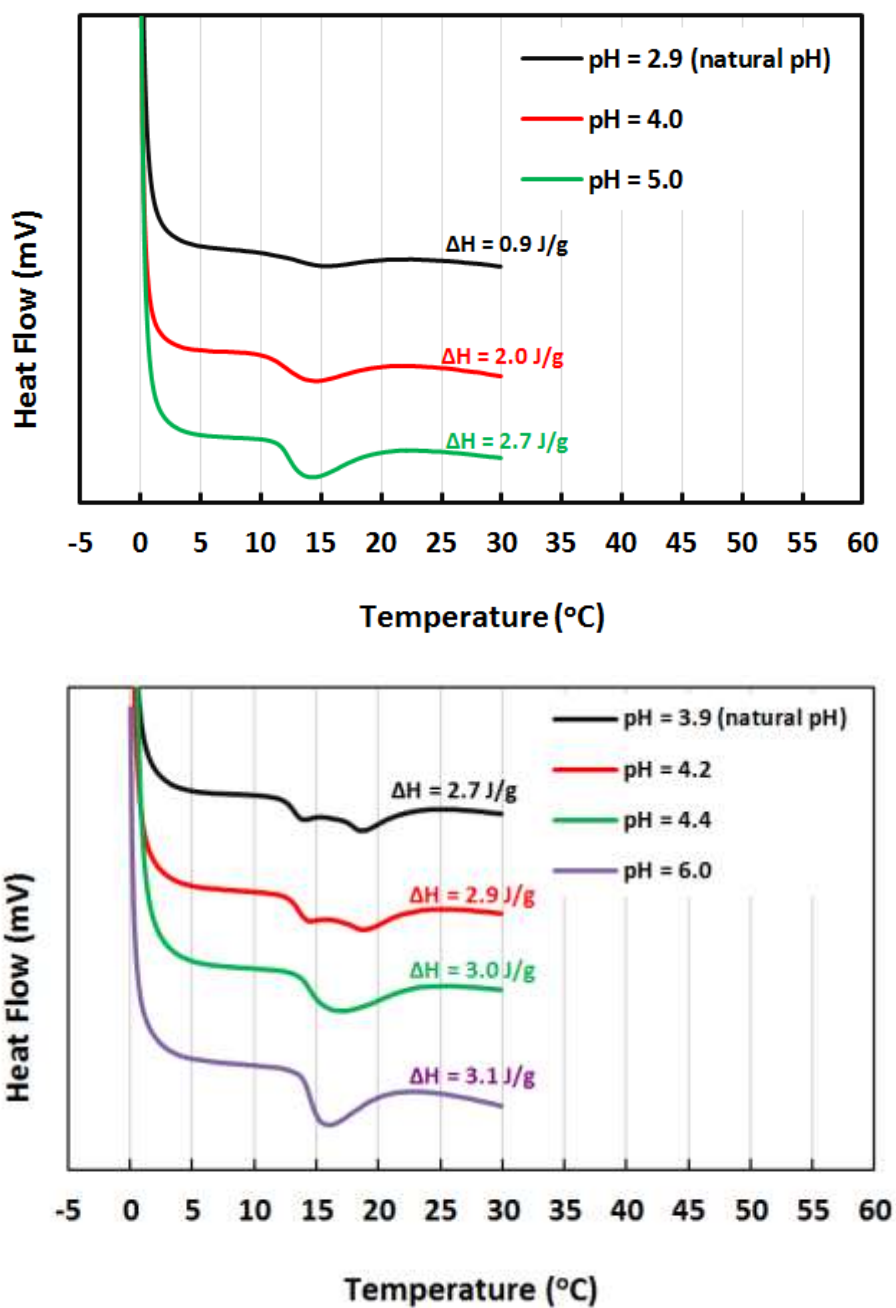


**Figure 4.7** Effect of pH on DSC Thermograms of 17.5% F127 + 4% PAA 1.8k (top) and 17.5% F127 + 0.5% PAA 450k (bottom); Estimated uncertainty:  $\Delta H \pm 0.2 \text{ J/g}$

From the DSC thermograms for the high M.W. PAA (450k) depicted in Figure 4.6 (bottom), several trends are observed with increase in PAA

concentration: (1) the onset temperature of the endothermic peak (CMT) decreases; (2) the endothermic process may split into two overlapping peaks with the first peak temperature lower and the second higher than the peak temperature of pure F127 solution; (3) the area under the first peak increases, while that under the second decreases; (4) for the PAA concentration  $\geq 0.75$  wt%, the second peak disappears. Note that the 1% PAA sample is already turbid, and dissolution becomes impossible beyond this concentration. Besides,  $\Delta H$  also decreases with increasing PAA (450k) concentration, similar to the effect of PAA (1.8k). Observations 2-4 are characteristic of the high M.W. PAA only. The reason for the peak splitting will be discussed later.

Figure 4.7 shows the effect of pH on the DSC thermograms. Interestingly, the peak splitting observed for PAA (450k) at natural pH does not occur when pH is high enough. Also,  $\Delta H$  increases with increasing pH. At the highest pH investigated for each M.W. of PAA, the onset temperature of endothermic peak is slightly lower than the value for the pure F127 solution, so is  $\Delta H$ .

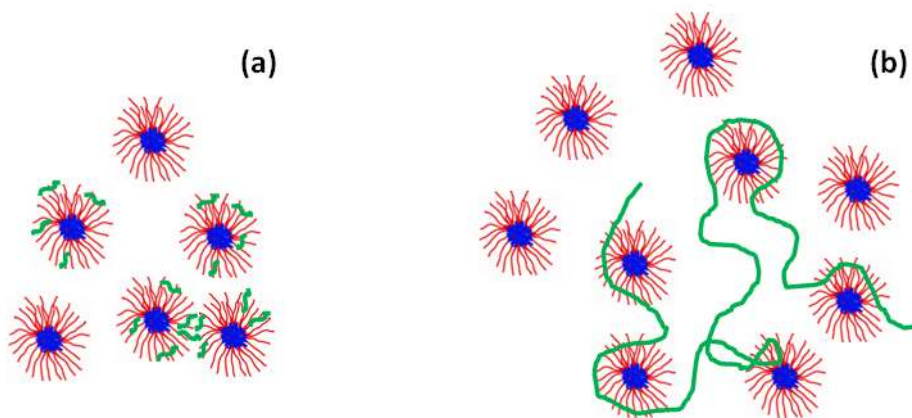
As pointed out earlier, some F127 chains can be associated with PAA ( $T < \text{CMT}$ ) via hydrogen bonding, and serve as nuclei for aggregation. For short PAA, these bound F127 molecules are easy for access by others, leading to formation of aggregates at a lower temperature, each comprising both bound F127 and unbound counterpart. The aggregates remain micelle-like with formation involving dehydration of PPO and nonzero  $\Delta H$ , as long as the bound F127 is not dominant in composition. Moreover, the enhanced affinity via the hydrophobic interaction between PPO and PAA backbone provides a more conducive

environment for aggregation, thereby requiring lesser dehydration and smaller  $\Delta H$ . With increasing PAA concentration, this effect becomes stronger and more F127 bound on PAA is present in the sample, eventually leading to vanishing  $\Delta H$ . Under this particular condition, the amount of added PAA is sufficient to cause self-assembly of polymer with no need to consume energy, but it is not clear whether the micelle-like structure will still remain or complexes with a different structure will emerge. At high pH, in contrast, the F127 unimers associated with PAA are considerably reduced due to the protonation of PAA. The copolymer molecules are expected to form micelles F127 in the ordinary way, except that the medium is the PAA solution instead of water. This could account for the slightly smaller CMT and  $\Delta H$  values when compared to the pure F127 system.

For the splitting of endothermic process obtained in F127/PAA(450k)/H<sub>2</sub>O system (Figure 4.6 (bottom)), the first peak (peak at lower temperature) is attributed to the formation of F127 aggregates on the PAA chains and the second peak to the formation of F127 free micelles in the bulk. Since the PAA chains are long, it is not easy for the unbound F127 to access the bound counterpart due to the steric constraint from the PAA. Therefore, a portion of the unbound F127 chains could form free micelles instead at a slightly higher temperature. At natural pH, with increase in PAA (450k) concentration, the fraction of F127 bound on PAA chains increases, explaining the growth of first peak relative to the second peak that eventually disappears at high enough PAA concentration. At high pH, the disappearance of peak splitting indicates that free micelles dominate, and F127 aggregates on PAA chains nearly vanish. A similar claim for split in

micellization process in high M.W. PAA solution has been reported for small nonionic surfactant C<sub>8</sub>E<sub>5</sub> via a surface tension study.<sup>125</sup> In such systems, the surfactant has been found to form micelles on the PAA chains at concentrations slightly lower than their actual CMC with a reduced aggregation number.<sup>125-127</sup> These findings are qualitatively analogous to our reduced CMT.

It is well known that the F127 micelles are thermoreversible.<sup>11, 12</sup> To check if the F127 micellization on the PAA chains is thermoreversible, we carried out heating-cooling-heating ramps for the system F127/PAA(450k)/H<sub>2</sub>O using DSC (refer to Figure A7 in Appendix). In the first round of heating, two overlapping endothermic peaks are seen as expected. In the subsequent cooling process, exothermic peaks with sizes same as the endothermic ones during the prior heating are seen, clearly illustrative of the thermoreversibility. When the second round of heating proceeds afterward, the two endothermic peaks identical to those in the first round are observed, indicating that both the PAA-bound micelles and the free F127 micelles are again formed.



**Scheme 4.1.** Complexes of F127 micelle and PAA chains with molecular weights of (a) 1.8k and (b) 450k g/mol for  $T > \text{CMT}$ .

## 4.2.3. Gelation

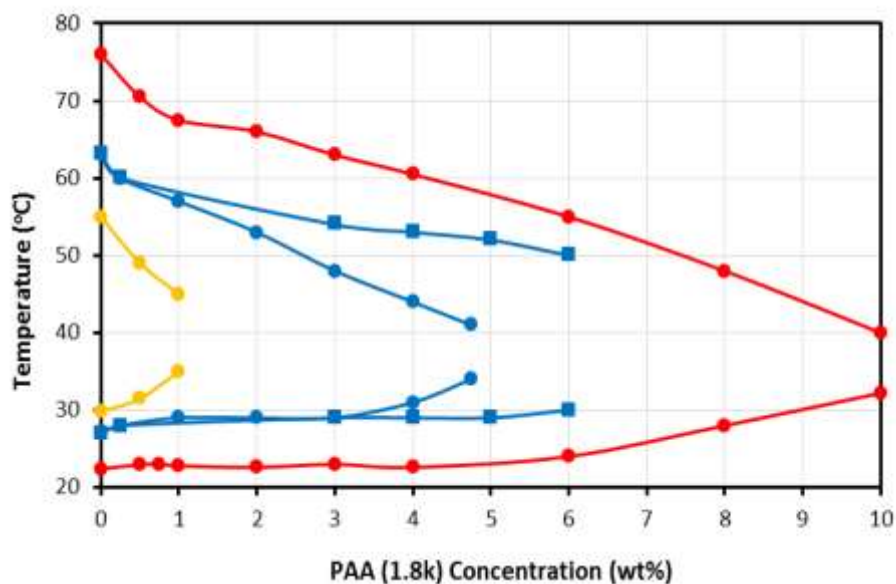


**Figure 4.9** Effects of PAA (1.8k) on the gel behavior of F127 at different concentrations; 20% (red), 17.5% (blue, circles) and 16% (yellow) at natural pH and 17.5% (blue, squares) at pH = 5

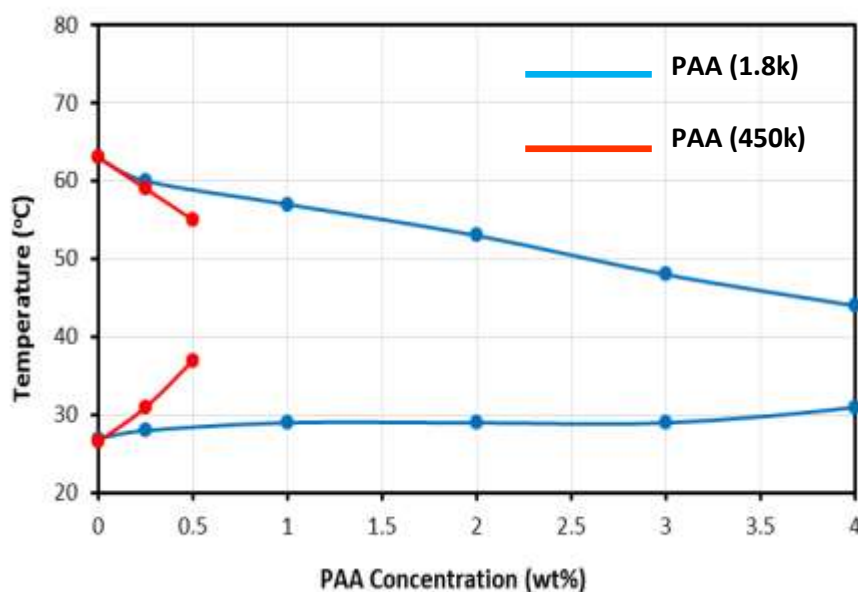


**Figure 4.8** Effect of PAA molecular weight on the gel behavior of 17.5% F127; Low M.W PAA (blue) and high M.W PAA (red)

Using the tube inversion method, we measured the critical gelation temperature (CGT) and gel melting temperature ( $T_m$ ). Figure 4.8 shows the variations of these two temperatures with the concentration of PAA (1.8k). It can be seen that the addition of PAA increases the CGT, but decreases  $T_m$ , thereby reducing the gel region of F127. The observed effects are dependent on 1) PAA concentration: the higher the PAA concentration, the greater the reduction in the gel region as shown in Figure 4.8; 2) F127 concentration: the higher the F127 concentration, the larger the amount of PAA is required to have an impact on the gelation; 3) PAA molecular weight: high M.W. PAA is more effective in reducing the gel region when compared to low M.W. PAA (see Figure 4.9); 4) pH of the medium – the higher the pH, the smaller the decrease in gel region caused by PAA (see Figure 4.8). Interestingly,  $T_m$  shows a stronger dependence on PAA concentration than CGT.

Our finding on the effect of PAA M.W. contradicts the behavior reported by Dos Santos et al.<sup>75</sup> using small angle X-ray scattering (SAXS). They found that PAA with smaller M.W. is more effective in destroying the structured phases of Pluronic P104. Important dissimilarities between their study and ours are 1) Methodology: they examine the evolution of structural phases using SAXS to find the sol-gel point, while rheometry and tube inversion technique is used in this work to determine this transition point. The contradictory findings are believed not due to this difference in methodology since the microstructure change associated with the sol-gel transition should also be detectable by rheometry. 2) Pluronic species: the Pluronic considered in their study was P104. To find if this

could be the reason for the contradicting results, the CGT for Pluronic P105 in the presence of PAA of both low and high M.W. were also measured (results not shown). The sol-gel behavior of P105 should closely resemble the P104 because of their similar block lengths. It is found that M.W. of PAA has a similar effect on P105 to that on F127; the higher the PAA chain length, the smaller the gel region. Therefore the difference in Pluronic species is not the reason. 3) Sample preparation: mixing and equilibration of samples were done using a centrifuge at 25°C in their study, as opposed to the traditional cold method<sup>13</sup> followed by storage at <5°C for equilibration in the present approach. According to their experimental procedure, the mixing took a considerably long time (sometimes days), so did the following equilibration at 25°C. In contrast, for the samples prepared here at low temperature, varying the storage time from a few days to a week or even a month is found to have no effect on the observed results. This leads to speculate that the difference in the sample preparation method could probably be the reason for the contradictory claims, although the exact cause remains unclear.

To study the gel strength of F127 in the presence of PAA, temperature sweeps for oscillatory flow test were carried out for selected samples using the rheometer with the results shown in Figure 4.10 and 4.11. The gelation in F127 is due to association of the micelles in an ordered arrangement when the PEO corona dehydrates.<sup>23, 28-30</sup> Two interesting observations are made. First, the addition of PAA results in two different slopes for the curve  $G'$  vs temperature during gelation before the plateau value of the gel is reached. Second, the

temperature interval for the transition increases with the PAA addition. This finding implies that the PAA exerts an influence on the structural evolution by means of hindering both the initial caging and the subsequent structural rearrangement of micelles. The PAA chains bound to F127 aggregates restrict the translational movement of the latter, and could hence lead to order disruption. This obstacle is more pronounced with increasing PAA chain length, accounting for the observed effect of PAA M.W. in gel suppression. The presence of PAA also decreases the elasticity of the formed gel as seen in Figure 4.10 and 4.11. Even below the gelation point, the addition of PAA also leads to a rise in  $G'$  by one or two orders of magnitude when compared to the pure F127 solution. As mentioned earlier, F127 aggregates bound on PAA chains with high M. W. could result in physical crosslinking of the latter (interchain association), forming large complexes and enhancing  $G'$ . PAA with low M.W. could connect micelles to form small clusters, and enhance the elasticity slightly.

At high pH, the added PAA results in a smaller decrease in the gel region as shown in Figure 4.8. Since the binding between PAA and F127 micelles hardly occurs, micelles can move and adjust their arrangement more easily in favor of gel formation.



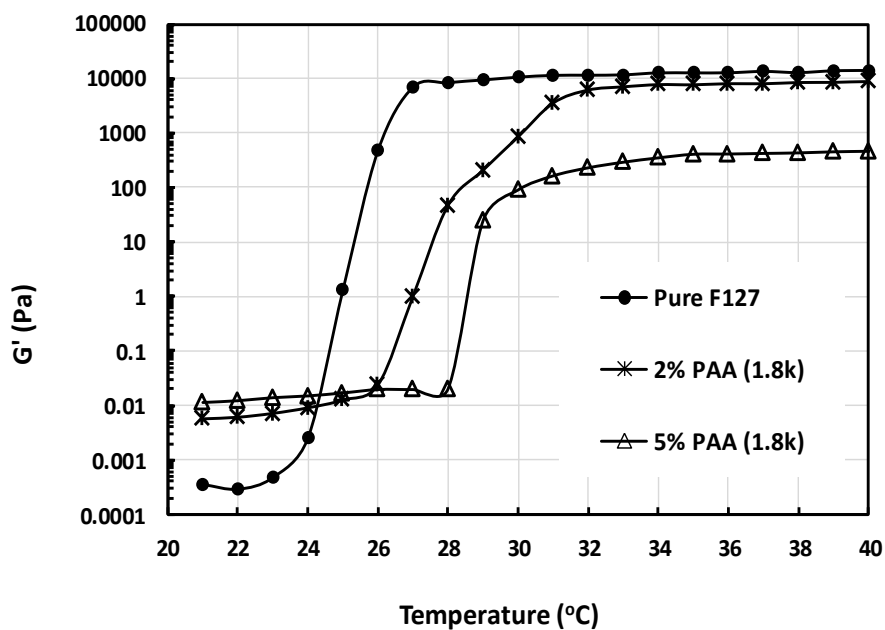


**Figure 4.10** Effects of PAA (1.8k) conc. on oscillatory temperature sweeps of F127/water system; F127 conc. = 17.5%

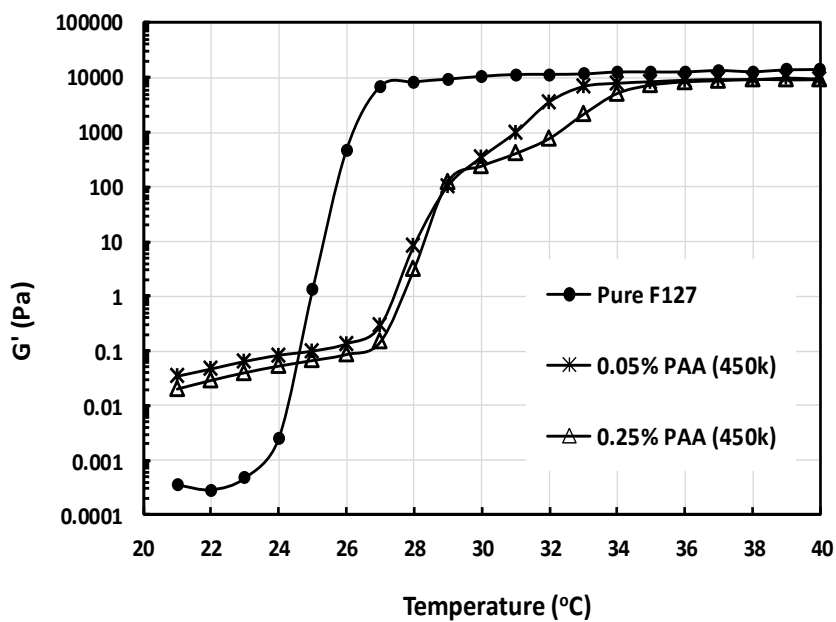


**Figure 4.11** Effects of PAA (450k) conc. on oscillatory temperature sweeps of F127/water system; F127 conc. = 17.5%

#### 4.2.4. Comparison with other commonly studied additives

It is interesting to compare the effect of PAA with other commonly studied additives like n-alkanols and salts with F127. Usually, if additives reduce  $\Delta H$ , they increase the CMT of F127<sup>19, 106</sup> (eg. ethanol), and vice versa (eg. butanol)<sup>19, 34</sup>. PAA however does not fall in any of these two categories because it decreases both CMT and  $\Delta H$  of F127. In the literature, the effect of small molecules as additives such as alcohols is thought to be associated with solvency change or their influence on water structure for hydration/dehydration. PAA is a weak polyelectrolyte with molecular size much larger than water. Therefore, its behavior cannot be appropriately explained by the mechanism of those medium-modifying additives. Moreover, the interaction between F127 and PAA via hydrogen bonding is exercised in a more direct manner. Figure 4.12 compares the effect of PAA on DSC thermogram of F127 with that of homopolymer poly(ethylene oxide) (PEO) with comparable M.W, which was examined in the last

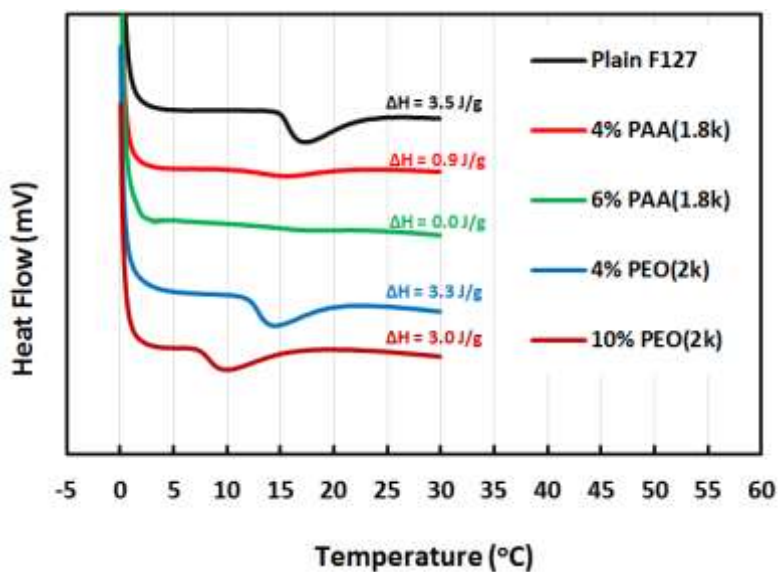


**Figure 4.12** DSC Thermograms of 17.5% F127 with the addition of PAA (1.8k) and PEO (2k); Estimated uncertainty:  $\Delta H \pm 0.2$  J/g

chapter. For PAA system,  $\Delta H$  becomes undetectable when the homopolymer concentration is 6%, while the decrease in  $\Delta H$  value is meagre for PEO even at relatively high concentration (10%). This suggests that the interaction for F127/PAA is much stronger than for F127/PEO. However, an interesting commonality between PAA and PEO is that they both reduce the CMT of F127, but increase the CGT or even curb the gelation.

### 4.3. Conclusion

Micellization and gelation have been studied to understand the role of PAA in the behavior of Pluronic F127 triblock copolymer. It is found that, the critical micellization and gelation temperatures (CMT and CGT), enthalpy of micellization ( $\Delta H$ ) and the gel strength depend strongly on medium pH, PAA concentration and molecular weight.

For the micellization, addition of PAA lowers the CMT of F127, unlike the behavior claimed in a prior study.<sup>122</sup> Hydrogen bonding between COOH of PAA and PEO blocks of F127 leads to a decreased effective block length of PEO, thereby enhancing the ease of micellization. Hydrophobic interaction between PPO blocks and aliphatic backbone of PAA increase their affinity, hence providing a more suitable environment for PPO in favor of aggregation without consuming as much energy in dehydration. At high enough concentration of PAA, DSC may no longer show any detectable endothermic peak. It is not clear if the corresponding formed complexes remain micelle-like. At high pH, to the

contrary, both CMT and  $\Delta H$  become weakly affected by the presence of PAA because the deprotonated the PAA chains are not favorable for the association with F127.

For the gelation, the CGT is increased, and the gel strength ( $G'$ ) is reduced in the presence of PAA of both low and high M.W. The effect is greater for high M.W PAA. Order disrupting for the packed F127 micelles due to PAA is responsible for the observed changes in CGT and  $G'$ . The present study can advance the understanding of structure-property relationships, and facilitate the effectual exploitation of block copolymer + PAA systems in various applications such as ocular drug delivery.

## 5. Sol-Gel Behavior of Pluronic Binary Mixture with Non-identical PPO Block Lengths

---

In this chapter, first of all, relevant literature on the nature of micelles in triblock copolymer binary mixtures is reviewed. The present study is aimed to shed light on the nature of micelles in PEO-PPO-PEO copolymer binary mixtures with different PPO block lengths. In concentrated regime, gelation and rheology of the mixtures are also explored. Experimental in this section has been carried out using dynamic light scattering (DLS), differential scanning calorimetry (DSC), small angle X-ray scattering (SAXS), polarized light microscopy (PLM), tube inversion technique and rheometry.

### 5.1. Introduction

In general, for a mixture of two block copolymers, the micelles can be any of the two types: (1) mixed micelles containing both polymer species, and (2) two separate families of micelles each incorporating only one polymer species (separate or pristine micelles). As mentioned in the Chapter 1 the mixture of copolymers with similar hydrophobicity most likely forms mixed micelles, although the hydrophobic blocks could be different in length and chemical structure. Therefore for Pluronic copolymers, mixtures with similar PPO block lengths are expected to form mixed micelles since they have equivalent hydrophobicity. This has indeed been verified using light scattering<sup>31</sup> For the mixtures with different PPO block lengths or hydrophobicity, there exist different claims on the nature of micelles. Gaisford et al.<sup>81</sup> used a UV spectrometric

method to find that mixtures F77 + F127 and F87 + F127 with dissimilar PPO block lengths exhibited two different CMT values. This observation led them to claim separate micellization for those having dissimilar PPO block lengths. Very recently, Zhang et al. used differential scanning calorimetry (DSC) to detect two endothermic peaks for the system F127 + F68 with dissimilar PPO block lengths, and interpreted this finding as a result of separate or independent micellization.<sup>82</sup> Having similar observation in an early study on P105+L64 with different PPO block length,<sup>83</sup> Zhou et al., on the contrary, speculated otherwise without further investigation because structural analysis was the main focus in their study.

The literature outlined above indicates that further detailed investigations are required to unravel the nature of micelles in Pluronics with dissimilar PPO block lengths. Moreover, there are very few studies on gelation behavior of mixed Pluronics.<sup>31, 84</sup> Therefore, the aim of this work is to examine micellization and gelation of mixed Pluronics with varying temperature using DLS, DSC, cloud point measurements, tube inversion, rheometry, SAXS, birefringence and <sup>13</sup>C - NMR. We study two mixtures F127+P105 and F127+L64 (F127: EO<sub>98</sub>PO<sub>67</sub>EO<sub>98</sub>; P105: EO<sub>37</sub>PO<sub>56</sub>EO<sub>37</sub>; L64: EO<sub>13</sub>PO<sub>30</sub>EO<sub>13</sub>). They are chosen for the following reasons: (1) the CMT values of parent Pluronics are very close to each other in F127+P105, but far apart in F127+L64, allowing us to study the effect of CMT difference on the self-assembly, (2) the parent Pluronics in each of the two mixtures form spherical micelles with different sizes, discernable by DLS, and (3) the properties of these Pluronics fall in the range that can be conveniently characterized by the aforementioned methods.

## 5.2. Results and discussion

### 5.2.1. Critical micellization temperature

DSC measurements were carried out for various weight ratios of F127:L64 and F127:P105 keeping the total polymer concentration at 25%. The thermograms are shown in Figure 5.1, where the broad endothermic peak is due to dehydration of PPO blocks of Pluronic when the temperature is high enough.<sup>12</sup> Since the dehydration of PPO block is the driving force for micelle formation, the endothermic peak has customarily been regarded as the CMT.

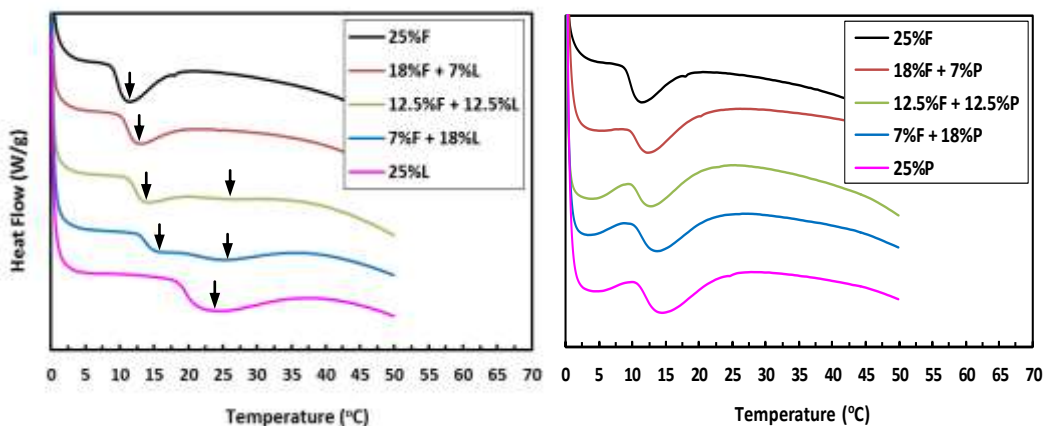


**Figure 5.1** DSC thermograms of various weight ratios for F + L (left) and F + P (right); F:F127, P:P105, L:L64

One can see from Figure 5.1 that each pure Pluronic has a single endothermic peak with peak temperature at 11.4°C (F127), 23.2°C (L64) and 14.7°C (P105). It shows that the micellization temperatures of F127 and L64 are more than 11°C apart, while those of F127 and P105 are very close (just ~3°C apart). Since pure F127 and P105 each form micelles at very similar temperatures, their mixture also exhibits only one endothermic peak (Figure 5.1 (right)). This single peak corresponds to dehydration and micellization of both F127 and P105.

Unlike F127+P105, the mixture F127+L64 has two peaks in their thermogram as indicated with arrow marks for easy reading (Figure 5.1 (left)). It has been reported that Pluronic with greater PPO block length forms micelles at lower temperature than those with smaller PPO block length.<sup>82, 83</sup> The low-temperature peak observed for F127+L64 in Figure 5.1(left) corresponds to the dehydration of F127, and the other peak signals the dehydration of L64. This observation shows that even upon mixing, the two Pluronics would dehydrate only at their respective critical temperatures. Nevertheless, the presence of two peaks in DSC curve does not necessarily attest separate micellization of the two Pluronics. To further examine the micellization behavior of mixtures, dynamic light scattering (DLS) experiments were conducted.

CMT of Pluronics at low concentration can be characterized by light scattering method since the unimer-micelle transition will cause a significant increase in the scattering intensity.<sup>16, 17</sup> Figure 5.2 illustrates the change in scattered light intensity with temperature for pure F127, L64, P105 and the mixtures F127+L64 and F127+P105. The CMT is determined by the point of intersection between two tangential lines (as demonstrated for the case of pure F127) except for pure L64. For pure L64, an additional peak is observed just before the onset of micellization. As pointed out by Kositza et al.,<sup>128</sup> this peak with high scattering intensity is attributed to hydrophobic impurities (least soluble) that form large aggregates to share a common hydrophobic environment just before the CMT is reached. Once the micelles form at temperatures  $\geq$  CMT, these impurities are thought to solubilize within the core of the micelles.<sup>31, 128</sup>



Therefore, the temperature at the peak is designated as the CMT for pure L64.<sup>31</sup> The CMT values obtained from this scattering method for F127 (~25°C) and L64 (~34°C) are around 9°C apart, while the CMT for P105 (~25°C) is nearly the same as that for F127. The difference between CMT values of parent Pluronics is similar to that obtained by DSC as shown in Figure 5.1, despite very different polymer concentrations.

For F127+L64, the scattering intensity starts to increase at ~25°C. This increase in intensity is due to formation of F127 micelles since the dehydration point of F127 has been reached. With further increase in temperature for

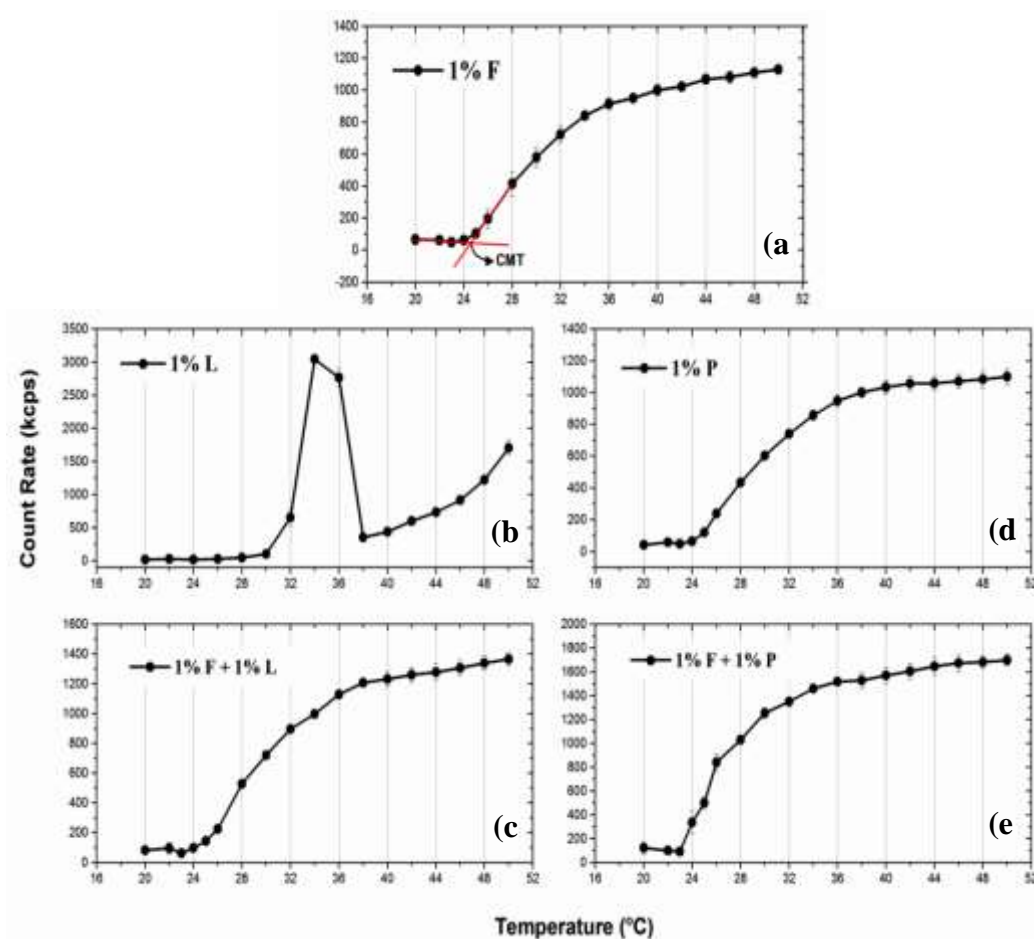


**Figure 5.2** Light scattering intensity vs. temperature for 1%F (a), 1%L (b), 1%F + 1%L (c), 1%P (d) and 1%F + 1%P (e); F:F127, P:P105, L:L64

dehydration of L64 (~34°C), if this species underwent independent micellization to form separate micelles, a slope increase in the scattering intensity curve would be expected because of a sudden increase in the total number of micelles.<sup>78, 80</sup> However, such a slope increase is not observed for temperature up to 50°C. In fact, the scattering intensity vs. temperature curve for F127+L64 appears very similar to that for pure F127. This analogy suggests that instead of forming separate micelles, L64 chains tend to participate in the already existing F127 micelles. Another interesting observation is that the high intensity peak arising from the impurities in pure L64 is completely absent in F127+L64, indicating the solubilization of the impurities into the core of F127 micelles instead of forming large aggregates.

### 5.2.2. Size analyses

To further confirm this behavior, the size distribution of micelles for parent Pluronics and for the mixtures F127+L64 and F127+P105 is examined. Distribution of hydrodynamic radius  $R_h$  may provide clues for the existence of mixed micelles or separate/independent micelles.<sup>31, 80, 129</sup> For the mixtures, a single peak with a narrow size distribution is indicative of existence of mixed/co-micelles,<sup>31, 129</sup> while a single broad peak or a bimodal size distribution suggests two separate micelle families.<sup>80</sup> The intensity-weighted size distributions at 40°C and 60°C are presented in Figure 5.3 and Figure 5.4. The obtained  $R_h$  of parent Pluronics are in good agreement with the literature.<sup>99, 130-132</sup> Note that the size distribution of 1% L64 at 60°C becomes very broad with the peak centered at ~163 nm shown in Figure 5.4. This is due to the micellar clustering reported for

pure L64 above 52°C.<sup>128</sup> For F127+L64 or F127+P105, a single sharp peak with a rather narrow size distribution (PDI <0.1) is always observed, suggesting the presence of mixed micelles. In particular at 60°C, the peak size for F127+L64 becomes very small (10.47 nm) and the distribution becomes very narrow (PDI <0.1) in stark contrast to the behavior of pure L64. This drastic difference provides evidence for the formation of mixed micelles, in which the long PEO blocks of F127 prevent the micelles from clustering via steric stabilization.

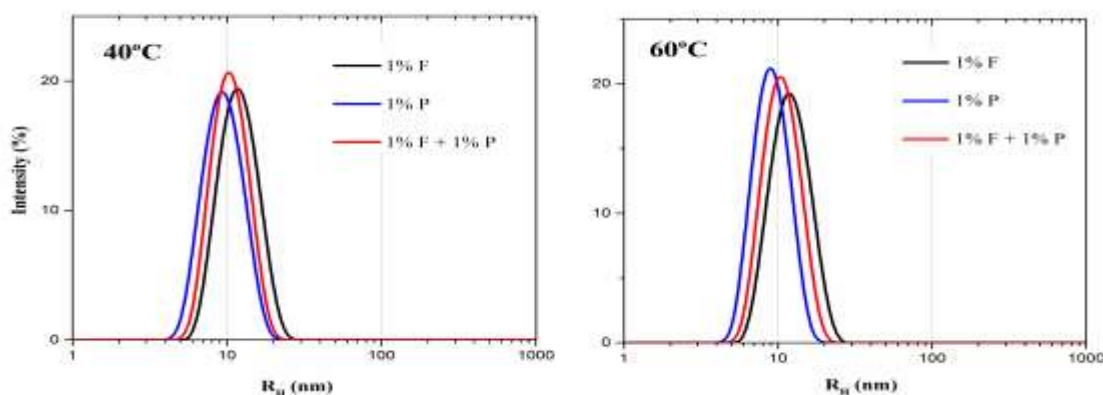


**Figure 5.3**  $R_h$  distribution of pluronic mixture F + P (F:F127 and P:P105) at 40°C (left) and 60°C (right)

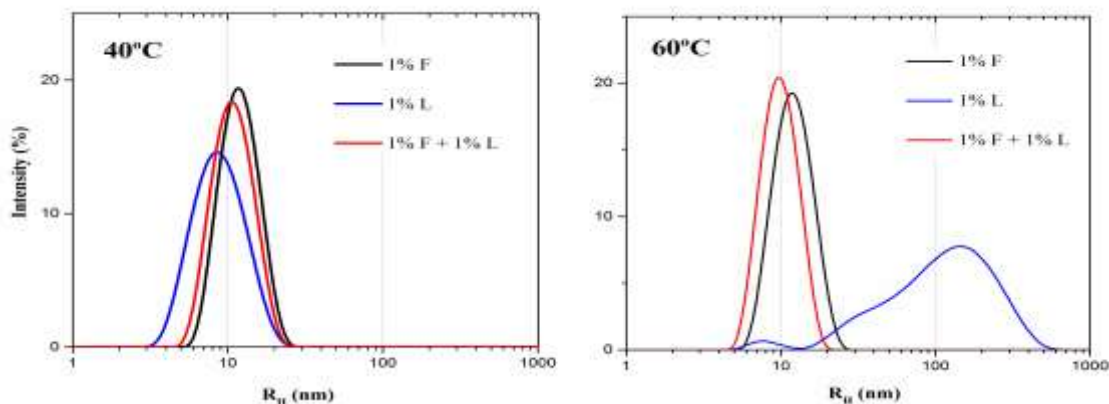


**Figure 5.4**  $R_h$  distribution of Pluronic mixture F+L (F:F127 and L:L64) at 40°C (left) and 60°C (right)

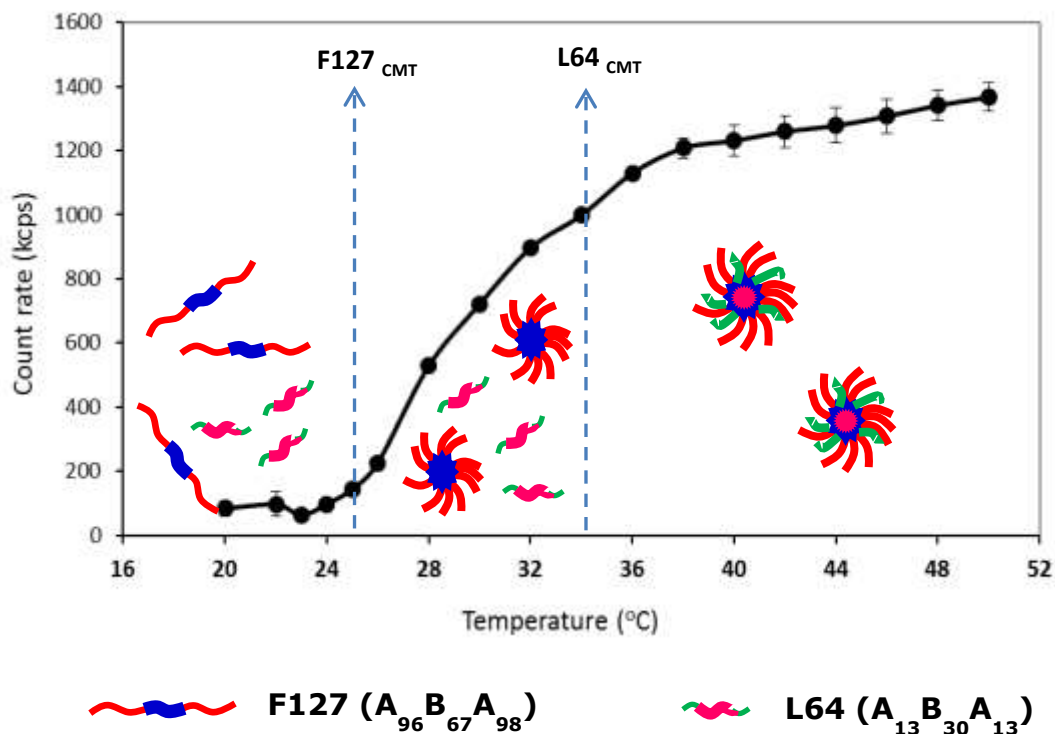
### 5.2.3. Cloud point (CP) studies

**Table 5.1** CP temperatures of pure Pluronics and their mixtures

Sample	CP (°C)
<b>Effect of increasing F127 concentration</b>	
0.5% L64	52
0.5% L64 + 0.5% F127	74
0.5% L64 + 1% F127	-
0.5% L64 + 2% F127	-
<b>Effect of weight ratios L64:F127 (total polymer concentration = 1%)</b>	
1% L64	52
0.75% L64 + 0.25% F127	64
0.5% L64 + 0.5% F127	74
0.25% L64 + 0.75% F127	-
1% F127	-
Maximum tested temperature = 84°	

Clouding is an indication of instability of micellar solutions; at high temperature, micelles may form large aggregates, resulting in cloudy appearance. This phenomenon happens to pure L64 or P105 solutions, but not to F127 in the temperature range investigated. Table 5.1 shows the measured CP for samples with L64 at 0.5% as the F127 concentration increases, and for samples at total polymer concentration 1% but different weight ratios of L64:F127. The CP temperature of pure L64 is in satisfactory agreement with the literature.<sup>133</sup> As the concentration or proportion of F127 is increased in the system, the CP temperature is increased dramatically. A similar trend is also observed for P105+F127 system (not shown). The progressive increase in CP with increasing

concentration of F127 suggests formation of mixed micelles with improved stability due to long PEO blocks of F127.



**Scheme 5.1** Nature of micelles with respect to temperature in F127+L64 mixture

From the above analyses, it is evident that both the mixtures studied form mixed micelles. For F127+L64, F127 forms micelles first as the temperature is increased to its PPO dehydration point. With further increase in temperature, most L64 will participate in the existing micelles when its PPO blocks dehydrate, as illustrated in Scheme 5.1. In addition, the hydrophobic impurities present in L64 are dissolved into F127 micelles. However, the possibility of pristine L64 micelles formed at small amount may not be ruled out entirely, although the used experimental methods cannot detect. For F127+P105, the two species dehydrate around the same temperature to form mixed micelles. Therefore, it is concluded

that a mixture of Pluronics even with different PPO block lengths can form mixed micelles, despite a considerable difference between the CMT values of their parent Pluronics. This contradicts the earlier claim that mixture of Pluronics with different CMT values forms separate micelles.<sup>81, 82</sup>

#### 5.2.4. Gelation and rheology

The phase behavior for various ratios of F127:L64 with total polymer concentration fixed at 25% is studied when the temperature is varied. Figure 5.5 shows the temperature ranges of sol and gel states of each sample based on the tube inversion method. Pure 25% F127 gels at 18°C, which is in good agreement with the literature.<sup>31, 36</sup> An interesting observation is that samples with certain F127:L64 ratios form gel again (2<sup>nd</sup> gel) after the first gel melts. The sample

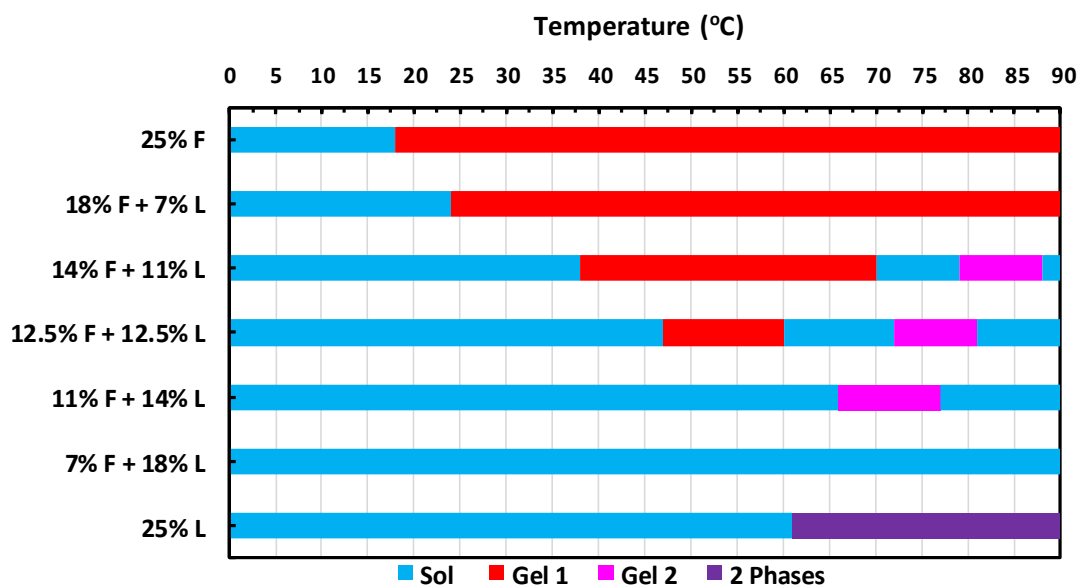


**Figure 5.5** Sol-gel behavior of F+L (F:F127, L:L64) system determined by tube inversion technique

appearance at different temperature is illustrated in Figure 5.7.

To gain more insight on this behavior, oscillatory temperature sweeps are carried out to measure the storage and loss moduli ( $G'$  and  $G''$ ) with the

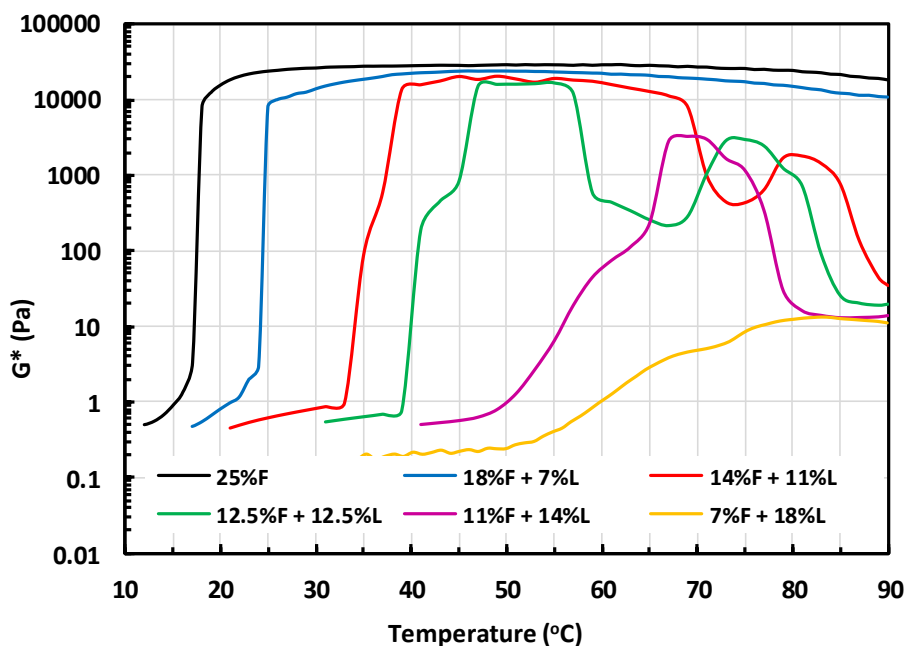


**Figure 5.6** Oscillatory temperature sweeps of varying ratios of F: L (F:F127, L:L64) with total polymer concentration fixed at 25%

rheometer. Figure 5.6 plots the complex modulus  $G^*$  against temperature. Since pure 25% L64 phase separates when its cloud point temperature ( $61^\circ\text{C}$ ) is reached, rheological experiments are not carried out. Figure 5.6 confirms the existence of two gel states for the systems 14%F127 + 11%L64 and 12.5%F127 + 12.5%L64. Other than the existence of two gel regions, we also find that  $G'$  dominates over  $G''$  even in the region in between them, although the results are not shown. According to the literature, gels could be classified into hard gels ( $G' > 1000$  Pa) and soft gels ( $G' < 1000$  Pa).<sup>31, 36</sup> This soft gel goes undetected in the

tube inversion technique due to its very small yield stress ( $< 40\text{Pa}$ ). The finding of two hard gel states separated by a soft gel with respect to temperature change is new for mixed triblock copolymer systems. Other observed characteristics are described below:

1) For hard gel 1, its CGT increases and its temperature range becomes narrower as the proportion of L64 increases in the mixture. This gel for all Pluronics ratios studied here appears clear in most part of its temperature range but becomes turbid just before the commencement of the degelation, except for the pure F127 gel.

2) The soft gel appears transparent in all the mixtures except at temperatures near the CGT of hard gel 2, where the sample turns hazy and is about to transform to the hard gel. This CGT becomes lower with decreasing F127 proportion in the mixture. With further increase in temperature, the gel haziness increases progressively towards opaqueness. Since  $G'$  of this hard gel is found to be always smaller than that of hard gel 1, the latter is stiffer.



**Figure 5.7** Images of tilted glass tubes with the mixture 12.5% F127 + 12.5% L64 at different temperatures; the sample appearance did not change after one week



3) Hard gel 2 is formed during the temperature ramp up but not attainable during the ramp down, whereas hard gel 1 is more or less thermoreversible (Figure 5.8). This implies that it is kinetically difficult to rehydrate the sample for restoration of the second hard gel during the cooling process. This observation remains qualitatively unaffected when the heating/cooling rate was varied in the investigated range (see Figure 5.9). All these complex behaviors are not completely understood.

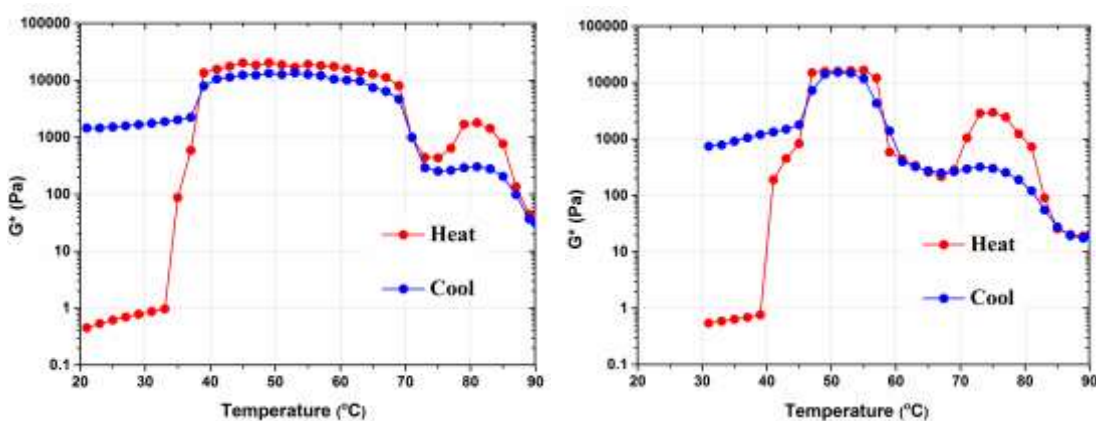


**Figure 5.8** Oscillatory temperature ramp up and ramp down for 14% F + 11%L (left) and 12.5%F + 12.5%L (right); F:F127, L:L64

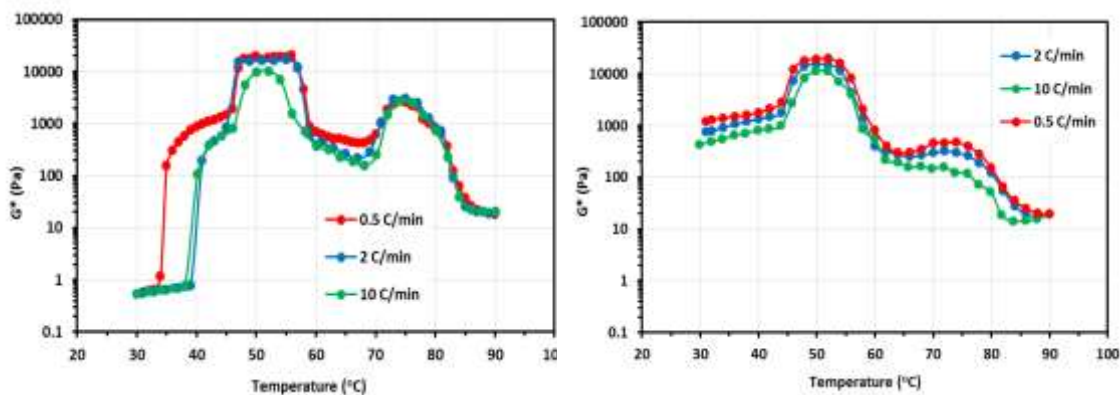


**Figure 5.9** Effect of heating rate (left) and cooling rate (right) on  $G^*$  of 12.5%F127+12.5%L64 mixture

Newby et al.<sup>84</sup> investigated the phase behavior of the mixture P85+P123. Since each of the parent Pluronics alone in aqueous solution has two gel phases, it is not surprising to see a similar behavior for their mixture. In the system considered in this work, to the contrary, neither of the parent Pluronics (F127 and L64) exhibits two gel states when it is alone. In fact, pure L64 at 25% does not form gel at any temperature, while pure F127 has only one gel phase. The presence of two different gel regions separated by a liquid or soft gel phase was reported previously only for very few pure Pluronics with relatively short PEO block lengths such as P103,<sup>134, 135</sup> P94<sup>30</sup> and P85.<sup>30, 136</sup> The second gel of P85 results from hexagonal packing of cylindrical micelles,<sup>30, 137, 138</sup> while that of P103

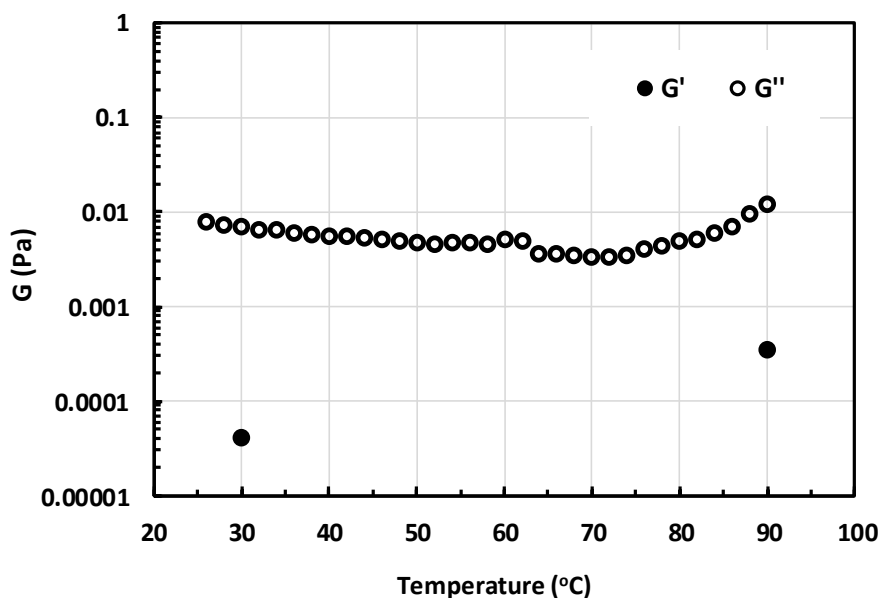


**Figure 5.10** Oscillatory temperature sweep for the mixture 1% F127 + 1% L64

is attributed to a disordered macrophase (turbid) driven by strong hydrophobic attraction between the micelles.<sup>134, 135</sup> Interestingly, P85 exhibited a 2nd gel region even at very low concentrations down to 0.5 - 1.0wt%.<sup>136</sup> The resulting

elasticity at such low concentrations was attributed to hindered rotation of rodlike micelles formed at high temperatures. Unlike P85, the mixture 1%F127 + 1%L64 shows negligible elasticity even at temperature up to 90°C (Figure 5.10). This observation implies that rodlike micelles are very unlikely to form for F127+L64 at low concentrations.

### 5.2.5. Microstructure

To get more information on the microstructures of these different gel regions, SAXS analysis was also carried out. As reported in the literature, the Bragg reflections always tend to become very weak in lyotropic liquid crystalline phases such as those found in Pluronics<sup>28</sup> due to short range disorder in the structure.

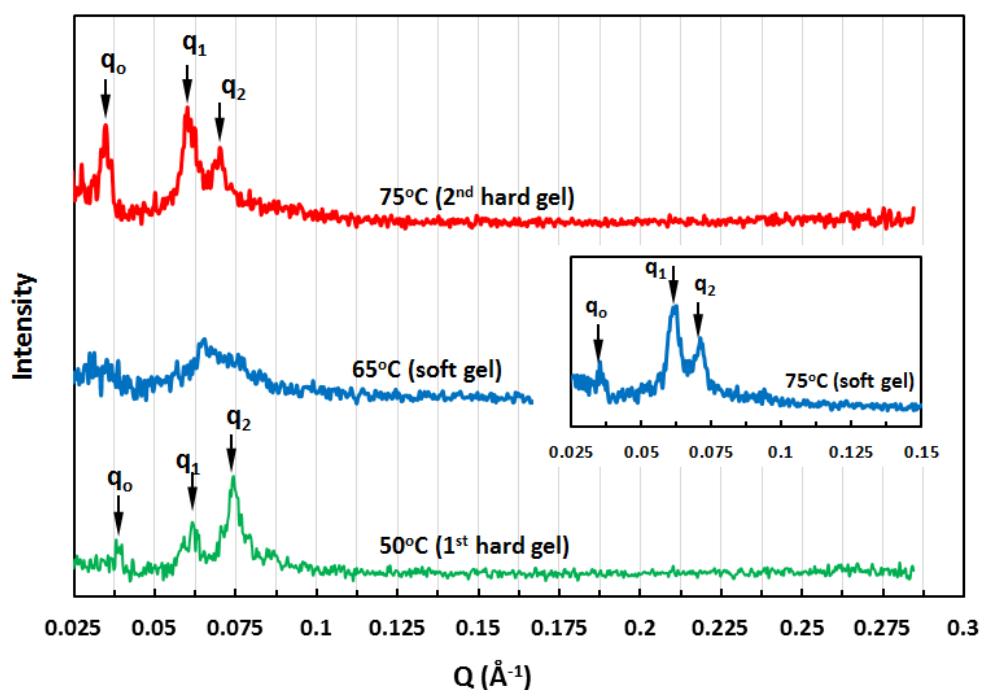


**Figure 5.11** SAXS patterns for the mixture 12.5% F + 12.5% L at different gel regions; Inset: SAXS pattern for soft gel region of 14%F + 11%L; (F:F127, L:L64)

However, these reflections are sufficient to reveal the packing of micelles.<sup>28, 29, 36</sup> The SAXS spectra of pure 25% F127 and pure 25% L64 are shown in Figure A4 in appendix. The relative positions of the peaks show a face centered cubic structure (FCC) for pure F127 gel in agreement with the literature.<sup>29</sup> Pure 25% L64 exhibits only a broad peak characteristic of a disordered system because it never forms a gel at any temperature. We note that the fundamental peak ( $q_0$ ) could not be seen for pure F127 at certain temperatures (not shown). This problem has also been reported previously for similar systems,<sup>29, 139</sup> but the exact cause is not fully understood.

Figure 5.11 shows the SAXS profiles of the mixture 12.5%F127 + 12.5%L64 at three different temperatures. At 75°C (2<sup>nd</sup> hard gel region), three distinct peaks are observed at  $q_0 = 0.034$ ,  $q_1 = 0.061$  and  $q_2 = 0.070$  (1/Å). These relative positions resemble those for a hexagonal crystalline phase (1:  $3^{1/2}$ :  $4^{1/2}$ ) more than for a cubic one (refer Table A2 in appendix for detailed indexation of the peaks). At 50°C (1<sup>st</sup> hard gel region), the fundamental peak is suppressed, similar to certain other systems as pointed out earlier. But the higher order peaks are clearly seen, and indexed to a face centered cubic phase [1:  $(8/3)^{1/2}$ :  $(11/3)^{1/2}$ ]. To confirm, the samples for birefringence under crossed polaroids was also examined using polarized light microscopy (PLM). The second hard gel exhibits birefringence, but the first one does not. This verifies that the first hard gel is isotropic, while the second one is anisotropic. At 65°C (intermediate soft gel region), the SAXS spectrum shows a relatively broad peak compared to the other two temperatures. This is attributed to either a less ordered phase or a mixture of

coexisting phases (cubic, hexagonal and disordered). For comparison, the mixture of different composition (14%F127 + 11%L64) was also examined. To the contrary, the soft gel (75°C) exhibits a hexagonal structure as shown in the inset of Figure 5.11, while the SAXS patterns of hard gels 1 and 2 are similar to those for the mixture 12.5%F127 + 12.5%L64 (not shown).

To check if the core-corona micelle structure is retained at high temperature,  $^{13}\text{C}$  NMR studies for the same sample (12.5%F127 + 12.5%L64) was carried out at different temperatures with the results shown in Figure A5 in appendix. It is found that the core-corona micelle structure remains even in the temperature range of the second hard gel.

Pluronic micelles tend to grow with temperature in order to reduce the surface to volume ratio and the associated interfacial energy,<sup>28</sup> so does their volume fraction,<sup>30</sup> if they remain stable. The thermal stability is enhanced with an increase in PEO content (block length).<sup>28</sup> When the critical value ( $\Phi_c \sim 0.53$ ) is reached, the spherical micelles tend to pack themselves into cubic arrangement to become a gel.<sup>23, 30</sup> For F127+L64, the effective PEO content decreases when the F127 proportion is reduced in the mixture. This leads to smaller micelles compared to pure F127 as shown in Figure 5.4, because the thickness of the less dense corona decreases. Therefore, the effective micelle volume fraction will reach the critical value ( $\Phi_c \sim 0.53$ ) at relatively higher temperature to form the cubic phase. Also, the decrease in the apparent volume of corona leads to weaker repulsion between the micelles and hence a lower stability against degelation. This explains the narrower temperature range of the first gel with decreasing F127 proportion.

With further increase in temperature, micelles may change their shape in order to incorporate more polymer molecules to be packed into the aggregates via chain stretching to reduce interfacial energy. Hence, rodlike micelles with small curvature become more favorable because of low surface to volume ratio when compared to the spherical counterpart.<sup>28</sup> Formation of rodlike micelles is also facilitated by weaker repulsion between the micelles, which can be achieved more easily with small PEO blocks. As such, one would expect a decline in the sphere to rod transition temperature with decreasing PEO content.<sup>30</sup> When the proportion of L64 is increased in the mixture F127+L64, the effective PEO content decreases and hence the steric repulsion between the micelles also decreases. This explains why the rodlike micelles can be formed to become the second hard gel for the mixture, while pure F127 does not form a hexagonal phase in the temperature range studied. Note that pure F127 was reported to undergo sphere to rod transition only at 95°C.<sup>30</sup> When L64/F127 mass ratio becomes high enough, only the anisotropic gel can form or no gelation can take place whatsoever as seen in Figure 5.5 and 5.6. This is because the effective PEO content becomes too low for the micelle volume fraction to reach the critical packing condition. In fact, pure 25% L64 turns cloudy at 61°C and then phase separates due to very weak steric repulsion between the micelles.

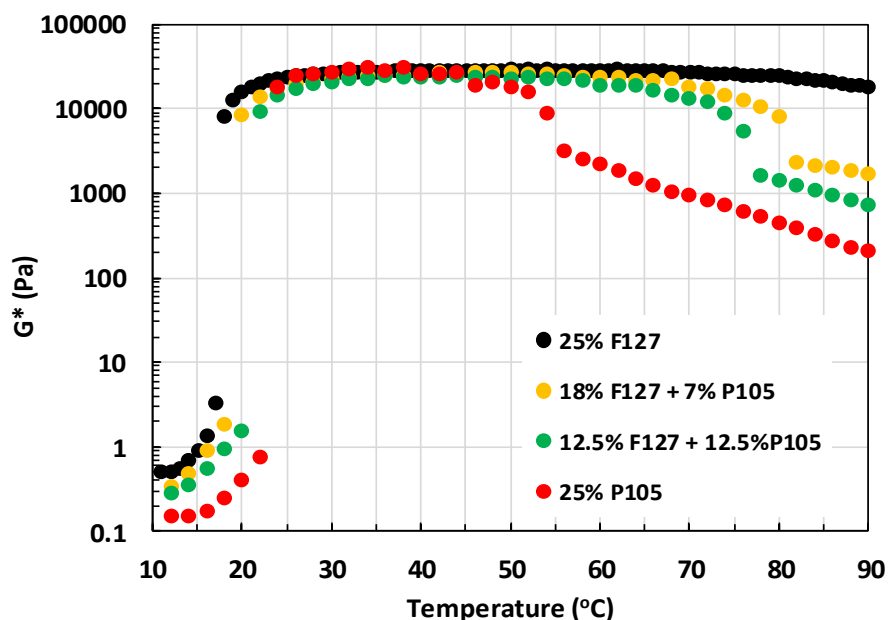


**Figure 5.12** Oscillatory temperature sweeps of varying ratios of F127: P105 with total polymer concentration fixed at 25%

The gelation behavior of F127+P105 mixture is comparatively simple since it has only one clear hard gel phase (Figure 5.12). The sol to gel transition and gel to sol transition (melting) temperatures of the mixtures lie in between the transitions points of pure F127 and P105.

### 5.3. Conclusion

Sol/gel behavior of aqueous Pluronic triblock copolymer binary mixtures with dissimilar PPO block lengths (F127 + L64 and F127 + P105) has been investigated. Our DSC studies revealed that the polymers dehydrate only at their own critical temperatures even after mixing. However, concerted studies on micelle size distribution, temperature dependence of scattering intensity, and CP

confirm the formation of mixed micelles. For F127 + L64 upon heating, F127 chains dehydrate first to form micelles followed by the L64 dehydration and participation in existing F127 micelles at higher temperature. For F127 + P105, since CMT values of F127 and P105 are quite similar, cooperative aggregation takes place directly around the same temperature leading to mixed micelles. Our results show that a mixture of Pluronics with a considerable difference between the CMT values of their parent Pluronics can form mixed micelles, unlike the behavior in the earlier reports.<sup>81, 82</sup>

Rheology of F127 + L64 mixture exhibits two hard gel states separated by a soft gel. The presence of two hard gel states is unexpected since neither of the two parent Pluronics exhibits such two gel states in the investigated temperature range. The elasticity of first hard gel is always higher than that of second hard gel. Tube inversion method, PLM and SAXS analysis show that the first hard gel is clear, non-birefringent and cubic structured, while the second one is found to be hazy with micelles hexagonally packed showing birefringence. Also, the first hard gel can form in both temperature ramp up and down, whereas the second one is attained only in the heating process as evidenced by oscillatory temperature sweeps. These findings demonstrate that mixture of block copolymers is a promising approach to tune/control the gel structure and properties.



## 6. Effect of Pluronics and Other Additives on Rheology of Corn Starch Suspension

---

In this chapter, firstly, relevant literature on the rheology of concentrated corn starch (CS)/H<sub>2</sub>O suspension is reviewed. The present work is aimed to study the influence of Pluronic F127 block copolymer, poly (ethylene oxide) (PEO) homopolymer and poly (ethylene glycol) with 200 g/mol (PEG) on the shear thickening behavior of CS/H<sub>2</sub>O suspension. Experimental in this section has been carried out using shear and oscillatory rheometry, Fourier transform infra-red spectroscopy (FTIR) and optical microscopy.

### 6.1. Introduction

Non-Newtonian fluids are those which deviate from the Newton's law of viscosity. They are used in our day- to-day life (food, inks, cleaning agents, personal care products, etc) and find application in different industries such as pharmaceutical, concrete, mining, etc. One among them is shear thickening fluid (STF) whose viscosity increases with shear rate/stress. The shear rate/stress at which the viscosity starts to increase is called critical shear rate/stress. Generally, shear thinning (decrease in viscosity with shear rate/stress) is observed before and after the shear thickening regime.<sup>140, 141</sup> The precise mechanism behind the shear thickening behavior could vary from case to case, and is still debatable. While the general mechanisms behind the shear thickening for particle dispersions was believed to be dilation<sup>94, 142</sup> or formation of hydroclusters,<sup>85, 143-145</sup> very recently Waitukaitis et al.<sup>146, 147</sup> claimed that neither of these mechanisms alone can

explain the act of a person running on the corn starch (CS) suspension without sinking. They showed that a rapidly growing solid front created by the impact is the reason for very high momentum absorption. STFs are currently tested for their potential use in commercial applications such as liquid armor.<sup>148</sup>

Corn starch (CS) in water is often used to demonstrate the shear thickening behavior in classrooms owing to its easy availability and low cost. CS suspensions have also been used by researchers<sup>87, 92-95</sup> to probe the shear thickening mechanism. Brown et al.<sup>93</sup> found that the slope of the shear thickening regime increased with increasing packing fraction and the viscosity diverged at a critical packing fraction. In their other article,<sup>140</sup> the shear thickening is found to be lost if the yield stress of the system is above a threshold. Fall et al.<sup>149</sup> studied the rheology of CS suspensions with the help of magnetic resonance imaging (MRI) to probe the local velocity profiles. They reported that the discontinuous shear thickening begins at the end of shear localization regime when all the fluid is sheared. From this observation they interpreted that the existence of non-flowing regions in the system will tend to delay or prevent the shear thickening effect. Bischoff White et al.<sup>95</sup> studied the extensional rheology of CS suspensions using a filament stretching rheometer. At moderate strains, the extensional viscosity increased with increase in extensional rate followed by brittle fracture above a critical extension rate. Crawford et al.<sup>87</sup> reported that at least 52.5 wt% of CS in water is required to induce sufficient solid like behavior to safely allow an average-weight person to walk on the CS suspension without sinking.

Though a significant number of studies have used CS/H<sub>2</sub>O suspension to study the different characteristics of shear thickening effect, the rheology of CS suspension has not been studied by modifying the composition of the continuous phase or by the adding polymers to the suspension. In this thesis, a block copolymer (Pluronic F127) and a homopolymer (poly (ethylene oxide); PEO) of different molecular weights (2000 to 35,000 g/mol) have been used to study the polymer effects on the rheology of CS/H<sub>2</sub>O suspension. Effect of both concentration and molecular weight of PEO are examined. The notion behind the choice of Pluronic F127 is to examine the role of temperature triggered gelation of F127 on the shear triggered gelation (shear thickening) of CS suspensions. Moreover, poly (ethylene glycol) (PEG) with a very low molecular weight of 200 g/mol is used to mix with water to study the effect of solvent mixture composition (PEG200: water) on the rheology of CS suspensions. Both steady shear and oscillatory rheometry have been used to conduct the investigation. The interaction between the CS particles and PEO is studied using Fourier transform infrared spectroscopy (FTIR).

## **6.2. Choice of CS packing fraction**

Wall slip, particle sedimentation and migration (secondary flows) are the various phenomena commonly associated with particle suspensions that may affect their rheometry measurements.<sup>92</sup> Rough plates (roughened by attaching sand paper) were used for comparison to check any wall slip for smooth plates, and no significant differences were noticed. Particle migration arising from inhomogeneous flow is prevented by using cone and plate geometry. For the pure

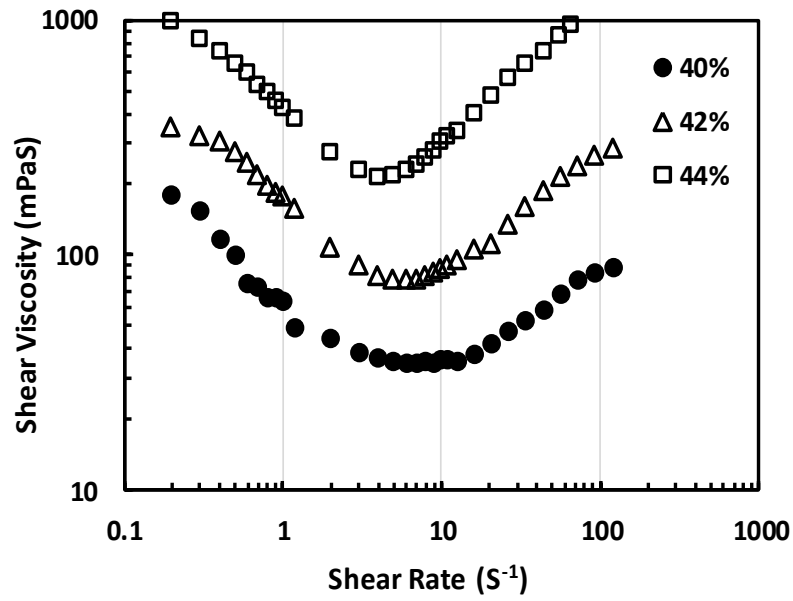


**Figure 6.1** Flow curves of CS suspension at different weight fractions

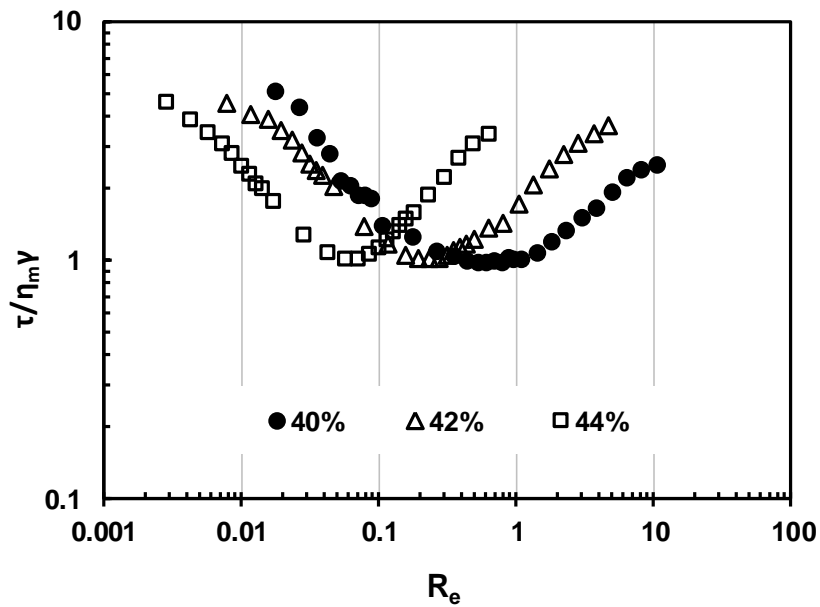


**Figure 6.2**  $(\tau/\eta_m\gamma)$  vs.  $Re$  plot curves for CS weight fractions studied in Figure 6.1

CS suspensions, the sedimentation effect is prevented by the methodology prescribed by Frith et al.<sup>92</sup> The flow curves (shear viscosity against shear rate) for various weight percentages of CS suspensions are shown in Figure 6.1. For all the concentrations investigated here, shear thinning is observed at low shear rates, while shear thickening is evident at higher shear rates. The critical shear rate denotes the rate for the onset of shear thickening. With increase in CS weight fraction, the critical shear rate decreases, while the intensity of shear thickening (defined as the positive slope of viscosity curve) increases. The dependences of both critical shear rate and the intensity of shear thickening on particle weight fraction are in agreement with the literature.<sup>87, 93, 149</sup>

To ensure that the measured viscosity increase arises from the shear thickening effect instead of the inertial effect, a plot of Stokes flow contribution ( $\tau/\eta_m\dot{\gamma}$ ) against Reynolds number ( $Re$ ) is made in Figure 6.2, where  $\tau$ ,  $\eta_m$  and  $\dot{\gamma}$  denote applied shear stress, minimum suspension viscosity at the onset of shear thickening and shear rate. Brown et al.<sup>150</sup> showed that if the curves in such a plot collapse onto a single one at high  $Re$  ( $>10$ ), the observed viscosity increase is caused by inertia, not from the real shear thickening. It can be seen from Figure 6.2 that the normalized stress curves do not behave this way. It indicates that the shear thickening observed for all the concentrations studied in Figure 6.1 is not erred by any inertial effect of hydrodynamics. The maximum packing fraction for CS studied here (S4180 SIGMA-ALDRICH) is found to be  $\phi_m = 53$  wt%. The physical appearance of suspension above this maximum packing fraction is shown in Figure 6.3. In the present study, 44 wt% is chosen as the suitable concentration



**Figure 6.3** Physical appearance of CS suspended in water for concentration just above the maximum packing fraction ( $\phi_m$ )

for two reasons. First, it exhibits about one order of magnitude of viscosity increase in the shear thickening regime. Second, it remains a workable suspension as the suspensions (>44 wt%) are too thick for rheometer loading. The largest shear rate for viscosity measurement is  $\sim 100 \text{ s}^{-1}$  since the viscometric flow becomes uncertain beyond this rate.

### 6.3. Results & Discussion

#### 6.3.1. Effects of F127

The effects of F127 addition on the flow curve of 44% CS are shown in Figure 6.4. Temperature was maintained constant at  $25^\circ\text{C}$  for experiments in Figure 6.4. At this temperature, F127 exists as micelles for the concentrations used in this study. Temperature was not varied in this experiment because increase in temperature swells the corn starch granules which in turn changes the rheology of pure corn starch suspension. With increase in F127 concentration, three main observations are made: 1) the intensity of shear thickening (extent of

viscosity increase) gradually diminish, shifting to higher critical shear stress values, and the shear thickening is completely absent at 4% F127; 2) the viscosity at the lower shear stress region ( $<1$  Pa) increases drastically and diverges at 4% of F127; 3) the change in the viscosity is greater in the low shear stress region than in high shear stress region.

To probe the effect of F127 gelation on the shear thickening of CS, particles were dispersed in F127 concentration of 15% and above. For all the samples prepared in this way, the suspensions became too thick to be loaded on to the rheometer (not shown). Moreover, such samples did not flow under  $180^\circ$  inversion of the beaker signifying the presence of yield stress. Temperature was maintained constant at  $25^\circ\text{C}$  for experiments in Figure 6.4. At this temperature, F127 exist as micelles for the concentrations used in this study. Temperature was

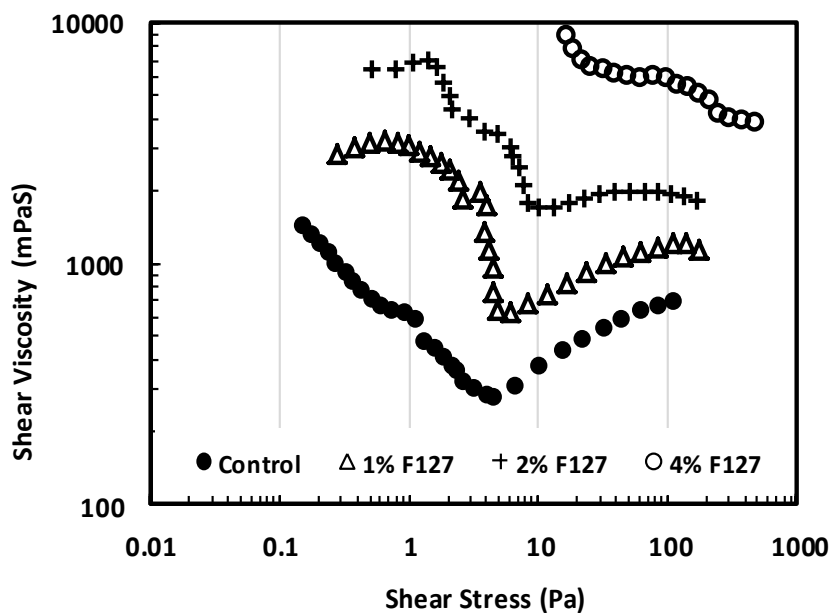


**Figure 6.4** Flow curves of 44% CS with increasing F127 concentration; control = pure 44% CS

not varied in this experiment because increase in temperature swells the corn starch granules which in turn changes the rheology of pure corn starch suspension.

To understand the mechanism behind the loss of shear thickening in detail, simpler polymer system: homopolymer poly (ethylene oxide) (PEO) is chosen to examine the role of polymer additive on the rheology of CS suspensions. Further experiments in this section will be on the effect of PEO homopolymer and PEG200 solvent on the rheology of CS suspensions.

### 6.3.2. Effects of PEO homopolymer

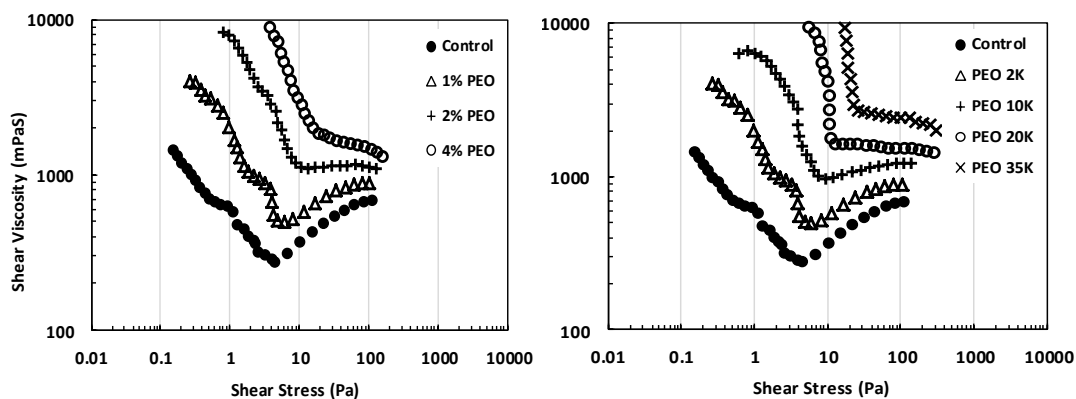


**Figure 6.5** Flow curves of 44% CS with increasing PEO2k concentration (left); with increasing molecular weight of 1% PEO (right); control = pure 44% CS

The influence of homopolymer PEO2k concentration and its molecular weight on the rheology of 44% CS suspension are shown in Figure 6.5. Qualitatively the observed behavior is very similar to the effect of F127. With increase in PEO concentration/molecular weight, the shear thickening shows a decreased intensity,



and shifts to higher critical shear stress, while the viscosity in low shear stress region increases drastically. For the suspensions with PEO at 2% and above or having M.W of 10k and above, the measured viscosity in the low shear stress region failed to attain a steady state even when the rheometer equilibrium time was set to 60 sec for each specified stress/rate. This failure signals the possibility of a large yield stress in these suspensions.

### 6.3.3. Yielding

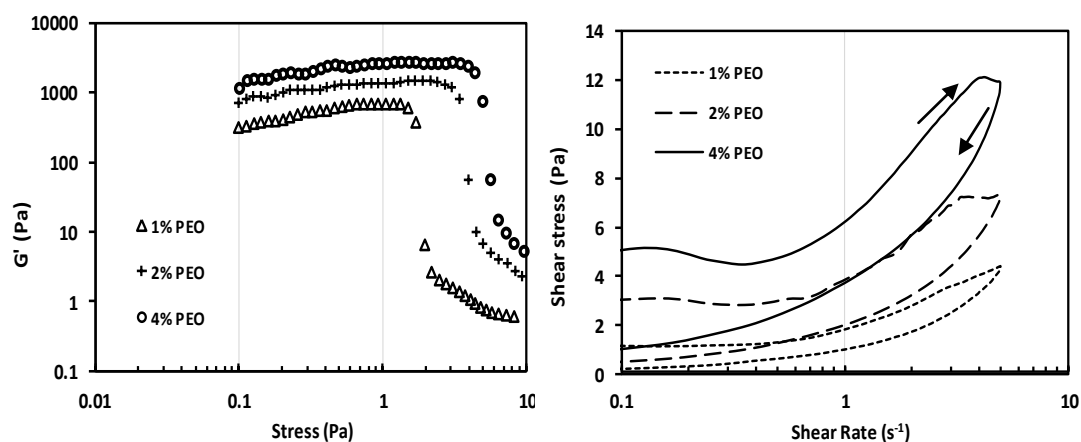


**Figure 6.6** Effect of concentration of PEO2k on oscillatory stress sweep (left) and thixotropy (right) of CS suspensions; CS concentration = 44%

To gain more insights on the macroscopic behaviour of these suspensions in the low shear stress regime, oscillatory stress sweeps were carried out. The advantage of oscillatory rheology in the linear viscoelastic regime is that it can probe the material nearly at rest without disturbing its microstructure. In this region, our data show that elastic modulus ( $G'$ ) is greater than viscous modulus ( $G''$ ) for the investigated frequency range, indicating that the suspensions are more elastic (solid like) than viscous (liquid like). Figure 6.6 (left) presents the

results for the oscillatory stress sweeps of CS suspensions with increasing PEO2k concentration. As seen, the plateau  $G'$  remains constant until a drastic drop takes place at a particular stress, denoting the yielding behavior associated with breakdown of the microstructure. The yield stress of a material can be measured in a number of ways as documented in the literature.<sup>151</sup> In this study, the stress for the crossover of  $G'$  and  $G''$  is taken as the yield stress.<sup>151</sup> The yield stress and the  $G'$  plateau obtained in the Figure 6.6 (left) are tabulated in Table 6.1. As seen, both properties increase with increase in PEO concentration.

Figure 6.7 shows the images of CS suspensions with two different molecular weights of PEO on the rheometer plate before flow tests. The physical appearance shows that the pure CS suspension spreads and lies flat on the plate. For the suspensions with PEO2k and PEO20k, the presence of yield stress is visually observable, because the material can partially hold its own weight.

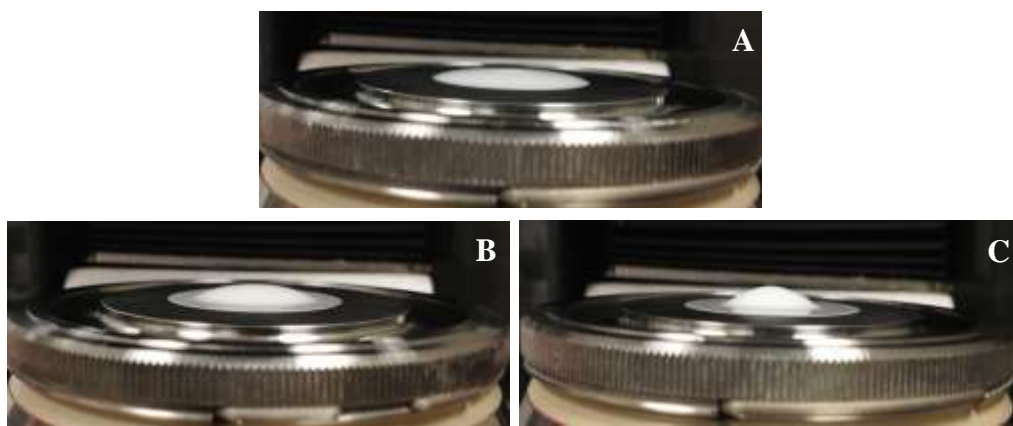
**Table 6.1** Effect of PEO concentration on  $G'$  (Pa), yield Stress (Pa) and thixotropic loop area (Pa/S) of CS suspension; PEO M.W = 2k; CS conc. = 44%

PEO Concentration (wt%)	$G'$ (Pa) at $\tau = 1$ Pa	Yield Stress (Pa)	Thixotropic Loop Area (Pa/S)
1	$0.68 \times 10^3$	1.8	5.2
2	$1.4 \times 10^3$	3.8	10.9
4	$5.4 \times 10^3$	5.4	14.6

Yield stress fluids can be of two types<sup>152, 153</sup>: simple (non-thixotropic) or thixotropic. The former is independent of the flow history and the origin of the

yield stress is repulsion between the suspended particles.<sup>153</sup> For the thixotropic type, the yield stress is due to attraction between the particles and the properties of these fluids depend on the flow history.<sup>153</sup> To identify the type of yield stress fluid that CS/PEO/H<sub>2</sub>O suspensions belong to, thixotropic experiments to probe the effect of flow history were performed. In this experiment, the shear rate is first ramped up from 0.1s<sup>-1</sup> to 5s<sup>-1</sup> followed by immediate ramp down for the same range, and the corresponding shear stresses are measured. The curves of shear stress against shear rate are plotted in Figure 6.6 (right). It is found that for each tested sample, the ramp up curve lies above the ramp down curve, indicating stress hysteresis and hence thixotropy. Since this hysteresis loop is also sensitive to the ramp speed, the speed has been fixed with ramp up for 30 sec and ramp down for 30 sec. The loop area can be determined from the figure to reflect the extent of thixotropy, and can also be regarded as an indirect measure of the extent of flocculation.<sup>153</sup> The calculated area for different PEO concentration is tabulated in Table 6.1. It can be found that the thixotropic loop area increases with increasing PEO concentration. The results suggest that weak attractive forces exist between the CS particles, leading to their flocculation. The applied stress tends to break the aggregates, and this breakdown process takes some time, leading to viscosity decrease with time. Since the thixotropic loop area increases with increasing PEO content, the particle flocculation is believed to become more significant. From both oscillatory stress and thixotropy studies, it is inferred that with increase in PEO concentration/M.W, the CS particles show a higher tendency to flocculate via inter-particle attraction, thereby leading to a percolated

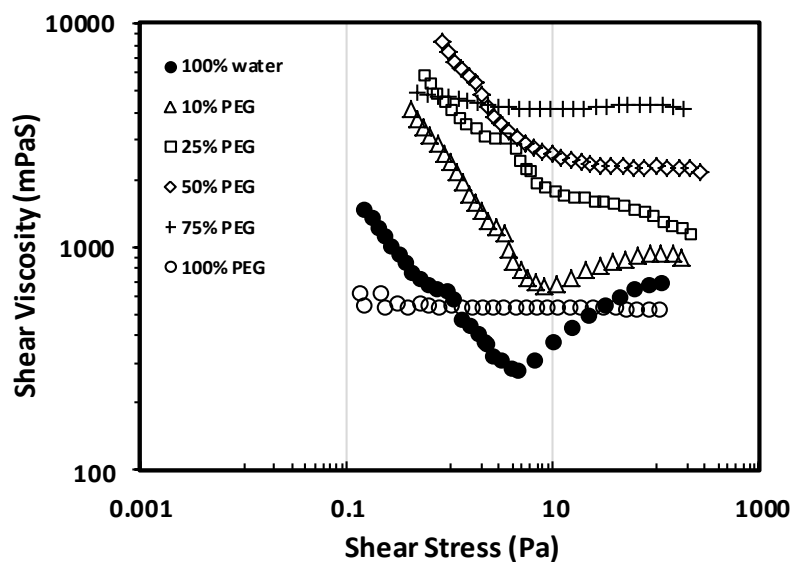
structure with increased elasticity and yield stress, which could be destroyed by a sufficiently strong flow.



**Figure 6.7** Photographs of pure CS (A), CS + PEO2k (B) and CS + PEO20k (C) suspensions on the rheometer plate after cone withdrawal; CS conc. = 44%; PEO conc. = 4%

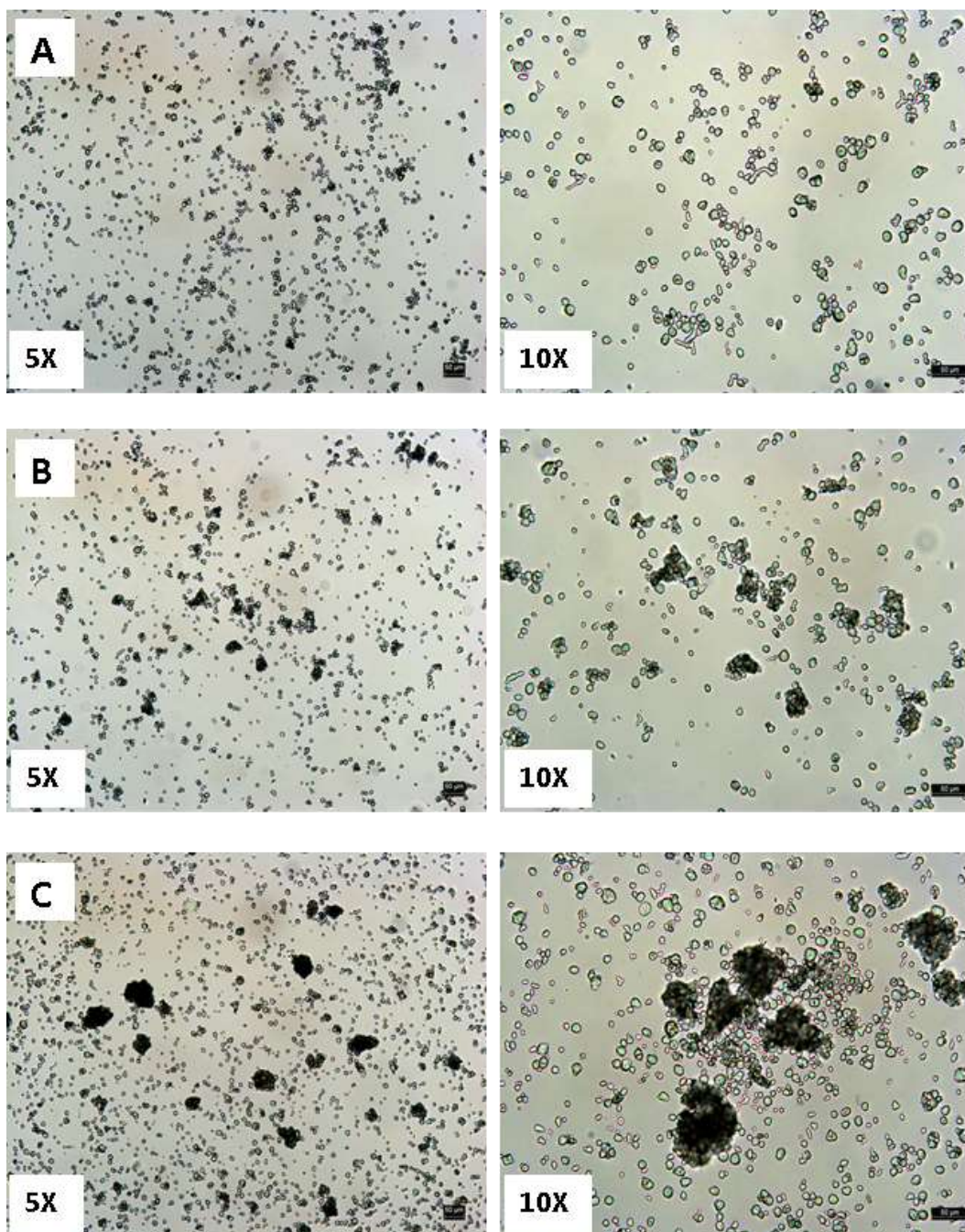
### 6.3.4. Solvent effect of PEG200

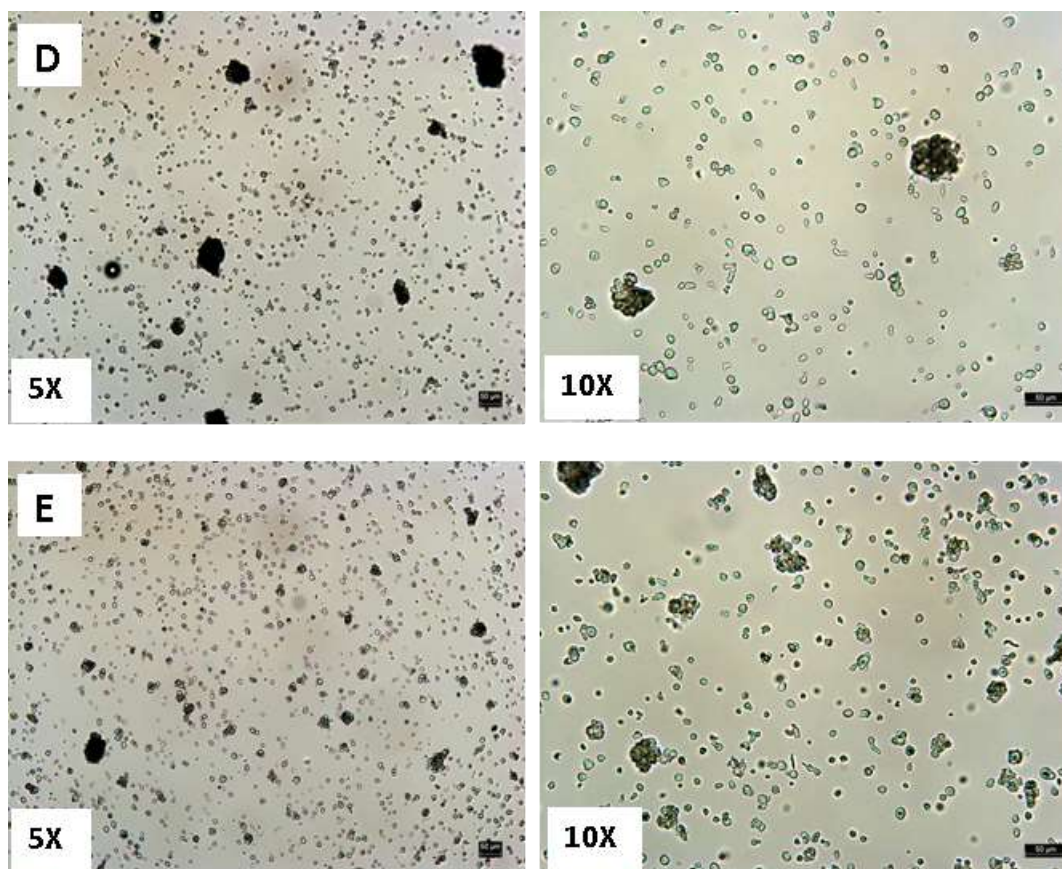
The solvent effect of PEG200 on the rheology of CS is investigated using a binary solvent comprising water and PEG200 at varying composition. The flow curves shown in Figure 6.8 are found to be more complex. In the binary solvent, the suspension rheology strongly depends on the weight fraction of PEG ( $\Phi_{\text{PEG}}$ ). Note that  $\Phi_{\text{PEG}} = 0$  and 1 denote pure water and pure PEG200, respectively. For the samples with  $\Phi_{\text{PEG}} \leq 25\%$ , the shear thickening in high shear stress regime decreases with increasing PEG concentration. For the sample with  $\Phi_{\text{PEG}} = 50\%$ , near Newtonian behaviour is seen at high stress region while the shear thinning still holds at low stress region. For the samples with  $\Phi_{\text{PEG}} > 50\%$ , the extent of shear thinning at low stress region decreases with increasing PEG concentration, and the behaviour becomes near Newtonian at both low and high shear stress region. The viscosity for the entire flow curve is found to decrease with PEG



**Figure 6.8** Shear flow curves of 44% CS in various fraction of PEG200/water

weight fraction. It is interesting to find that CS in pure PEG200 exhibits a perfect Newtonian behaviour in the shear stress range investigated.





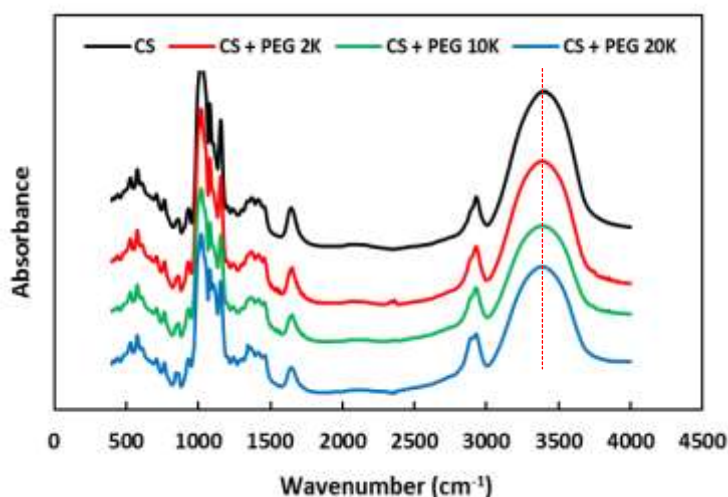
**Figure 6.9** Microscopic images of 1% CS in various fraction of PEG200/water; pure water (A), 25% PEG200 (B), 50% PEG200 (C), 75% PEG200 (D), pure PEG200 (E)

Figure 6.9 shows the images of 1% CS in different solvent compositions obtained by optical microscopy. In 100% water, CS particles appear well dispersed, while small aggregates can be seen for  $\Phi_{\text{PEG}}=25\%$ , and relatively large ones are spotted for  $\Phi_{\text{PEG}}=50\%$ . Surprisingly, the size of the aggregates is decreased when the PEG200 concentration is further increased above 50%. These structural differences seem to show some correlation to the rheological behavior as shown in Figure 6.8. The greater the tendency for CS to aggregate in the

presence of PEG at appropriate compositions, the higher the viscosity in the small stress regime.

### 6.3.5. Interaction between CS particles and PEO

It is essential to study the interaction between the CS particles and PEO homopolymers to understand the mechanism behind the decrease in shear thickening of CS in the presence of PEO. FTIR has been used to study the interaction between starch and PEG in starch-PEO blends<sup>154-156</sup> and also between silica particles and PEO homopolymers.<sup>157, 158</sup> CS particles contain hydroxyl groups at their surface making them very hydrophilic. Vibrational changes in these -OH groups are expected if the PEO chains get adsorb on the surface of CS particles via hydrogen bonding. The FTIR spectra for pure CS and for the CS-PEO mixture are shown in Figure 6.10. The broad peak in the range of 3000 to 3700  $\text{cm}^{-1}$  corresponds to -OH absorption band of CS.<sup>155, 159, 160</sup> For cellulose-PEO



**Figure 6.10** Effect of PEG M.W. on FTIR spectra for CS : PEG weight ratio = 7.5:2.5



blend, Kondo et al.<sup>154</sup> observed a considerable change in shape and position of the -OH peak ( $> 20\text{cm}^{-1}$  shift in peak position) as the PEO amount is increased. They attributed this change to strong hydrogen bonding between the cellulose and PEO chains. Similar observation and argument were made by Kim et al.<sup>155</sup> for CS-PEO blends.

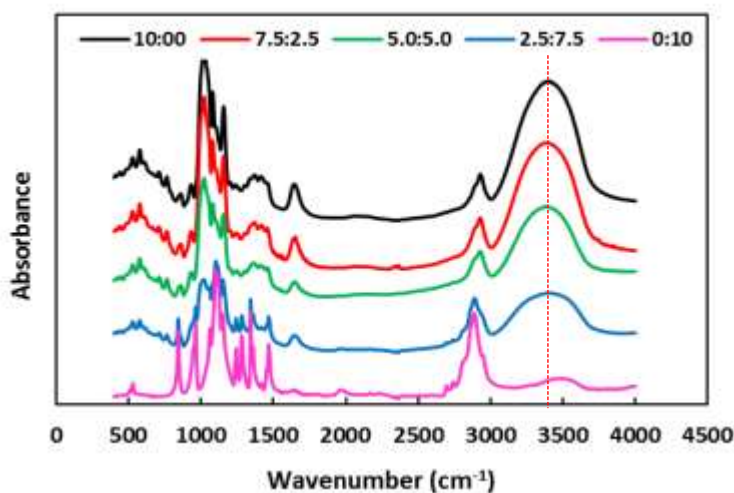


**Figure 6.11** Effect of weight ratio of CS : PEG on FTIR spectra; total concentration =10 wt%; PEG M.W. = 2K

In contrast to the behavior of the blends reported in the literature, it is found from Figure 6.11 that as the fraction of PEO is increased in the CS suspension neither a significant shift in the -OH peak nor any shape change is observed. Note that a slight peak shift shown in Table 6.2 when compared to the pure CS is well within the experimental uncertainty. The only notable change is the decrease in the intensity of -OH peak with increasing PEO fraction due to the decreased CS amount in the mixture. Figure 6.10 displays the effect of PEG M.W. on the FTIR spectra of CS+PEO. As seen, there is no change in either peak shape or wavenumber with varying PEO molecular weight.

**Table 6.2** Effect of CS : PEO ratio and PEO M.W on the shift of –OH peak relative to pure CS

	<b>Sample (CS :PEO)</b>	<b>Shift of the OH peak position (cm<sup>-1</sup>)</b>
Effect of CS:PEO ratio (PEO M.W. = 2K)	7.5 : 2.5	-0.6
	5.0 : 5.0	-0.3
	2.5 : 7.5	-0.3
Effect of PEO M.W. (CS : PEO = 7.5 : 2.5)	CS + PEO2k	-0.6
	CS + PEO10k	-1.3
	CS + PEO20k	-0.6

These observations show that there is no strong hydrogen bonding between the CS particles and PEO in the system considered in this work, unlike the blend systems studied by others.<sup>154, 155</sup> Hydrophobic interaction is also unlikely because both CS particles and PEO are hydrophilic in nature. Therefore, the PEO chains prefer to be dissolved completely in the bulk water and not adsorbed on the CS surface.

### 6.3.6. Discussion

The suspension viscosity measured in our system is influenced by two effects: 1) the inter-particle interaction, and 2) the viscosity of the dispersing liquid (water + polymer). To better see the contribution of inter-particle interaction, the relative viscosity, which is the suspension viscosity normalized by the value of dispersing

liquid, is plotted in Figure 6.12. The normalized viscosity is always much greater than unity, and the curve trend shown in this figure does not differ much from that in Figure 6.5 (left), indicating that the contribution of the dispersing medium to the suspension viscosity is very little

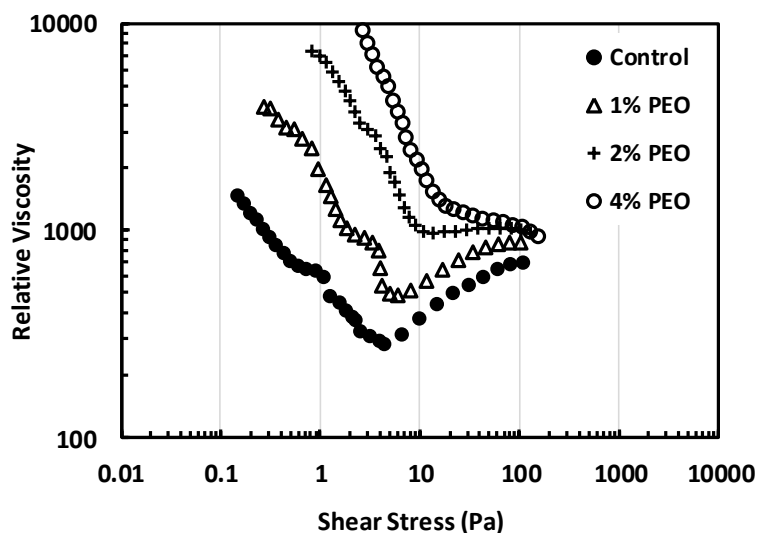


**Figure 6.12** Relative viscosity vs. shear stress for CS suspension with increasing PEO weight percentages; CS conc. = 44%; PEO M.W = 2k; control = pure 44% CS

Following sections discuss the possible mechanisms accountable for the loss of shear thickening in CS/PEO/H<sub>2</sub>O systems. Three factors (electrostatic interactions, hydrogen bonding interactions and depletion forces) are considered and addressed as follows.

### 6.3.6.1 Electrostatic interactions

Some types of starch granules such as wheat and potato are reported to possess negative surface charge at their natural pH.<sup>161, 162</sup> The amylose and amylopectin chains that form the starch granules are neutral macromolecules

carrying no charge. Therefore, the origin of granule surface charge was thought to arise from surface proteins. Although negative charge on CS has not been reported in the literature, CS holds some common features with the other types of starches. If electrostatics plays a key role in the stability of CS suspensions, decreasing the solvent polarity (by changing from water to PEO200) would reduce the degree of surface ionization and thereby the stability of CS suspensions. To investigate this possibility, the effect of pH on the rheology of CS suspended in water was studied with the results shown in Figure 6.13. The isoelectric point of wheat starch lies between pH 2 and 4.<sup>161</sup> At the isoelectric point, particles would tend to flocculate, and hence could supposedly cause a considerable change in the suspension viscosity at low shear rate/stress. However, Figure 6.13 shows that the pH has a very weak effect on the CS suspension viscosity. Moreover, for both the pH experiment and salt-addition experiment, no perceptible change in the sample appearance could be observed, namely, it looks

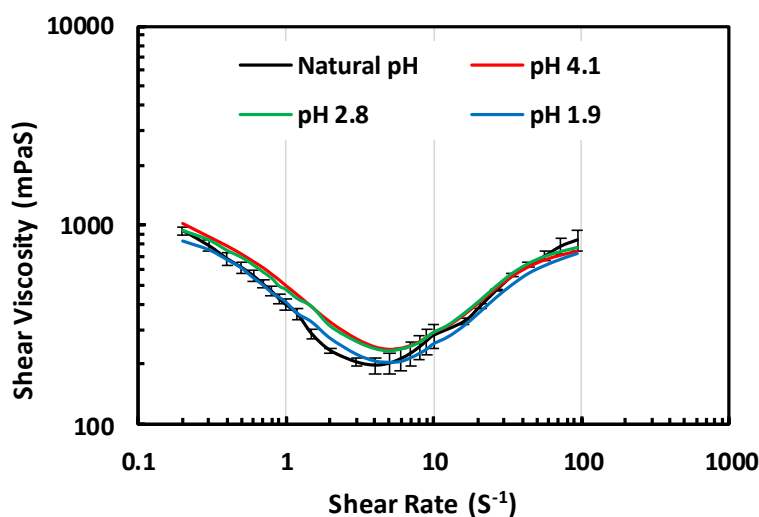


**Figure 6.13** Effect of pH on flow curves of 44% CS in water

like what is shown in Figure 6.7A. From these analyses, it is concluded that the electrostatics has a negligible effect on the stability and the shear thickening behavior of CS suspensions.

### 6.3.6.2 Hydrogen bonding interactions

CS particles have hydroxyl (-OH) groups on their surface making them highly hydrophilic. These hydroxyl groups form hydrogen bonds with water resulting in good surface wettability. FTIR studies showed that PEO homopolymers do not have strong affinity towards the CS surface, and therefore they are more likely to stay in the bulk water. A prior study reported that addition of PEG to water decreases the polarity of the resulting medium.<sup>105</sup> This finding implies that the CS hydroxyl groups have a lower tendency to form hydrogen bonding with the binary solvent (PEO + H<sub>2</sub>O) than with pure water. The reduced polarity can also be viewed as a decrease in solvency to disperse the CS particles, leading to their aggregation as observed for dilute suspensions in Figure 6.9 and larger low-shear viscosity in the concentrated regime shown in Figure 6.8. This behavior becomes more pronounced with increasing PEO concentration until the degree of percolation for particle aggregation reaches the maximum. Further increase in PEO concentration could lead to more dense aggregates with compromised percolation. This may account for the decrease in viscosity that varies rather weakly with stress, like a Newtonian fluid.

### 6.3.6.3 Depletion forces

The decrease in solvent polarity have been reported to be much more dependent on the PEO concentration than its molecular weight.<sup>105</sup> In Figure 6.5, it is observed that the suppression of shear thickening depends significantly on both concentration and M.W. of added PEO. Therefore, the above discussed solvency change cannot explain this behavior. It is well known that non-adsorbing polymers can result in depletion flocculation of the suspended particles.<sup>163, 164</sup> A prior study on depletion flocculation of large particles<sup>165</sup> shows that the larger the particles, the lower the polymer concentration is required to induce depletion attraction. In the system considered in this work, the ratio of CS particle diameter (10 $\mu$ m on average) to the PEO polymer coil size is very large. Therefore, PEO even at low concentration is expected to cause depletion flocculation of CS particles. This is more likely at high particle loading, since the inter-particle distance is very small, leading to depletion of PEO and smaller osmotic pressure in the gap. The resulting osmotic pressure difference between the outside and the inside of the gap gives rise to weak attraction between the CS particles. The strength of attraction between the CS particles increases with the PEO M.W. and concentration, so does the flocculation. This constitutes an explanation for the observed dependences of suspension yield stress on the PEO concentration and molecular weight.

For CS particles dispersed in pure water, one can see large viscosity at both low and high shear rates. Although both are associated with formation of particle clusters, the physical origins are different. When the flow is absent or

weak, particle aggregation (gelation) is a thermodynamic phenomenon, whereas particle clustering at high stress (shear thickening) is a hydrodynamic effect giving rise to strong jamming and viscous dissipation.<sup>166</sup> Addition of polymer in the studied system leads to an enhancement in the thermodynamic effect (aggregation of CS particles). The increased inter-particle attraction could alleviate the resistance to their approach to one another under a large shear force. When the gelation becomes sufficiently strong, the thermodynamic effect dominates over the hydrodynamic one, thereby preventing the occurrence of shear thickening.<sup>166, 167</sup>

#### **6.4. Conclusion**

The effects of Pluronic F127, PEO with a wide range of molecular weight (2000 to 35,000 g/mol) and the binary solvent water +PEG (M.W.=200 g/mol) on the rheology of concentrated aqueous corn starch (CS) suspensions have been studied. Pure CS suspensions exhibit shear thickening behavior in the high stress regime. With increase in PEO M.W./concentration or F127 concentration, the shear thickening shifts to higher stress values with reduced intensity and eventually disappear. Oscillatory stress sweeps, visual observation and thixotropy studies indicate that the yield stress and the extent of particle aggregation increase when the PEO M.W./concentration is increased.

The effect of PEO200 in the binary solvent on the rheology of CS suspensions is more complex. For the suspensions with PEO < 50%, the shear thickening in high shear stress regime becomes less pronounced with increasing PEO

concentration, while the shear thinning behaviour in low shear stress region is more significant. The suspension viscosity is also found to increase with increasing PEO concentration. For the suspensions with PEO > 50%, to the contrary, the viscosity and the extent of shear thinning both decrease with increasing PEO concentration, and the suspension behaviour is progressively similar to that of a Newtonian fluid. In fact, CS in pure PEO200 is perfectly Newtonian in the shear stress range investigated.

The FTIR studies show that PEO has no affinity (hydrogen bonding) with CS surface, and hence behaves as non-adsorbing homopolymer in the suspensions. As such, the aggregation of CS particles can be attributed to 1) the depletion effect of the non-adsorbing PEO homopolymers leading to attraction between CS particles at high concentration and 2) reduced polarity effect of PEO on water (deteriorated solvency). The yield stress arising from the CS aggregation is enhanced by PEO addition, leading to the greater importance of the thermodynamic effect relative to the hydrodynamic jamming. Therefore, shear thickening becomes weaker and becomes completely absent at high enough PEO concentrations/MW.



## **7. Conclusions and Recommendations**

---

This chapter summarizes the major contributions and significance of the research work in this thesis. Limitations are also addressed followed by suggested potential future works.

### **7.1. Conclusions**

The motivation for studying the micellization, gelation and rheology of triblock copolymers with polymer/particle additives was based on their enormous advantage in various applications, ranging from medical technologies to cosmetics fields. The overall objective of this thesis work was to investigate the influence of additives, namely non-ionic homopolymer (poly (ethylene oxide); PEO), ionic homopolymer (poly (acrylic acid); PAA), triblock copolymer (Pluronic® L64 or P105) and a particle suspension (corn starch; CS) on the micellization and gelation behavior of amphiphilic triblock copolymer Pluronic® F127 (EO<sub>98</sub>PO<sub>67</sub>EO<sub>98</sub>) in aqueous medium.

In Chapter 3, the influence of PEO molecular weight and concentration on the sol/gel behavior of F127 in aqueous medium was examined. Emphasis was placed on exploring the underlying mechanism behind the loss of F127 gelation in presence of PEO as reported in the literature. From this study, it was observed that short PEO chains promote gelation of F127, while long chains delay or even curb the gel formation. The findings also demonstrate that the PEO always decreases the critical micellization temperature modestly with least change in micellization enthalpy irrespective of its chain length. These findings indicate that the added

PEO does not hinder the micelle formation but only the gel formation. This contrasting effect on micellization and gelation was unexpected since it was believed that, in general species such as ethanol, methanol that are reported to hinder the gelation process also hinder the micellization process sturdily owing to their better solvency for F127 chains. Micelle size measurement and Cryo-TEM micrographs provided the evidence for micellar aggregation via bridging of long PEO chains or via depletion, thereby impeding the ordering of micelles for gel formation. Therefore it was proposed that the disturbing or hindering effect is the underlying mechanism for the observed gel suppression.

In Chapter 4, the role of PAA on the micellization and gelation behavior of F127 in aqueous medium was explored. It was found that, the critical micellization and gelation temperatures (CMT and CGT), enthalpy of micellization ( $\Delta H$ ) and the gel strength depend strongly on medium pH, PAA concentration and molecular weight. For the micellization, addition of PAA lowers the CMT of F127, unlike the behavior claimed in a prior study.<sup>122</sup> Even though the micelles are formed at lower temperature, the  $\Delta H$  was found to be reduced with PAA which is unexpected. At high pH, to the contrary, both CMT and  $\Delta H$  become weakly affected by the presence of PAA because the deprotonated the PAA chains are not favorable for the association with F127. For the gelation, the CGT is increased, and the gel strength ( $G'$ ) is reduced in the presence of PAA of both low and high M.W. The effect is greater for high M.W PAA. Order disrupting for the packed F127 micelles due to PAA was proposed to be the reason for the observed changes in CGT and  $G'$ . The results obtained

advance the understanding of structure-property relationships, and facilitate the effectual exploitation of block copolymer + PAA systems in various applications such as ocular drug delivery.

Sol/gel behavior of mixture of two Pluronic species (F127+L64 and F127+P105) with non-identical hydrophobic (PPO) block lengths in aqueous medium was explored in Chapter 5. Emphasis was placed on the nature of micelles (either mixed or separate micelles), nature of gelation, gel strength and microstructure. From DLS, DSC and cloud point (CP) temperature experiments, it was concluded that PEO-PPO-PEO block copolymers even with non-identical hydrophobic block (PPO) lengths can form mixed micelles via cooperative aggregation. From rheometry, F127/L64/H<sub>2</sub>O was observed to exhibit two hard gel states separated by a soft gel with increase in temperature, although the species individually do not show such behavior. The first hard gel formed at lower temperature appeared clear with a cubic packing structure, while the second hard gel at higher temperature was hexagonally structured and appeared hazy. Interestingly, the second hard gel is observed only during the temperature ramp up process, whereas the first gel is seen both in the ramp up and down processes. The aforementioned behavior does not occur for F127/P105/H<sub>2</sub>O system.

In Chapter 6, the influence of block copolymer (F127), homopolymer (PEO) and a binary solvent water + PEG (MW = 200 g/mol) on the rheology of concentrated aqueous corn starch (CS) suspensions was explored. The shear thickening behavior of CS shifts to higher stress values with reduced intensity and eventually disappears with increase in PEO M.W/concentration or F127

concentration. The FTIR studies showed that PEO has no affinity (hydrogen bonding) with CS surface, and hence behaves as non-adsorbing homopolymer in the suspensions. As such, the aggregation of CS particles was attributed to 1) the depletion effect of the non-adsorbing PEO homopolymers leading to attraction between CS particles at high concentration and 2) reduced polarity effect of PEO on water (deteriorated solvency). The yield stress arising from the CS aggregation is enhanced by PEO addition, leading to the greater importance of the thermodynamic effect relative to the hydrodynamic jamming. Therefore, shear thickening becomes weaker and is completely absent at high enough PEO concentrations/MW.

To conclude, sound knowledge about the interaction of block copolymers with polymers for a particular application is desirable and important. The work presented here contributes to the advancement of structure-property relationships of these systems, and can facilitate the effective exploitation of block copolymer + polymeric additive systems in various applications such as drug delivery.

## **7.2. Recommendations**

- 1) Although the microstructural ordering of copolymer micelles are successfully probed using Cryo-TEM or SAXS in this study, probing the structural properties of micelles such as core radius ( $R_c$ ), hard sphere radius ( $R_{hs}$ ) and inter-micellar spacing of the micelles is still not an easy task. To obtain a better and more affirmative understanding on the Pluronic + polymeric additive systems, further research can be done using small angle neutron

scattering (SANS), if available, which can estimate the  $R_c$ ,  $R_{hs}$ , inter-micellar spacing and aggregation number of the micelles.

- 2) In Chapter 3, formation of micellar aggregates that impede the ordering of micelles was proposed to be the underlying mechanism for the loss of F127 gelation. But the micellar aggregates can arise from two phenomena: 1) PEO chains can form hydrogen bonds with two or more F127 micelles thereby bridging the micelles attached to them, or 2) large PEO chains are not attached to the micelles, present in the bulk water can result in depletion zone between two micelles leading to micelle aggregates. Therefore the exact phenomenon still remains unclear. A further study on the interaction by isothermal titration calorimetry (ITC) which is very sensitive to any weak interactions will provide important information to elucidate the exact underlying mechanism. Any strong change in the enthalpy value of Pluronics with addition of PEO may indicate the attachment of PEO chains on F127 micelles while the absence of any changes may signify the lack of any interaction.
- 3) Investigations of mixed micelles using dissipative particle dynamics (DPD) simulations also deserve attention. Chapter 5 reports the formation of mixed micelles for the Pluronics mixture (F127+ L64) with non-identical hydrophobic block lengths. However, the possibility of pristine L64 micelles formed at small amount may not be ruled out entirely, although the used experimental methods cannot detect. DPD simulations can be carried out to study the existence of pristine micelles, if any, in the mixed Pluronic

- copolymer systems. DPD simulations can also fetch microscopic information such as the composition of the micellar core and corona.
- 4) In the Chapter 4, the changes in CMT, micelle size,  $\Delta H$ , CGT and  $G'$  brought by linear PAA to the copolymer F127 were quantified and the underlying mechanism was elucidated. However the recent successful use of Pluronic/PAA/H<sub>2</sub>O system in ocular drug delivery involves usage of cross linked PAA rather than linear PAA.<sup>53, 54</sup> The behavior of Pluronic + cross linked PAA system is expected to be qualitatively similar to the Pluronic + linear PAA system studied here, but quantitatively they may show considerably difference. Therefore the influence of the cross linked PAA on the above mentioned properties should be studied in order to use the Pluronic + cross linked PAA system effectively in ocular drug delivery.
  - 5) The practical application of Pluronics for drug delivery performance or lithographic purpose is beyond the scope of the present study. Nevertheless, it would be fascinating to further study the drug loading capacity, encapsulation efficiency and release properties of Pluronic + polymer + H<sub>2</sub>O systems. Recently, it was found that the addition of 0.5 wt% PEO35k to 1 wt% F127 increased the solubilization capacity of 1 wt% F127 to a value approaching double that of 2.5% of pure F127.<sup>71</sup> This study suggests that the addition of simple homopolymers can be an alternative to attain a greater drug loading capacity without increasing the surfactant concentrations, which can be expensive and pharmaceutically undesirable. Similar work could be done to quantify the drug loading capacity with the addition of polyelectrolytes such

## *Conclusions and Recommendations*

as PAA and PMAA. It will provide feedback ideas on how to better tune the complexes to achieve desirable properties in order to add practical value in pharmaceutical realm.

**BIBLIOGRAPHY**

---

1. Jonsson, B., *Surfactants and polymers in aqueous solution*. John Wiley & Sons: 1998.
2. Laughlin, R. G., *The aqueous phase behavior of surfactants*. Academic Press London: 1994; Vol. 6.
3. Larsson, K.; Larsson, K., *Lipids: molecular organization, physical functions and technical applications*. Oily Press Dundee,, Scotland: 1994.
4. Rosen, M. J.; Kunjappu, J. T., *Surfactants and interfacial phenomena*. John Wiley & Sons: 2012.
5. Alexandridis, P.; Lindman, B., *Amphiphilic block copolymers: self-assembly and applications*. Elsevier: 2000.
6. Alexandridis, P., Amphiphilic copolymers and their applications. *Current Opinion in Colloid & Interface Science* **1996**, 1, (4), 490-501.
7. Dumortier, G.; Grossiord, J. L.; Agnely, F.; Chaumeil, J. C., A review of poloxamer 407 pharmaceutical and pharmacological characteristics. *Pharmaceutical Research* **2006**, 23, (12), 2709-2728.
8. Agrawal, A. K.; Das, M.; Jain, S., In situ gel systems as 'smart' carriers for sustained ocular drug delivery. *Expert opinion on drug delivery* **2012**, 9, (4), 383-402.
9. He, C.; Kim, S. W.; Lee, D. S., In situ gelling stimuli-sensitive block copolymer hydrogels for drug delivery. *Journal of Controlled Release* **2008**, 127, (3), 189-207.
10. Alexandridis, P.; Alan Hatton, T., Poly (ethylene oxide)-poly (propylene oxide)-poly (ethylene oxide) block copolymer surfactants in aqueous solutions and at interfaces: thermodynamics, structure, dynamics, and modeling. *Colloids and Surfaces A: Physicochemical and Engineering Aspects* **1995**, 96, (1), 1-46.
11. Alexandridis, P.; Holzwarth, J. F.; Hatton, T. A., Micellization of poly (ethylene oxide)-poly (propylene oxide)-poly (ethylene oxide) triblock copolymers in aqueous solutions: thermodynamics of copolymer association. *Macromolecules* **1994**, 27, (9), 2414-2425.
12. Wanka, G.; Hoffmann, H.; Ulbricht, W., Phase diagrams and aggregation behavior of poly(oxyethylene)-poly(oxypropylene)-poly(oxyethylene) triblock copolymers in aqueous solutions. *Macromolecules* **1994**, 27, (15), 4145-4159.



13. Schmolka, I. R., Artificial skin I. Preparation and properties of pluronic F-127 gels for treatment of burns. *Journal of biomedical materials research* **1972**, 6, (6), 571-582.
14. Alexandridis, P.; Alan Hatton, T., Poly (ethylene oxide) • poly (propylene oxide) • poly (ethylene oxide) block copolymer surfactants in aqueous solutions and at interfaces: thermodynamics, structure, dynamics, and modeling. *Colloids and Surfaces A: Physicochemical and Engineering Aspects* **1995**, 96, (1), 1-46.
15. Zhou, Z.; Chu, B., Light-scattering study on the association behavior of triblock polymers of ethylene oxide and propylene oxide in aqueous solution. *Journal of colloid and interface science* **1988**, 126, (1), 171-180.
16. Alexandridis, P.; Nivaggioli, T.; Hatton, T. A., Temperature effects on structural properties of Pluronic P104 and F108 PEO-PPO-PEO block copolymer solutions. *Langmuir* **1995**, 11, (5), 1468-1476.
17. Li, Y.; Xu, R.; Bloor, D.; Holzwarth, J.; Wyn-Jones, E., The binding of sodium dodecyl sulfate to the ABA block copolymer Pluronic F127 (EO97PO69EO97): an electromotive force, microcalorimetry, and light scattering investigation. *Langmuir* **2000**, 16, (26), 10515-10520.
18. Cardoso da Silva, R.; Olofsson, G.; Schillen, K.; Loh, W., Influence of ionic surfactants on the aggregation of poly (ethylene oxide)-poly (propylene oxide)-poly (ethylene oxide) block copolymers studied by differential scanning and isothermal titration calorimetry. *The Journal of Physical Chemistry B* **2002**, 106, (6), 1239-1246.
19. Armstrong, J.; Chowdhry, B.; Mitchell, J.; Beezer, A.; Leharne, S., Effect of cosolvents and cosolutes upon aggregation transitions in aqueous solutions of the poloxamer F87 (poloxamer P237): A high sensitivity differential scanning calorimetry study. *Journal of Physical Chemistry* **1996**, 100, (5), 1738-1745.
20. Sarkar, B.; Ravi, V.; Alexandridis, P., Micellization of amphiphilic block copolymers in binary and ternary solvent mixtures. *Journal of colloid and interface science* **2013**, 390, (1), 137-146.
21. Nivaggioli, T.; Alexandridis, P.; Hatton, T. A.; Yekta, A.; Winnik, M. A., Fluorescence probe studies of pluronic copolymer solutions as a function of temperature. *Langmuir* **1995**, 11, (3), 730-737.

22. Vadnere, M.; Amidon, G.; Lindenbaum, S.; Haslam, J. L., Thermodynamic studies on the gel-sol transition of some pluronic polyols. *International journal of pharmaceutics* **1984**, 22, (2), 207-218.
23. Mortensen, K.; Pedersen, J. S., Structural study on the micelle formation of poly (ethylene oxide)-poly (propylene oxide)-poly (ethylene oxide) triblock copolymer in aqueous solution. *Macromolecules* **1993**, 26, (4), 805-812.
24. Nolan, S. L.; Phillips, R. J.; Cotts, P. M.; Dungan, S. R., Light scattering study on the effect of polymer composition on the structural properties of PEO-PPO-PEO micelles. *Journal of colloid and interface science* **1997**, 191, (2), 291-302.
25. Rassing, J.; Attwood, D., Ultrasonic velocity and light-scattering studies on the polyoxyethylene—polyoxypropylene copolymer Pluronic F127 in aqueous solution. *International Journal of Pharmaceutics* **1982**, 13, (1), 47-55.
26. Lam, Y. M.; Grigorieff, N.; Goldbeck-Wood, G., Direct visualisation of micelles of Pluronic block copolymers in aqueous solution by cryo-TEM. *Physical Chemistry Chemical Physics* **1999**, 1, (14), 3331-3334.
27. Mortensen, K.; Talmon, Y., Cryo-TEM and SANS Microstructural Study of Pluronic Polymer Solutions. *Macromolecules* **1995**, 28, (26), 8829-8834.
28. Alexandridis, P.; Zhou, D.; Khan, A., Lyotropic liquid crystallinity in amphiphilic block copolymers: temperature effects on phase behavior and structure for poly (ethylene oxide)-b-poly (propylene oxide)-b-poly (ethylene oxide) copolymers of different composition. *Langmuir* **1996**, 12, (11), 2690-2700.
29. Mezmarich, N. A.; Juggernaut, K. A.; Batzli, K. M.; Love, B. J., Structural changes in PEO-PPO-PEO gels induced by methylparaben and dexamethasone observed using time-resolved SAXS. *Macromolecules* **2011**, 44, (19), 7792-7798.
30. Mortensen, K., Structural studies of aqueous solutions of PEO-PPO-PEO triblock copolymers, their micellar aggregates and mesophases; a small-angle neutron scattering study. *Journal of Physics: Condensed Matter* **1996**, 8, (25A), A103.
31. Chaibundit, C.; Ricardo, N. M.; de MLL Costa, F.; Yeates, S. G.; Booth, C., Micellization and gelation of mixed copolymers P123 and F127 in aqueous solution. *Langmuir* **2007**, 23, (18), 9229-9236.
32. Malmsten, M.; Lindman, B., Effects of homopolymers on the gel formation in aqueous block copolymer solutions. *Macromolecules* **1993**, 26, (6), 1282-1286.

33. Mortensen, K.; Batsberg, W.; Hvidt, S., Effects of PEO-PPO diblock impurities on the cubic structure of aqueous PEO-PPO-PEO pluronic micelles: fcc and bcc ordered structures in F127. *Macromolecules* **2008**, 41, (5), 1720-1727.
34. Jiang, J.; Li, C.; Lombardi, J.; Colby, R. H.; Rigas, B.; Rafailovich, M. H.; Sokolov, J. C., The effect of physiologically relevant additives on the rheological properties of concentrated Pluronic copolymer gels. *Polymer* **2008**, 49, (16), 3561-3567.
35. Chaibundit, C.; Ricardo, N. M. P. S.; Costa, F. D. M. L. L.; Wong, M. G. P.; Hermida-Merino, D.; Rodriguez-Perez, J.; Hamley, I. W.; Yeates, S. G.; Booth, C., Effect of ethanol on the micellization and gelation of pluronic P123. *Langmuir* **2008**, 24, (21), 12260-12266.
36. Chaibundit, C.; Ricardo, N. M. P. S.; Murny, C. A.; Madec, M. B.; Yeates, S. G.; Booth, C., Effect of ethanol on the gelation of aqueous solutions of Pluronic F127. *Journal of Colloid and Interface Science* **2010**, 351, (1), 190-196.
37. Wanka, G.; Hoffmann, H.; Ulbricht, W., The aggregation behavior of poly-(oxyethylene)-poly-(oxypropylene)-poly-(oxyethylene)-block-copolymers in aqueous solution. *Colloid and Polymer Science* **1990**, 268, (2), 101-117.
38. Jiang, J.; Burger, C.; Li, C.; Li, J.; Lin, M. Y.; Colby, R. H.; Rafailovich, M. H.; Sokolov, J. C., Shear-Induced Layered Structure of Polymeric Micelles by SANS. *Macromolecules* **2007**, 40, (11), 4016-4022.
39. Hamley, I. W.; Mai, S.-M.; Ryan, A. J.; Fairclough, J. P. A.; Booth, C., Aqueous mesophases of block copolymers of ethylene oxide and 1, 2-butylene oxide. *Physical Chemistry Chemical Physics* **2001**, 3, (15), 2972-2980.
40. Daga, V. K.; Watkins, J. J., Hydrogen-bond-mediated phase behavior of complexes of small molecule additives with poly (ethylene oxide-b-propylene oxide-b-ethylene oxide) triblock copolymer surfactants. *Macromolecules* **2010**, 43, (23), 9990-9997.
41. Kim, H.-C.; Park, S.-M.; Hinsberg, W. D., Block copolymer based nanostructures: materials, processes, and applications to electronics. *Chemical reviews* **2009**, 110, (1), 146-177.
42. Tirumala, V. R.; Daga, V.; Bosse, A. W.; Romang, A.; Ilavsky, J.; Lin, E. K.; Watkins, J. J., Well-ordered polymer melts with 5 nm lamellar domains from blends of a

- disordered block copolymer and a selectively associating homopolymer of low or high molar mass. *Macromolecules* **2008**, 41, (21), 7978-7985.
43. Attwood, D.; Zhou, Z.; Booth, C., Poly (ethylene oxide) based copolymers: solubilisation capacity and gelation. *Expert opinion on drug delivery* **2007**, 4, (5), 533-546.
44. Oerlemans, C.; Bult, W.; Bos, M.; Storm, G.; Nijsen, J. F. W.; Hennink, W. E., Polymeric micelles in anticancer therapy: targeting, imaging and triggered release. *Pharmaceutical research* **2010**, 27, (12), 2569-2589.
45. Dumortier, G.; El Kateb, N.; Sahli, M.; Kedjar, S.; Boulliat, A.; Chaumeil, J., Development of a thermogelling ophthalmic formulation of cysteine. *Drug development and industrial pharmacy* **2006**, 32, (1), 63-72.
46. Wei, G.; Xu, H.; Ding, P. T.; Li, S. M.; Zheng, J. M., Thermosetting gels with modulated gelation temperature for ophthalmic use: the rheological and gamma scintigraphic studies. *Journal of Controlled Release* **2002**, 83, (1), 65-74.
47. Barichello, J. M.; Morishita, M.; Takayama, K.; Chiba, Y.; Tokiwa, S.; Nagai, T., Enhanced rectal absorption of insulin-loaded Pluronic® F-127 gels containing unsaturated fatty acids. *International journal of pharmaceuticals* **1999**, 183, (2), 125-132.
48. Park, Y.-J.; Yong, C. S.; Kim, H.-M.; Rhee, J.-D.; Oh, Y.-K.; Kim, C.-K.; Choi, H.-G., Effect of sodium chloride on the release, absorption and safety of diclofenac sodium delivered by poloxamer gel. *International journal of pharmaceuticals* **2003**, 263, (1), 105-111.
49. El Gendy, A. M.; Jun, H.; Kassem, A. A., In vitro release studies of flurbiprofen from different topical formulations. *Drug development and industrial pharmacy* **2002**, 28, (7), 823-831.
50. Shin, S.-C.; Cho, C.-W.; Oh, I.-J., Enhanced efficacy by percutaneous absorption of piroxicam from the poloxamer gel in rats. *International journal of pharmaceuticals* **2000**, 193, (2), 213-218.
51. Barichello, J. M.; Morishita, M.; Takayama, K.; Nagai, T., Absorption of insulin from Pluronic F-127 gels following subcutaneous administration in rats. *International journal of pharmaceuticals* **1999**, 184, (2), 189-198.

52. Pec, E.; Wout, Z.; Johnston, T., Biological activity of urease formulated in poloxamer 407 after intraperitoneal injection in the rat. *Journal of pharmaceutical sciences* **1992**, 81, (7), 626-630.
53. Asasutjarit, R.; Thanasanchokpibull, S.; Fuongfuchat, A.; Veeranondha, S., Optimization and evaluation of thermoresponsive diclofenac sodium ophthalmic in situ gels. *International journal of pharmaceutics* **2011**, 411, (1), 128-135.
54. Qi, H.; Chen, W.; Huang, C.; Li, L.; Chen, C.; Li, W.; Wu, C., Development of a poloxamer analogs/carbopol-based in situ gelling and mucoadhesive ophthalmic delivery system for puerarin. *International journal of pharmaceutics* **2007**, 337, (1), 178-187.
55. Tirumala, V. R.; Romang, A.; Agarwal, S.; Lin, E. K.; Watkins, J. J., Well ordered polymer melts from blends of disordered triblock copolymer surfactants and functional homopolymers. *Advanced Materials* **2008**, 20, (9), 1603-1608.
56. Yong, C. S.; Choi, J. S.; Quan, Q. Z.; Rhee, J. D.; Kim, C. K.; Lim, S. J.; Kim, K. M.; Oh, P. S.; Choi, H. G., Effect of sodium chloride on the gelation temperature, gel strength and bioadhesive force of poloxamer gels containing diclofenac sodium. *International Journal of Pharmaceutics* **2001**, 226, (1), 195-205.
57. Ricci, E.; Lunardi, L.; Nanclares, D.; Marchetti, J., Sustained release of lidocaine from Poloxamer 407 gels. *International Journal of Pharmaceutics* **2005**, 288, (2), 235-244.
58. Jain, N.; George, A.; Bahadur, P., Effect of salt on the micellization of pluronic P65 in aqueous solution. *Colloids and Surfaces A: Physicochemical and Engineering Aspects* **1999**, 157, (1), 275-283.
59. Bahadur, P.; Pandya, K.; Almgren, M.; Li, P.; Stilbs, P., Effect of inorganic salts on the micellar behaviour of ethylene oxide-propylene oxide block copolymers in aqueous solution. *Colloid and Polymer Science* **1993**, 271, (7), 657-667.
60. Alexandridis, P.; Holzwarth, J. F., Differential scanning calorimetry investigation of the effect of salts on aqueous solution properties of an amphiphilic block copolymer (poloxamer). *Langmuir* **1997**, 13, (23), 6074-6082.
61. Su, Y.-l.; Liu, H.-z.; Wang, J.; Chen, J.-y., Study of salt effects on the micellization of PEO-PPO-PEO block copolymer in aqueous solution by FTIR spectroscopy. *Langmuir* **2002**, 18, (3), 865-871.

62. Pandit, N.; Trygstad, T.; Croy, S.; Bohorquez, M.; Koch, C., Effect of salts on the micellization, clouding, and solubilization behavior of pluronic F127 solutions. *Journal of colloid and interface science* **2000**, 222, (2), 213-220.
63. Yong, C. S.; Choi, J. S.; Quan, Q.-Z.; Rhee, J.-D.; Kim, C.-K.; Lim, S.-J.; Kim, K.-M.; Oh, P.-S.; Choi, H.-G., Effect of sodium chloride on the gelation temperature, gel strength and bioadhesive force of poloxamer gels containing diclofenac sodium. *International journal of pharmaceutics* **2001**, 226, (1), 195-205.
64. Li, Y.; Xu, R.; Couderc, S.; Bloor, M.; Wyn-Jones, E.; Holzwarth, J., Binding of sodium dodecyl sulfate (SDS) to the ABA block copolymer Pluronic F127 (EO97PO69EO97): F127 aggregation induced by SDS. *Langmuir* **2001**, 17, (1), 183-188.
65. Li, Y.; Xu, R.; Couderc, S.; Bloor, D.; Holzwarth, J.; Wyn-Jones, E., Binding of tetradecyltrimethylammonium bromide to the ABA block copolymer Pluronic F127 (EO97 PO69 EO97): electromotive force, microcalorimetry, and light scattering studies. *Langmuir* **2001**, 17, (19), 5742-5747.
66. Hellweg, T., Block Copolymer Surfactant Mixtures in Aqueous Solution: Can we Achieve Size and Shape Control by Co-Micellization? In *Self Organized Nanostructures of Amphiphilic Block Copolymers II*, Springer: 2011; pp 1-27.
67. Kurumada, K.-i.; Robinson, B. H., Viscosity studies of pluronic F127 in aqueous solution. In *Trends in Colloid and Interface Science XVI*, Springer: 2004; pp 12-15.
68. Jangher, A.; Griffiths, P.; Paul, A.; King, S.; Heenan, R.; Schweins, R., Polymeric micelle disruption by cosolvents and anionic surfactants. *Colloids and Surfaces A: Physicochemical and Engineering Aspects* **2011**, 391, (1), 88-94.
69. Gilbert, J. C.; Richardson, J. L.; Davies, M. C.; Palin, K. J.; Hadgraft, J., The effect of solutes and polymers on the gelation properties of pluronic F-127 solutions for controlled drug delivery. *Journal of Controlled Release* **1987**, 5, (2), 113-118.
70. Ricardo, N. M. P. S.; Costa, F. D. M. L. L.; Bezerra, F. W. A.; Chaibundit, C.; Hermida-Merino, D.; Greenland, B. W.; Burattini, S.; Hamley, I. W.; Keith Nixon, S.; Yeates, S. G., Effect of water-soluble polymers, polyethylene glycol and poly(vinylpyrrolidone), on the gelation of aqueous micellar solutions of Pluronic copolymer F127. *Journal of Colloid and Interface Science* **2012**, 368, (1), 336-341.
71. Oliveira, C. P.; Vasconcellos, L. C. G.; Ribeiro, M. E. N. P.; Ricardo, N. M. P. S.; Souza, T. V. D. P.; Costa, F. D. M. L. L.; Chaibundit, C.; Yeates, S. G.; Attwood, D., The

- effect of polymeric additives on the solubilisation of a poorly-soluble drug in micellar solutions of Pluronic F127. *International Journal of Pharmaceutics* **2011**, 409, (1-2), 206-208.
72. Zhang, H.; Yu, L.; Ding, J., Roles of hydrophilic homopolymers on the hydrophobic-association-induced physical gelling of amphiphilic block copolymers in water. *Macromolecules* **2008**, 41, (17), 6493-6499.
73. Costa, T.; Seixas de Melo, J.; Miguel, M. d. G.; Lindman, B. r.; Schillén, K., Complex Formation between a Fluorescently-Labeled Polyelectrolyte and a Triblock Copolymer. *The Journal of Physical Chemistry B* **2009**, 113, (18), 6205-6214.
74. Cole, M. L.; Whateley, T. L., Interaction of nonionic block copolymeric (Poloxamer) surfactants with poly (Acrylic Acid), studied by photon correlation spectroscopy. *Journal of colloid and interface science* **1996**, 180, (2), 421-427.
75. Dos Santos, S.; Luigjes, B.; Piculell, L., Associative phase behaviour and disintegration of copolymer aggregates on adding poly (acrylic acid) to aqueous solutions of a PEO-PPO-PEO triblock copolymer. *Soft Matter* **2010**, 6, (19), 4756-4767.
76. Owen, S. C.; Chan, D. P.; Shoichet, M. S., Polymeric micelle stability. *Nano Today* **2012**, 7, (1), 53-65.
77. Ebrahim Attia, A. B.; Ong, Z. Y.; Hedrick, J. L.; Lee, P. P.; Ee, P. L. R.; Hammond, P. T.; Yang, Y.-Y., Mixed micelles self-assembled from block copolymers for drug delivery. *Current Opinion in Colloid & Interface Science* **2011**, 16, (3), 182-194.
78. Liu, T.; Nace, V. M.; Chu, B., Self-assembly of mixed amphiphilic triblock copolymers in aqueous solution. *Langmuir* **1999**, 15, (9), 3109-3117.
79. Ricardo, N. M.; Chaibundit, C.; Yang, Z.; Attwood, D.; Booth, C., Association behavior of mixed triblock copoly (oxyalkylene) s (type EBE and ESE) in aqueous solution. *Langmuir* **2006**, 22, (3), 1301-1306.
80. Harrison, W. J.; Aboulgasem, G. J.; Elathrem, F. A.; Nixon, S. K.; Attwood, D.; Price, C.; Booth, C., Micelles and gels of mixed triblock copoly (oxyalkylene) s in aqueous solution. *Langmuir* **2005**, 21, (14), 6170-6178.
81. Gaisford, S.; Beezer, A. E.; Mitchell, J. C., Diode-array UV spectrometric evidence for cooperative interactions in binary mixtures of Pluronics F77, F87, and F127. *Langmuir* **1997**, 13, (10), 2606-2607.

82. Zhang, M.; Djabourov, M.; Bourgaux, C.; Bouchemal, K., Nanostructured Fluids from pluronic® Mixtures. *International Journal of Pharmaceutics* **2013**, 454, (2), 599-610.
83. Zhou, D.; Alexandridis, P.; Khan, A., Self-assembly in a mixture of two poly(ethylene oxide)-b-poly(propylene oxide)-b-poly(ethylene oxide) copolymers in water. *Journal of Colloid and Interface Science* **1996**, 183, (2), 339-350.
84. Newby, G. E.; Hamley, I. W.; King, S. M.; Martin, C. M.; Terrill, N. J., Structure, rheology and shear alignment of Pluronic block copolymer mixtures. *Journal of Colloid and Interface Science* **2009**, 329, (1), 54-61.
85. Wagner, N. J.; Brady, J. F., Shear thickening in colloidal dispersions. *Physics Today* **2009**, 62, (10), 27-32.
86. Barnes, H., SHEAR-THICKENING('DILATANCY') IN SUSPENSIONS OF NONAGGREGATING SOLID PARTICLES DISPERSED IN NEWTONIAN LIQUIDS. *J. Rheol.* **1989**, 33, (2), 329-366.
87. Crawford, N. C.; Popp, L. B.; Johns, K. E.; Caire, L. M.; Peterson, B. N.; Liberatore, M. W., Shear thickening of corn starch suspensions: Does concentration matter? *Journal of colloid and interface science* **2013**.
88. Egres Jr, R.; Lee, Y.; Kirkwood, J.; Kirkwood, K.; Wetzel, E.; Wagner, N. In *Liquid armor: protective fabrics utilizing shear thickening fluids*, Proceedings of the 4th International Conference of Safety and Protective Fabrics, Pittsburg, PA, 2004; 2004.
89. Srivastava, A.; Majumdar, A.; Butola, B., Improving the impact resistance of textile structures by using shear thickening fluids: a review. *Critical Reviews in Solid State and Materials Sciences* **2012**, 37, (2), 115-129.
90. Kang, T. J.; Hong, K. H.; Yoo, M. R., Preparation and properties of fumed silica/Kevlar composite fabrics for application of stab resistant material. *Fibers and Polymers* **2010**, 11, (5), 719-724.
91. Sun, L. L.; Xiong, D. S.; Xu, C. Y., Application of shear thickening fluid in ultra high molecular weight polyethylene fabric. *Journal of Applied Polymer Science* **2013**, 129, (4), 1922-1928.
92. Frith, W.; Lips, A., The rheology of concentrated suspensions of deformable particles. *Advances in colloid and interface science* **1995**, 61, 161-189.
93. Brown, E.; Jaeger, H. M., Dynamic jamming point for shear thickening suspensions. *Physical Review Letters* **2009**, 103, (8), 86001.



94. Fall, A.; Huang, N.; Bertrand, F.; Ovarlez, G.; Bonn, D., Shear thickening of cornstarch suspensions as a reentrant jamming transition. *Physical Review Letters* **2008**, 100, (1), 18301.
95. Bischoff White, E. E.; Chellamuthu, M.; Rothstein, J. P., Extensional rheology of a shear-thickening cornstarch and water suspension. *Rheologica Acta* **2010**, 49, (2), 119-129.
96. Escobar-Chávez, J.; López-Cervantes, M.; Naik, A.; Kalia, Y.; Quintanar-Guerrero, D.; Ganem-Quintanar, A., Applications of thermo-reversible pluronic F-127 gels in pharmaceutical formulations. *J Pharm Pharmaceut Sci* **2006**, 9, (3), 339-358.
97. Kaszuba, M.; Connah, M. T.; McNeil-Watson, F. K.; Nobbmann, U., Resolving concentrated particle size mixtures using dynamic light scattering. *Particle & Particle Systems Characterization* **2007**, 24, (3), 159-162.
98. Sarkar, B.; Ravi, V.; Alexandridis, P., Micellization of amphiphilic block copolymers in binary and ternary solvent mixtures. *Journal of colloid and interface science* **2012**.
99. Meznarich, N. A. K.; Love, B. J., The kinetics of gel formation for PEO-PPO-PEO triblock copolymer solutions and the effects of added methylparaben. *Macromolecules* **2011**, 44, (9), 3548-3555.
100. Bonacucina, G.; Spina, M.; Misici-Falzi, M.; Cespi, M.; Pucciarelli, S.; Angeletti, M.; Palmieri, G. F., Effect of hydroxypropyl  $\beta$ -cyclodextrin on the self-assembling and thermogelation properties of Poloxamer 407. *European Journal of Pharmaceutical Sciences* **2007**, 32, (2), 115-122.
101. Desbrières, J.; Hirrien, M.; Ross-Murphy, S. B., Thermogelation of methylcellulose: Rheological considerations. *Polymer* **2000**, 41, (7), 2451-2461.
102. Yuan, C. N.; Sheng, Y. J.; Tsao, H. K., Non-Brownian particle gel. *Applied Physics Letters* **2009**, 95, (23).
103. Walls, H. J.; Caines, S. B.; Sanchez, A. M.; Khan, S. A., Yield stress and wall slip phenomena in colloidal silica gels. *Journal of Rheology* **2003**, 47, (4), 847-868.
104. Shih, W. Y.; Shih, W. H.; Aksay, I. A., Elastic and yield behavior of strongly flocculated colloids. *Journal of the American Ceramic Society* **1999**, 82, (3), 616-624.

105. Singh, P.; Pandey, S., Solute-solvent interactions within aqueous poly(ethylene glycol): Solvatochromic probes for empirical determination and preferential solvation. *Green Chemistry* **2007**, 9, (3), 254-261.
106. Kwon, K. W.; Park, M. J.; Hwang, J.; Char, K., Effects of alcohol addition on gelation in aqueous solution of poly(ethylene oxide)-poly(propylene oxide)-poly(ethylene oxide) triblock copolymer. *Polymer Journal* **2001**, 33, (5), 404-410.
107. Bieze, T. W. N.; Barnes, A. C.; Huige, C. J. M.; Enderby, J. E.; Leyte, J. C., Distribution of Water around Poly(ethylene oxide): A Neutron Diffraction Study. *The Journal of Physical Chemistry* **1994**, 98, (26), 6568-6576.
108. Kjellander, R.; Florin, E., Water structure and changes in thermal stability of the system poly(ethylene oxide)-water. *Journal of the Chemical Society, Faraday Transactions 1: Physical Chemistry in Condensed Phases* **1981**, 77, (9), 2053-2077.
109. Naskar, B.; Ghosh, S.; Moulik, S. P., Solution behavior of normal and reverse triblock copolymers (pluronic L44 and 10R5) individually and in binary mixture. *Langmuir* **2012**, 28, (18), 7134-7146.
110. Wei, D.; Ge, L.; Guo, R., Binding characteristics between Poly (ethylene glycol) and hydrophilic modified ibuprofen in aqueous solution. *The Journal of Physical Chemistry B* **2010**, 114, (10), 3472-3481.
111. Feitosa, E.; Brown, W.; Wang, K.; Barreleiro, P. C. A., Interaction between poly(ethylene glycol) and C 12E 8 investigated by dynamic light scattering, time-resolved fluorescence quenching, and calorimetry. *Macromolecules* **2002**, 35, (1), 201-207.
112. Ge, L.; Zhang, X.; Guo, R., Microstructure of Triton X-100/poly (ethylene glycol) complex investigated by fluorescence resonance energy transfer. *Polymer* **2007**, 48, (9), 2681-2691.
113. Brackman, J. C.; Engberts, J. B. F. N., Polymer - Micelle interactions: Physical organic aspects. *Chemical Society Reviews* **1993**, 22, (2), 85-92.
114. Feitosa, E.; Brown, W.; Vasilescu, M.; Swanson-Vethamuthu, M., Effect of temperature on the interaction between the nonionic surfactant C12E5 and poly (ethylene oxide) investigated by dynamic light scattering and fluorescence methods. *Macromolecules* **1996**, 29, (21), 6837-6846.

115. Feitosa, E.; Brown, W.; Swanson-Vethamuthu, M., Interaction of the Nonionic Surfactant C12E8 with High Molar Mass Poly (ethylene oxide) Studied by Dynamic Light Scattering and Fluorescence Quenching Methods. *Langmuir* **1996**, 12, (25), 5985-5991.
116. Dormidontova, E. E., Influence of end groups on phase behavior and properties of PEO in aqueous solutions. *Macromolecules* **2004**, 37, (20), 7747-7761.
117. Malmsten, M.; Linse, P.; Zhang, K. W., Phase behavior of aqueous poly(ethylene oxide)/poly(propylene oxide) solutions. *Macromolecules* **1993**, 26, (11), 2905-2910.
118. Khutoryanskiy, V. V.; Dubolazov, A. V.; Nurkeeva, Z. S.; Mun, G. A., pH effects in the complex formation and blending of poly (acrylic acid) with poly (ethylene oxide). *Langmuir* **2004**, 20, (9), 3785-3790.
119. Khutoryanskiy, V. V.; Mun, G. A.; Nurkeeva, Z. S.; Dubolazov, A. V., pH and salt effects on interpolymer complexation via hydrogen bonding in aqueous solutions. *Polymer international* **2004**, 53, (9), 1382-1387.
120. Oyama, H. T.; Tang, W. T.; Frank, C. W., Effect of hydrophobic interaction in the poly (methacrylic acid)/pyrene end-labeled poly (ethylene glycol) complex. *Macromolecules* **1987**, 20, (8), 1839-1847.
121. Koussathana, M.; Lianos, P.; Staikos, G., Investigation of hydrophobic interactions in dilute aqueous solutions of hydrogen-bonding interpolymer complexes by steady-state and time-resolved fluorescence measurements. *Macromolecules* **1997**, 30, (25), 7798-7802.
122. Costa, T.; Schillén, K.; Miguel, M. d. G.; Lindman, B. r.; Seixas de Melo, J., Association of a Hydrophobically Modified Polyelectrolyte and a Block Copolymer Followed by Fluorescence Techniques. *The Journal of Physical Chemistry B* **2009**, 113, (18), 6194-6204.
123. Tirumala, V. R.; Vogt, B. D.; Lin, E. K.; Watkins, J. J. In *Influence of Strongly Interacting Homopolymers on the Long-Range Order in Semi-Crystalline, Amphiphilic Block Copolymer Templates*, The 2006 Annual Meeting, 2006; 2006.
124. Vallat, P.; Catala, J.-M.; Rawiso, M.; Schosseler, F., Conformational transitions of conjugated annealed polyelectrolytes. *EPL (Europhysics Letters)* **2008**, 82, (2), 28009.
125. D'Errico, G.; Ciccarelli, D.; Ortona, O.; Paduano, L.; Sartorio, R., Interaction between pentaethylene glycol n-octyl ether and poly (acrylic acid): Effect of the polymer molecular weight. *Journal of colloid and interface science* **2007**, 314, (1), 242-250.

126. D'Errico, G.; Ciccarelli, D.; Ortona, O.; Paduano, L.; Sartorio, R., Interaction between pentaethylene glycol n-octyl ether and low-molecular-weight poly (acrylic acid). *Journal of colloid and interface science* **2004**, 270, (2), 490-495.
127. Anghel, D. F.; Saito, S.; Băran, A.; Iovescu, A., Interaction between poly (acrylic acid) and nonionic surfactants with the same poly (ethylene oxide) but different hydrophobic moieties. *Langmuir* **1998**, 14, (19), 5342-5346.
128. Kositzka, M. J.; Bohne, C.; Alexandridis, P.; Hatton, T. A.; Holzwarth, J. F., Micellization dynamics and impurity solubilization of the block-copolymer L64 in an aqueous solution. *Langmuir* **1999**, 15, (2), 322-325.
129. Mingvanish, W.; Chaibundit, C.; Booth, C., Mixed micellisation of oxyethylene–oxybutylene diblock and triblock copolymers in water studied by light scattering. *Physical Chemistry Chemical Physics* **2002**, 4, (5), 778-784.
130. Bahadur, P.; Pandya, K., Aggregation behavior of Pluronic P-94 in water. *Langmuir* **1992**, 8, (11), 2666-2670.
131. Alexandridis, P.; Athanassiou, V.; Hatton, T. A., Pluronic-P105 PEO-PPO-PEO block copolymer in aqueous urea solutions: micelle formation, structure, and microenvironment. *Langmuir* **1995**, 11, (7), 2442-2450.
132. Zhou, L.; Schlick, S., Electron spin resonance (ESR) spectra of amphiphilic spin probes in the triblock copolymer EO13PO30EO13(Pluronic L64): hydration, dynamics and order in the polymer aggregates. *Polymer* **2000**, 41, (12), 4679-4689.
133. Mata, J.; Majhi, P.; Guo, C.; Liu, H.; Bahadur, P., Concentration, temperature, and salt-induced micellization of a triblock copolymer Pluronic L64 in aqueous media. *Journal of Colloid and Interface Science* **2005**, 292, (2), 548-556.
134. Park, M. J.; Char, K., Two Gel States of a PEO-PPO-PEO Triblock Copolymer Formed by Different Mechanisms. *Macromolecular Rapid Communications* **2002**, 23, (12), 688-692.
135. Park, M. J.; Char, K.; Kim, H. D.; Lee, C.-H.; Seong, B.-S.; Han, Y.-S., Phase behavior of a PEO-PPO-PEO triblock copolymer in aqueous solutions: Two gelation mechanisms. *Macromolecular Research* **2002**, 10, (6), 325-331.
136. Jørgensen, E. B.; Hvidt, S.; Brown, W.; Schillén, K., Effects of salts on the micellization and gelation of a triblock copolymer studied by rheology and light scattering. *Macromolecules* **1997**, 30, (8), 2355-2364.

137. Mortensen, K., Phase behaviour of poly (ethylene oxide)-poly (propylene oxide)-poly (ethylene oxide) triblock-copolymer dissolved in water. *EPL (Europhysics Letters)* **1992**, 19, (7), 599.
138. Mortensen, K.; Brown, W., Poly (ethylene oxide)-poly (propylene oxide)-poly (ethylene oxide) triblock copolymers in aqueous solution. The influence of relative block size. *Macromolecules* **1993**, 26, (16), 4128-4135.
139. Olsen, B. D.; Li, X.; Wang, J.; Segalman, R. A., Near-surface and internal lamellar structure and orientation in thin films of rod-coil block copolymers. *Soft Matter* **2009**, 5, (1), 182-192.
140. Brown, E.; Forman, N. A.; Orellana, C. S.; Zhang, H.; Maynor, B. W.; Betts, D. E.; DeSimone, J. M.; Jaeger, H. M., Generality of shear thickening in dense suspensions. *Nature materials* **2010**, 9, (3), 220-224.
141. Negi, A. S.; Osuji, C. O., New insights on fumed colloidal rheology—shear thickening and vorticity-aligned structures in flocculating dispersions. *Rheologica acta* **2009**, 48, (8), 871-881.
142. Hoffman, R. L., Discontinuous and dilatant viscosity behavior in concentrated suspensions III. Necessary conditions for their occurrence in viscometric flows. *Advances in colloid and interface science* **1982**, 17, (1), 161-184.
143. Brady, J. F.; Bossis, G., Rheology of concentrated suspensions of spheres in simple shear flow by numerical simulation. *Journal of Fluid Mechanics* **1985**, 155, 105-29.
144. Maranzano, B. J.; Wagner, N. J., The effects of particle size on reversible shear thickening of concentrated colloidal dispersions. *The Journal of Chemical Physics* **2001**, 114, 10514.
145. Kalman, D. P.; Wagner, N. J., Microstructure of shear-thickening concentrated suspensions determined by flow-USANS. *Rheologica acta* **2009**, 48, (8), 897-908.
146. Waitukaitis, S. R.; Jaeger, H. M., Impact-activated solidification of dense suspensions via dynamic jamming fronts. *Nature* **2012**, 487, (7406), 205-209.
147. Waitukaitis, S.; Roth, L.; Vitelli, V.; Jaeger, H., Dynamic jamming fronts. *EPL (Europhysics Letters)* **2013**, 102, (4), 44001.

148. Lee, Y. S.; Wetzel, E. D.; Wagner, N. J., The ballistic impact characteristics of Kevlar® woven fabrics impregnated with a colloidal shear thickening fluid. *Journal of materials science* **2003**, 38, (13), 2825-2833.
149. Fall, A.; Bertrand, F.; Ovarlez, G.; Bonn, D., Shear thickening of cornstarch suspensions. *Journal of Rheology* **2012**, 56, 575.
150. Brown, E.; Jaeger, H. M., The role of dilation and confining stresses in shear thickening of dense suspensions. *Journal of Rheology* **2012**, 56, 875.
151. Walls, H.; Caines, S. B.; Sanchez, A. M.; Khan, S. A., Yield stress and wall slip phenomena in colloidal silica gels. *Journal of Rheology* **2003**, 47, (4), 847-868.
152. Moller, P.; Fall, A.; Chikkadi, V.; Derks, D.; Bonn, D., An attempt to categorize yield stress fluid behaviour. *Philosophical Transactions of the Royal Society A: Mathematical, Physical and Engineering Sciences* **2009**, 367, (1909), 5139-5155.
153. Fall, A.; Paredes, J.; Bonn, D., Yielding and shear banding in soft glassy materials. *Physical Review Letters* **2010**, 105, (22).
154. Kondo, T.; Sawatari, C.; Manley, R. S. J.; Gray, D. G., Characterization of hydrogen bonding in cellulose-synthetic polymer blend systems with regioselectively substituted methylcellulose. *Macromolecules* **1994**, 27, (1), 210-215.
155. Kim, C.-H.; Kim, D.-W.; Cho, K. Y., The influence of PEG molecular weight on the structural changes of corn starch in a starch/PEG blend. *Polymer bulletin* **2009**, 63, (1), 91-99.
156. Yu, F.; Prashantha, K.; Soulestin, J.; Lacrampe, M.-F.; Krawczak, P., Plasticized-starch/poly (ethylene oxide) blends prepared by extrusion. *Carbohydrate polymers* **2012**.
157. Madathingal, R. R.; Wunder, S. L., Confinement Effects of Silica Nanoparticles with Radii Smaller and Larger Than  $R_g$  of Adsorbed Poly (ethylene oxide). *Macromolecules* **2011**, 44, (8), 2873-2882.
158. Voronin, E.; Gun'ko, V. M.; Guzenko, N.; Pakhlov, E.; Nosach, L.; Leboda, R.; Skubiszewska-Zięba, J.; Malysheva, M.; Borysenko, M.; Chuiko, A., Interaction of poly (ethylene oxide) with fumed silica. *Journal of colloid and interface science* **2004**, 279, (2), 326-340.
159. Jagadish, R.; Raj, B., Properties and sorption studies of polyethylene oxide–starch blended films. *Food Hydrocolloids* **2011**, 25, (6), 1572-1580.

160. Dean, K. M.; Do, M. D.; Petinakis, E.; Yu, L., Key interactions in biodegradable thermoplastic starch/poly (vinyl alcohol)/montmorillonite micro-and nanocomposites. *Composites Science and Technology* **2008**, 68, (6), 1453-1462.
161. Marsh, R.; Waight, S., The effect of pH on the zeta potential of wheat and potato starch. *Starch-Stärke* **1982**, 34, (5), 149-152.
162. Marshall, W. E.; Chrastil, J., Interaction of Food Proteins with Starch. In *Biochemistry of food proteins*, Springer: 1992; pp 75-97.
163. Jenkins, P.; Snowden, M., Depletion flocculation in colloidal dispersions. *Advances in colloid and interface science* **1996**, 68, 57-96.
164. Asakura, S.; Oosawa, F., Interaction between particles suspended in solutions of macromolecules. *Journal of Polymer Science* **1958**, 33, (126), 183-192.
165. Liang, W.; Tadros, T. F.; Luckham, P., Effect of volume fraction and particle size on depletion flocculation of a sterically stabilized latex dispersion induced by addition of poly (ethylene oxide). *Journal of Colloid and Interface Science* **1993**, 155, (1), 156-164.
166. Gopalakrishnan, V.; Zukoski, C., Effect of attractions on shear thickening in dense suspensions. *Journal of Rheology* **2004**, 48, 1321.
167. Jiang, T.; Zukoski, C. F., Role of Particle Size and Polymer Length in Rheology of Colloid–Polymer Composites. *Macromolecules* **2012**, 45, (24), 9791-9803.
168. Ma, J.; Guo, C.; Tang, Y.; Wang, J.; Zheng, L.; Liang, X.; Chen, S.; Liu, H., Microenvironmental and conformational structure of triblock copolymers in aqueous solution by <sup>1</sup>H and <sup>13</sup>C NMR spectroscopy. *Journal of Colloid and Interface Science* **2006**, 299, (2), 953-961.
169. Ma, J.-h.; Guo, C.; Tang, Y.-l.; Liu, H.-z., <sup>1</sup>H NMR spectroscopic investigations on the micellization and gelation of PEO-PPO-PEO block copolymers in aqueous solutions. *Langmuir* **2007**, 23, (19), 9596-9605.
170. Zeghal, M.; Auvray, L., Structure of hydrophobically and hydrogen-bonded complexes between amphiphilic copolymer and polyacid in water. *The European Physical Journal E* **2004**, 14, (3), 259-268.
171. Jeong, B.; Bae, Y. H.; Kim, S. W., Thermoreversible gelation of PEG-PLGA-PEG triblock copolymer aqueous solutions. *Macromolecules* **1999**, 32, (21), 7064-7069.

172. Hecht, E.; Mortensen, K.; Gradzielski, M.; Hoffmann, H., Interaction of ABA block copolymers with ionic surfactants: influence on micellization and gelation. *The Journal of Physical Chemistry* **1995**, 99, (13), 4866-4874.
173. Wang, Q.; Li, L.; Jiang, S., Effects of a PPO-PEO-PPO triblock copolymer on micellization and gelation of a PEO-PPO-PEO triblock copolymer in aqueous solution. *Langmuir* **2005**, 21, (20), 9068-9075.



## PUBLICATIONS & CONFERENCES

---

### Journal Publications

- 1) **Pragatheeswaran, A. M.**, Chen, S. B., Effect of Chain Length of PEO on the Gelation and Micellization of the Pluronic F127 Copolymer Aqueous System. *Langmuir* 29(31), 9694-9701 (2013).
- 2) **Pragatheeswaran, A. M.**, Chen, S. B., Chen, C. F., & Chen, B. H., Micellization and gelation of PEO-PPO-PEO binary mixture with non-identical PPO block lengths in aqueous solution. *Polymer* 55(20), 5284-5291 (2015).
- 3) **Pragatheeswaran, A. M.**, Chen, S. B., Effect of Poly(acrylic acid) on the Gelation and Micellization of the Pluronic F127 Copolymer Aqueous System. *Polymer*, under review.

### Conference Proceedings

- 1) **Pragatheeswaran, A. M.**, & Chen, S. B., Temperature Effects on Gelation of PEO<sub>x</sub>-PPO<sub>y</sub>-PEO<sub>x</sub> Triblock Copolymer Mixtures in Aqueous Solution. *6th Pacific Rim Conference on Rheology*, July 20-25 (2014), Melbourne, Australia.
- 2) **Pragatheeswaran, A. M.**, & Chen, S. B., Rheology of Non-Brownian Particulate Suspension in Poly (Ethylene Glycol)/Water Mixtures. *6th Pacific Rim Conference on Rheology*, July 20-25 (2014), Melbourne, Australia.
- 3) **Pragatheeswaran, A. M.**, & Chen, S. B., Interaction of nonionic block copolymer with poly(acrylic acid) and poly(ethylene oxide) in aqueous medium. *The Society of Rheology 86th Annual Meeting*, October 5-9 (2014), Philadelphia, PA.

## APPENDIX

---

### Effect of PEO contributed viscosity on F127 micelle size

The presence of free PEO may increase the medium viscosity and hence lead to overestimation of the micelle hydrodynamic radius. The viscosity of PEO solution without F127 was thus measured using the rheometer and a capillary viscometer at 40°C. Treating the medium as a continuum with this viscosity, the micelle size was determined with the result shown in Table A1. As expected, the hydrodynamic radius is reduced. For pure PEO20k and PEO35k solutions, the measured hydrodynamic radii are about 3 and 5 nm, respectively, which are not much smaller than the micelles size seen in Table A1. Hence, the continuum assumption becomes invalid, and the above assessment provides a lower bound for the micelle size. Researchers who studied the effect of PEO on the size of surfactant micelles considered only the water viscosity instead of the PEO solution viscosity.<sup>110-112</sup> Nevertheless, we acknowledge that free PEO may have certain effect on the diffusion of micelles. In this regards, the micelle hydrodynamic radius should fall between the two values in Table A1. The trend of size change remains the same though.

**Table A1.** Effect of medium viscosity on micelle size; F127 conc. = 1 wt%; PEO conc. = 2 wt%.

PEO MW (g/mol)	Hydrodynamic Radius (nm)	
	Water viscosity considered	PEO solution viscosity considered
Pure F127	12.18	-

2k	14.11	13.62
10k	18.92	13.89
20k	21.91	14.67
35k	39.41	23.11

### Effect of PEO on $^1\text{H-NMR}$ spectra of 1%F127

Figure A2 shows the  $^1\text{H-NMR}$  spectra of 1% F127 in  $\text{D}_2\text{O}$  at different temperatures. The peak at  $\sim 1\text{ppm}$  corresponds to methyl unit of PO group ( $\text{PO-CH}_3$ ), while the sharp peak at  $\sim 3.5\text{ppm}$  and the hyperfine peak to its right correspond to methylene units of EO and PO groups, respectively.<sup>12, 168, 169</sup> The  $\text{PO-CH}_3$  peak shows a clear triplet at low temperature. Above the CMT ( $>25^\circ\text{C}$ ), this triplet disappears completely and the peak broadens. This behavior has been attributed to transfer of  $\text{PO-CH}_3$  from a hydrated state to a hydrophobic environment.<sup>12, 168</sup> According to Ma et al.,<sup>168</sup> the peaks of  $\text{PO-CH}_3$  and  $\text{PO-CH}_2$  relative to that of  $\text{EO-CH}_2$  show upfield shift with increasing temperature. Our data also exhibit the same behavior in agreement with their observation.

When a poly(methacrylic acid) (PMA) was added to Pluronic solution, Zeghal et al.<sup>170</sup> found a drastic change in this  $\text{PO-CH}_3$  peak: the triplet shape was completely absent and the peak was broader even at temperature below CMT. Unlike a pure pluronic solution, no sharp transition in the shape of the peak was observed above CMT, but the line width increased with increasing temperature. They attributed the absence of peak's triplet to reduced mobility of the PPO moiety due to association of PMA homopolymer with PPO accompanied by loss

of water molecules. The progressive increase in the line width was ascribed to the heightened extent of complexation between PMA and PPO moiety with increasing temperature due to hydrophobicity. Therefore, the change in shape of the PO-CH<sub>3</sub> peak is an indication of strong interaction between PPO moiety of the pluronic and the homopolymer.

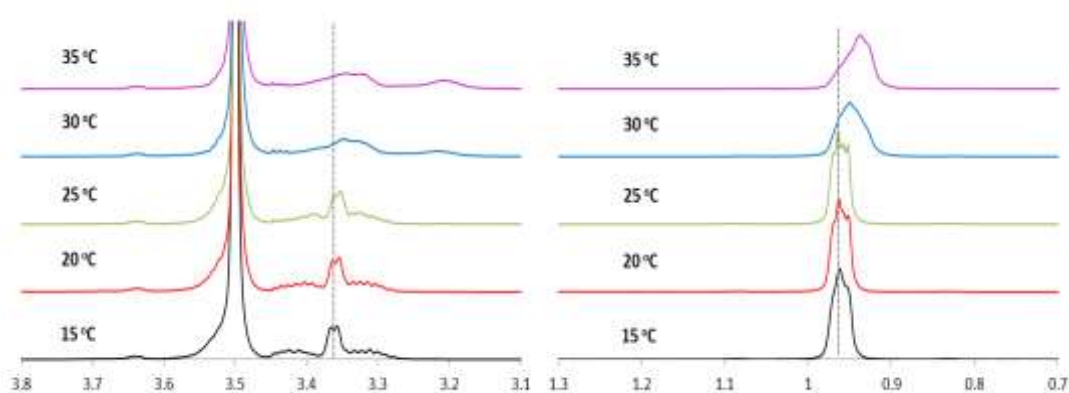


**Figure A2.** <sup>1</sup>H-NMR spectra of 1% F127 in D<sub>2</sub>O at various temperatures; 3.1-3.8ppm (left) and 0.7-1.3ppm (right)

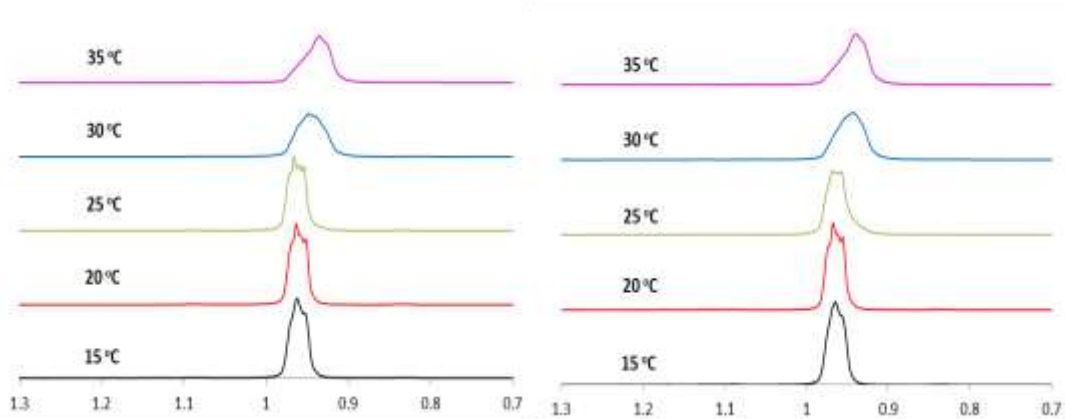


**Figure A3.** <sup>1</sup>H-NMR spectra of F127/PEO200/D<sub>2</sub>O solution (left) and F127/PEO35k/D<sub>2</sub>O (right) at various temperatures; F127 conc. = 1%; PEO conc. = 4%.

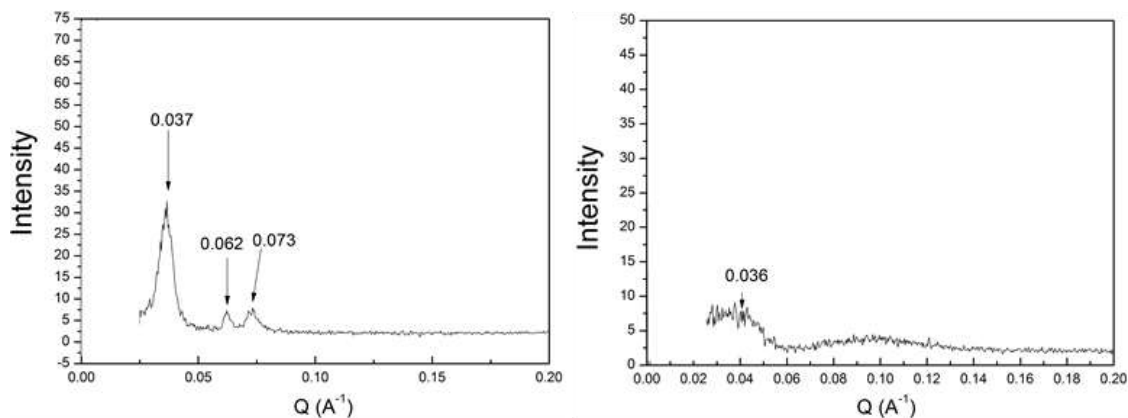
For the system considered in this thesis, the shape of PO-CH<sub>3</sub> peak for F127+PEO200 and F127+PEO35k are shown in Figure A3. In both systems, the peak triplet remains below CMT, but disappears above the CMT (>25°C) along with peak broadening, showing a similar behavior to that of pure F127 solution. Therefore, we conclude that the interaction between the PEO homopolymers and PPO moieties of pluronic is very weak or absent for the temperatures below and above the CMT. Any interaction between PEO moieties of F127 and PEO homopolymers could not be probed since the EO signal from the homopolymer overlapped with that of the F127 (not shown).

We also carried out <sup>13</sup>C NMR measurements to probe the conformational information of F127 in the presence of PEO homopolymer. For pure PEO or F127 solutions, the peaks and their shift with temperature are all in agreement with the literature.<sup>168</sup> For F127+PEO, there is no noticeable peak shift or shape change when compared to the pure F127 at the same concentration and temperature. It is therefore concluded that addition of PEO does not lead to conformational change of F127.

### **SAXS Analysis**

Figure A4 shows the SAXS intensity vs the wave vector for pure 25% F127 at 45°C and for 25% L64 at 55°C. The microstructures inferred from peak analysis for various cases are presented in Table A2. For the mixture 12.5%F127 + 12.5%L64 at 75°C, the deviation of observed reflections is 3.5% from the expected reflections of HCP and 9.9% from the expected FCC reflections, indicating that the microstructure resembles HCP more than the FCC. For all

other systems studied, the observed reflections are in very good match with the expected peaks (<3.5% of deviation).

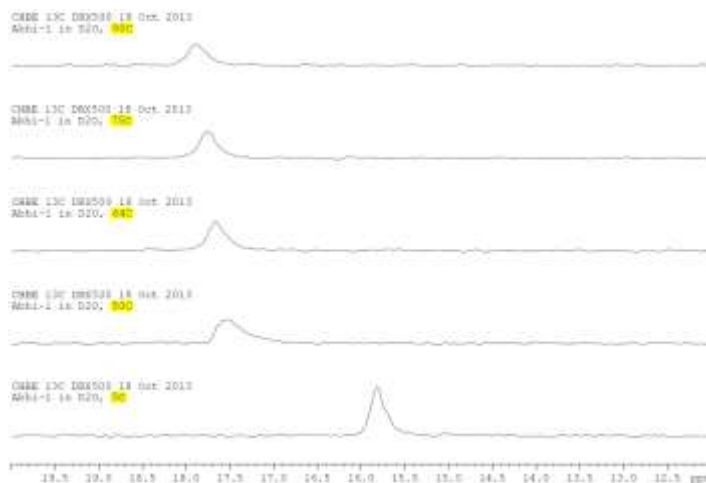


**Figure A4.** SAXS patterns of pure 25% F127 at 45°C (left) and pure 25% L64 at 55°C (right).

**Table A2.** Identified phases for different systems using SAXS.

Sample	Temperature (°C)	Sol/Gel State	Q <sub>0</sub>	Q <sub>1</sub>	Q <sub>2</sub>	Phase
25% F127	45	Hard gel	0.037	0.062	0.073	FCC
25% L64	55	Sol	-	-	-	No order (broad amorphous peak)
12.5% F127 + 12.5% L64	50	1 <sup>st</sup> hard gel	a	0.062	0.074	FCC
	65	Soft gel	-	-	-	Less ordered
	75	2 <sup>nd</sup> hard gel	0.034	0.061	0.070	HCP (more likely)

<sup>a</sup> No fundamental peak was observed

**$^{13}\text{C}$ -NMR for F127+L64 mixture**

**Figure A5.**  $^{13}\text{C}$  NMR spectra showing PPO- $\text{CH}_3$  signal for the mixture 12.5% F127+12.5%L64 in  $\text{D}_2\text{O}$  solution at various temperatures

Figure A5 shows the peak corresponding to the PPO- $\text{CH}_3$  group of 12.5%F127 + 12.5%L64 mixture at different temperatures. For this mixture, the CMT is  $12^\circ\text{C}$ . When temperature is increased from  $5^\circ\text{C}$  ( $T < \text{CMT}$ ) to  $50^\circ\text{C}$  ( $T \gg \text{CMT}$ ), the peak undergoes a large  $^{13}\text{C}$  chemical shift (increase in ppm value) and also broadening, which is attributed to the formation of non-polar microenvironment and change in the gauche/trans isomerism.<sup>168</sup> Jeong et al.<sup>171</sup> claimed that the core-shell micelle structure is lost at high temperature in PEG-PLGA-PEG system since they observed a relatively narrow (enhanced methyl peak) signal at high temperature. Unlike their system, the methyl peak of F127+L64 did not narrow down and retained its broadened shape. This indicates that the structure of the micelle (core-shell) is preserved even at high temperature (2<sup>nd</sup> hard gel region).

**Effect of F127 concentration on CMT of F127/PAA/H<sub>2</sub>O system**

Figure A6 plots the change in CMT with increasing PAA (1.8k) for two different F127 concentrations (17.5% system - obtained by DSC and 1% system - obtained by DPH solubilization technique). It shows that the CMT reduction is strongly dependent on the F127 concentration: the higher the F127 concentration, the smaller the CMT reduction at the same PAA concentration. For instance, 0.5% PAA can reduce the CMT of 1% F127 by  $\sim 8^{\circ}\text{C}$  while it can reduce the CMT of 17.5% F127 only by  $\sim 2^{\circ}\text{C}$ .

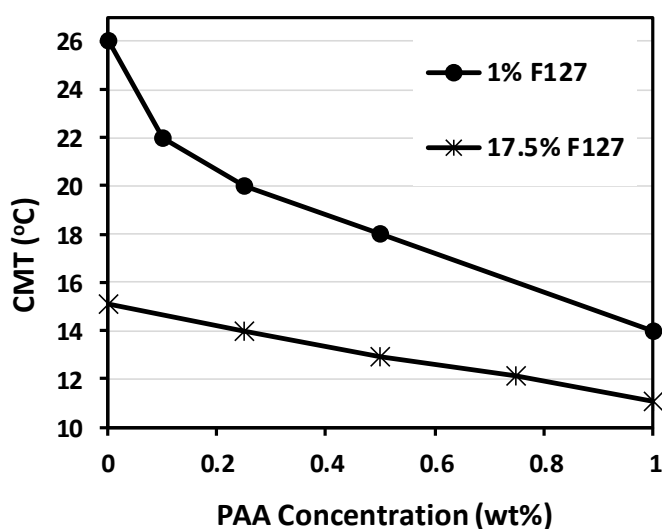


**Figure A6.** Effect of PAA (1.8k) concentration on CMT of dilute F127 (1%) and concentrated F127 (17.5%)



**Thermoreversibility of micellization process in F127/PAA/H<sub>2</sub>O**

Figure A7 presents the DSC thermogram from the heating-cooling-heating test of 17.5%F127+0.5%PAA (450k). The peak temperatures of the heating processes are slightly higher than those in the cooling process due to the difference in kinetics of micellization and demicellization of Pluronics.<sup>172, 173</sup>

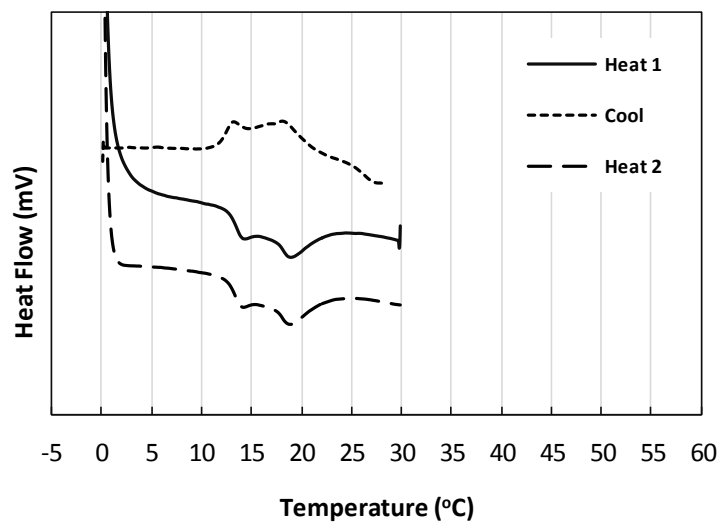


**Figure A7.** Thermoreversibility of micellization process shown by DSC for 17.5% F127 + 0.5% PAA (450k) at natural pH (= 3.9)